Faculty of Technology

The Validation of Predictive Geometallurgical Models for Concentrator Plant Process Design

Tomi Käyhkö

The Field of Process and Environmental Engineering

Master's Thesis

August 2019

TEKNILLINEN TIEDEKUNTA

Ennustavien geometallurgisten mallien validointi rikastamoiden prosessisuunnittelussa

Tomi Käyhkö

Prosessitekniikan tutkinto-ohjelma

Diplomityö

Elokuu 2019

TIIVISTELMÄ
OPINNÄYTETYÖSTÄ Oulun yliopisto Teknillinen tiedekunta

Koulutusohjelma (kandidaatintyö, diplomityö) Prosessitekniikan koulutusohjelma	Pääaineopintojen ala (lisensiaatintyö)
Tekijä Käyhkö, Tomi Santeri	Työn ohjaaja yliopistolla Sinche Gonzalez, M, lehtori

Työn nimi
Ennustavien geometallurgisten mallien validointi rikastamoiden suunnittelussa

Opintosuunta	Työn laji	Aika	Sivumäärä
Rikastustekniikka	Diplomityö	Elokuu 2019	88 s., 8 liitettä

Tiivistelmä

Geometallurgisten mallien käyttäminen rikastamoiden suunnittelussa ja tuotannossa yleistyy jatkuvasti. Ennustavalla mallinnuksella pyritään optimoimaan rikastamoiden ajoparametrejä jo valmiiksi ennen kuin malmi prosessoidaan rikastamolla. Rikkaimmat ja suurimmat malmiot maailmalla ovat pääosin käytetty ja tulevaisuudessa entistä köyhempiä ja vaikeammin rikastettavia malmeja joudutaan hyödyntämään, jotta metallien tuotanto saadaan pidettyä tarvittavalla tasolla. Prosessointia täytyy kehittää jatkuvasti ja tulevaisuudessa pyritään kehittämään erityisesti ennustavaa suunnittelua laitosten tuotannossa. Geometallurgisella mallilla tarkoitetaan metallurgien, kaivosinsinöörien ja geologien yhdessä luomaa mallia, jossa on yhdistetty data kaivossuunnitelmasta, kairaustuloksista ja metallurgisista kokeista.

Metallurgisten kokeiden tekeminen on kallista ja vie reilusti aikaa. Tässä työssä pyritään osoittamaan, että malmisekoituksille ei tarvitsisi erikseen tehdä metallurgisia kokeita vaan aikaa ja rahaa voidaan säästää mallinnus- ja simulointityöllä. Vaahdotusprosessia on tutkittu hyvin huolellisesti mutta geometallurgisten mallien suunnittelu- ja kehitystyöhön täytyy käyttää tulevaisuudessa enemmän rahaa ja aikaa.

Outotecin kehittämä simulointiohjelma HSC Chemistry® on suunnittelu- ja tuotantovaiheessa käytetty ohjelma, joka perustuu Outotecin tekemiin kokeisiin laboratorioissa ja tuotantolaitoksilla. Tämän työn tarkoituksena on validoida sen mallinnusta. Rikastamoilla syötteen laatu vaihtelee jatkuvasti, sillä malmi voi saapua prosessiin eri puolilta kaivosta ja syöte ei ole koskaan homogeeninen. Rikastamo tulee säätää sen mukaan, millaista malmia syötetään laitokselle.

Diplomityön aikana tehtiin yhteensä 16 eri vaahdotuskoetta neljällä eri malmityypillä, jotka ovat peräisin Rich Metal Groupin kaivokselta, Georgiasta. Kaivoksen malmio on jaettu eri geometallurgisiin yksiköihin, niiden mineralogisten ja metallurgisten ominaisuuksien perusteella. Vaahdotuskokeet suoritettiin Outotecin Porin tutkimuskeskuksessa. Koetoiminnan aikana jokaiselle yksikölle määritettiin vaahdotuskinetiikat, esi- ja kertausvaahdotuksessa. Laboratoriokokeissa ensimmäiseksi selvitettiin sopiva jauhatusaika vaahdotuskokeita varten. Laboratoriossa vaahdotusparametrejä ovat; vaahdotusilman syöttömäärä, kemikaalien annostelu, vaahdotuskoneen parametrit sekä vaahdotettavan malmin määrä. Vaahdotusten aikana eri malmien osuuksia muutettiin, muutoin vaahdotusolosuhteet pyrittiin pitämään vakioina.

Teoriaosuudessa perehdytään tärkeimpiin termeihin liittyen geometallurgiaan, vaahdotukseen ja vaahdotuksen simulointiin sekä mallinnukseen. Lisäksi validoinnin teoriaa avattu yhdessä kappaleessa, sillä simulointiohjelman validointi on tärkeässä roolissa tässä diplomityössä.

Kokeiden ja simulointien tulosten vertailu osoittaa, että tulokset vastaavat hyvin toisiaan ja näin ollen voidaan todeta että, HSC Sim simulointiohjelmaa voidaan käyttää malmisekoitusten mallinnukseen, mikäli eri malmien mineralogia on samankaltainen. HSC:tä voidaan käyttää malmisekoitusten mallinnukseen, mikäli vain päätejäsen-malmien metallurginen performanssi on tutkittu huolellisesti.

Muita tietoja

ABSTRACT
FOR THESIS

University of Oulu Faculty of Technology

Degree Programme (Bachelor's Thesis, Master's Thesis) Process Engineering		Major Subject (Licentiate Thesis)	
Author Käyhkö, Tomi Santeri		Thesis Supervisor Sinche Gonzalez, M, lecturer	
Title of Thesis The Validation of predictive geometallurgical models for concentrator plant process design			
Major Subject Mineral Processing	Type of Thesis Master's Thesis	Submission Date August 2019	Number of Pages 88 p., 8 App.

Abstract

The use of geometallurgical models is becoming more common in concentrator plant design and production phase. Predictive modelling aims to optimize process parameters before ore reaches the concentrator plant. Richest and easiest orebodies are already extracted, and in the future, more low-grade and complex orebodies should be exploited to reach enough metal production level. Mineral processing field should be developed all the time and especially predictive planning should be considered. Geometallurgical model means the model that is developed cooperated between metallurgists, mining engineers and geologists. Geometallurgical model combines data from mine plan, drill cores and metallurgical test works.

Metallurgical test works are expensive and take a lot of time. Validation aims to point out that it is possible to save money by doing comprehensive modelling and simulation work. Flotation process itself is very detailed studied but the use of geometallurgical models is still under development work.

HSC Chemistry® is simulation software developed by Outotec. HSC Sim is sub-program used in process design and production phase. The main objective of this thesis was to evaluate how experimental flotations with different ore blends will correspond to the current kinetic models of HSC Sim simulations for different ore blends.

In concentrator plants the ore feed keeps changing all the time, because ore might be delivered from different parts of mine and feed is always heterogeneous. The concentrator plant should be optimized based on mine plan and the kind of ore will be feed to the concentrator plant.

Overall 16 different flotation tests were accomplished during this thesis work. Test work was carried out using four different end-member ore types coming from Rich Metal Group mine site from Georgia. Deposit is distributed to different ore types and geometallurgical units. Flotation test work was conducted in Outotec Research Center in Pori. During experimentation, flotation kinetics were defined for four ore types in rougher and cleaner flotation. Experimental work started with grinding tests and optimal grinding times were defined. During flotation tests the distribution of ore types was changing, otherwise, flotation conditions remained constant.

Theory chapter explains the most important terms concerning to geometallurgy, flotation theory and flotation simulation and modelling. Theory chapter introduces the theory of validation due to the simulation model validation is the most important output of this thesis.

The correlation between experimental and simulated results is clear and results are close to each other. This means that the results are very promising and HSC Sim simulation software can be used to simulate flotation blends, if ores have similar mineralogy. In the future, more test work should be done with more different ores to validate HSC Sim simulation. Simulation of ore blends requires the deep metallurgical definition of end-member ores.

Additional Information

FOREWORD

This thesis project was carried out under the supervision of Outotec (Finland) Oy and it was written in Espoo between January and July 2019. Experimental phase of the thesis was done at Outotec Research Center in the city of Pori.

Firstly I would like to express my gratitude to my supervisors: Maria Sinche Gonzalez, PhD from University of Oulu and Jussi Liipo PhD from Outotec for the support and guidance during the whole thesis project. From Outotec side I also like to thank Janne Suhonen M.Sc. (Tech.) and Rodrigo Grau D.Sc. (Tech.) for sharing their advice and knowledge especially for modelling and simulation work. Additionally, I want to thank Rich Metals Group (JSC RMG Copper, Georgia) and Mr Sandro Khizanishvili for collaboration and ore samples used in the experimental part of the thesis.

I want also to thank my family, friends and football team members for being so supportive and helpful during all these years at University. Finally, I would like to express my appreciation to my energetic fellow students who made all these last years memorable.

In Oulu, 19.9.2019 Tomi Käyhkö

TABLE OF CONTENTS

TERMS AND ABBREVIATIONS

Au	gold
C	sampling constant for material to be sampled
$Ca(OH)_2$	calcium hydroxide
CC	cleaner concentrate
cc	chalcocite
ccp	chalcopyrite
CF	cleaner flotation
CT	cleaner tailings
Cu	copper
cupr	cuprite
c_i	component *i* concentration
f	shape factor
g	granulometric factor
GCT	Geometallurgical Comminution Test
ICP-OES	Inductively Coupled Plasma Optical Emission Spectroscopy
k_i	rate constant of component *i*
k_{max}	maximum rate constant
L	gross weight of sample required
l	liberation factor
M	minimum weight of sample required
m	mass
m	mineralogical composition factor
NSG	non-sulfide gangue
ORC	Outotec Research Center
py	pyrite
P80	80% passing particle size
pH	hydrogen potential
qtz	quartz
R	recovery
R_{max}	infinite recovery
RF	rougher flotation
RC	rougher concentrate

RMG	Rich Metal Group
RT	rougher tailings
rpm	rounds per minute
S	sulfur
V&V	Validation and Verification

1 INTRODUCTION

Geometallurgy takes both geological and metallurgical information to create a spatially-spaced model for a mineral processing industry (Lamberg, 2011). The use of geometallurgical models in concentrator plant process design and during plant operation is becoming more common all the time. New mining projects exploit more complex and low-grade ore bodies, which mean that the efficiency must be higher than before to reach the necessary metal production level.

Geometallurgical models can provide higher energy-efficiency in grinding circuit or better metallurgical performance in the flotation stage. Geometallurgical model helps to optimize the concentrator plant to process available ore and adapt the ore variation more beneficial way. Also, mining plant design projects will endeavor to favor more modelling besides flotation tests. Modelling and simulation will save money and time when a large part of the flotation tests can be replaced with modelling work. Usually, a geometallurgical model is developed during the pre-feasibility and feasibility stages of project implementation (Figure **1**).

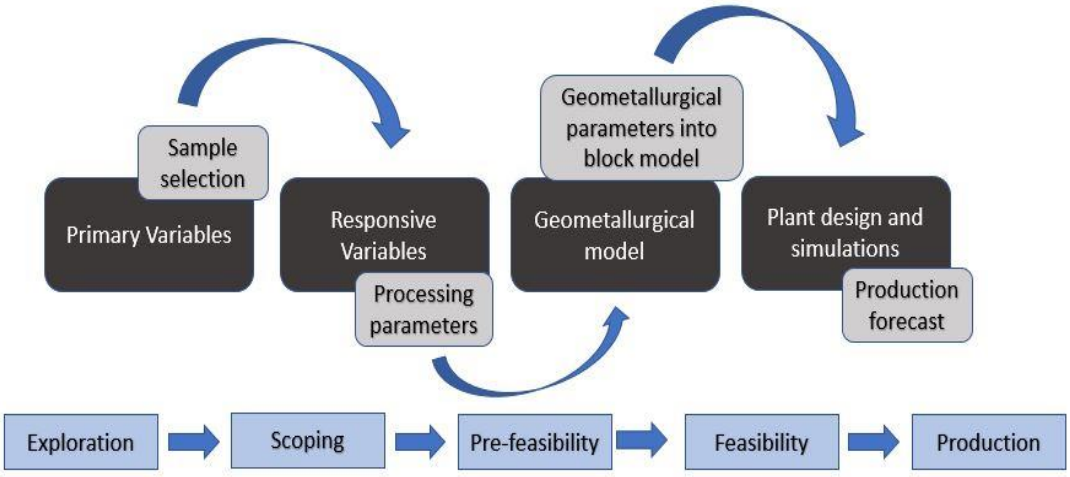

Figure 1. Mining project implementation phases (Lamberg, 2011).

HSC Sim is one module in HSC Chemistry® simulation and modelling software for metallurgical use and it is developed by Outotec. HSC Sim is used in metallurgical plant operations and the during process design stage. It covers all main metallurgical processes and it includes a huge database with more than 28 000 species used in chemical and metallurgical industry (Outotec, 2016). The main objective of this thesis was to evaluate how experimental flotations with different ore blends will correspond to the current kinetic models of HSC Sim simulations for different ore blends. The work included simulations with HSC Sim and lab-scale flotation tests with different ore types and blends. The comparison was made between the results of HSC Sim modelling and flotation test work. The number of tests performed was 16 with four different ore samples and in various combination ratios of ores.

There was an urgent need for this study because mining companies blend ores without necessary knowing how ore blends act in the flotation process. The topic of the thesis is unique so far because nothing comparable wasn´t done before. Results of the thesis are promising, and results correlate quite well.

The work started with grinding calibration tests to evaluate suitable grinding times for flotation tests. After grinding tests, rougher and cleaner kinetic tests were carried out for each ore. The main object of this research was to validate HSC software ore blending models with empirical test work.

The validation itself was done by comparing the results of feed analysis and back-calculated grades of elements and minerals in flotation tests. Rougher and cleaner flotation test was done for all reference ores and ore blends. Back-calculated feed grades are compared to mineralogical analysis results, this aspect gives more reliability for flotations done in this thesis. The most important factor for validation is compared results between experimental flotations and HSC simulations.

2 THEORY

Theory chapter gives fundamentals of geometallurgy, flotation, flotation modelling and plant designing approaches. Geometallurgy part introduces what is *Geometallurgy* and how it could be used in production and concentrator plant process design. Geometallurgy is a cooperation field for geologists and mineral processing engineers, and it occurs virtually in all mining operations. Predictive geometallurgy is a modern way to operate today mining projects. Predictive optimization of ore processing is based on automated mineralogy and characterization of ore. Creating of a predictive geometallurgical model requires also metallurgical test work campaign (van den Boogaart and Tolosana-Delgado, 2018).

Flotation theory section gives fundamentals of froth flotation that plays a key role in this thesis though. What are the most used reagents and what is needed to reach for optimal flotation performance.

Flotation circuit modelling is theoretical, and it is based on the kinetics of each particle in flotation conditions. Flotation simulation section introduces the theory behind different simulation models. Flotation modelling is a big part of the concentrator plant designing project and plant design sector showing the stages of an average project. Sulfide flotation has an own chapter including the most frequent flotation methods in the mining industry. Flotation itself is a widespread topic, so only more important approaches are presented more detailed in the theory chapter.

The validation of models is the most important output of this thesis. Validation method theory is presented in the last part of theory section. This section introduces the most important terms and different validation techniques used in model development and certification. Simulation models are used for decision making and problem solving and therefore they should be reliable.

2.1 Geometallurgy

Geometallurgy gives a quantitative understanding of the geological and mineralogical perspective of ores and combines this information with minerals processing and economics of valuable metals in minerals. Geometallurgy approach gives the opportunity to optimize the net present value and manage the mine plan online. Metallurgical recovery, ore loss and dilution are major variables during the determination of mine profitability.

Geometallurgy can be found also as mathematical geoscience because geometallurgical models are mathematical models based on geosciences like geology and mineralogy. The aim is to optimize and control the metallurgical performance even if geological variability is taken place. To keep the performance stable, models require information of ore deposit such as comminution energy, liberation, shape of particles, product recovery, hardness of ore, size reduction and concentrate quality. At today´s situation where ore bodies are more complex, and grades are getting lower is more important to develop predictive modelling. Mineral processing requires more knowledge and understanding of the ore's mineralogy. What the feed contains and what is the texture and shape of particles will be more important. (Andrea and Lopera, 2014; van den Boogaart and Tolosana-Delgado, 2018; Dominy *et al.*, 2018).

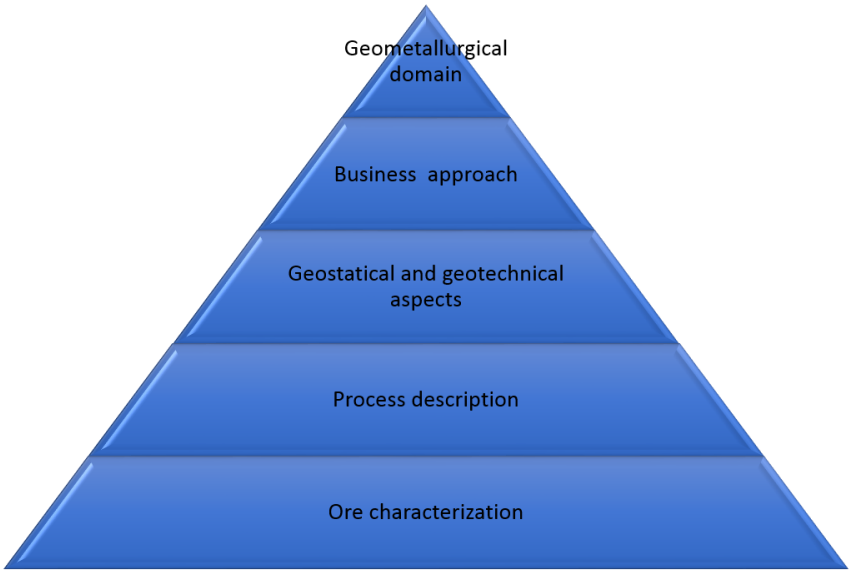

Figure 2. Geometallurgical approach of model development. (Lund, 2013)

Lund (2013), defined the geometallurgical concept as it is shown in Figure **2**, to cover main points while building the geometallurgical model. Ore characterization and process description are internal factors to cover single deposit outcome. Particularly the first one is the basic level factor and important for the model building process. Next metallurgists must cooperate with geologists to define the second level. Before a process definition, laboratory work should be carried out extensively. Top three sections cover external factors and what outcome scenarios model will have. These external factors define especially financial fluctuations in the global market. Geometallurgical domains are homogeneous regions or blocks in the block model with different processing properties like grindability or certain mineral recovery to concentrate. Determining a single geometallurgical domain for block model is straightforward. Combining geometallurgical domains together in the same mine plan is a complex engineering challenge and based on Lund (2013), we can´t be sure of that is even necessary for the model building. (Lund, 2013; Rajabinasab and Asghari, 2018)

Block modelling is an important part of mining projects pre-feasibility and feasibility study. The 3D block model is spatial, and it performs volumetric of each block and it is used to evaluate the value of an ore deposit. Geologists decide the geometry of orebody based on geological data from drill core samples. Ready-made model is created in XYZ grid system and each block has a uniform size. Each ore block can have its own value of grade, tonnage and other geological variables. Mining companies are doing drilling during exploration and possible later during the production phase. When there is enough data and drilling plan is comprehensive, a 3D block model is possible to create. Drilling plan should cover the whole orebody and all different ore variations inside the deposit. Databases from drill cores are created with quantitative and qualitative information. Many different companies have created tools which creates 3D block models for mining companies use. These 3D block models can perform many different variables from each block to support mine planning. Figure **3** represents a 3D block model of Chilean deposit including two pits, Alice and Productora. Each block has a certain color, which illustrates the Bond Work index. Block model like this can be used in mine planning to find an adequate grindability value for concentrator feed. (Geostat, 2018; Roy, Ground and Board, 2016; King and Macdonald, 2016)

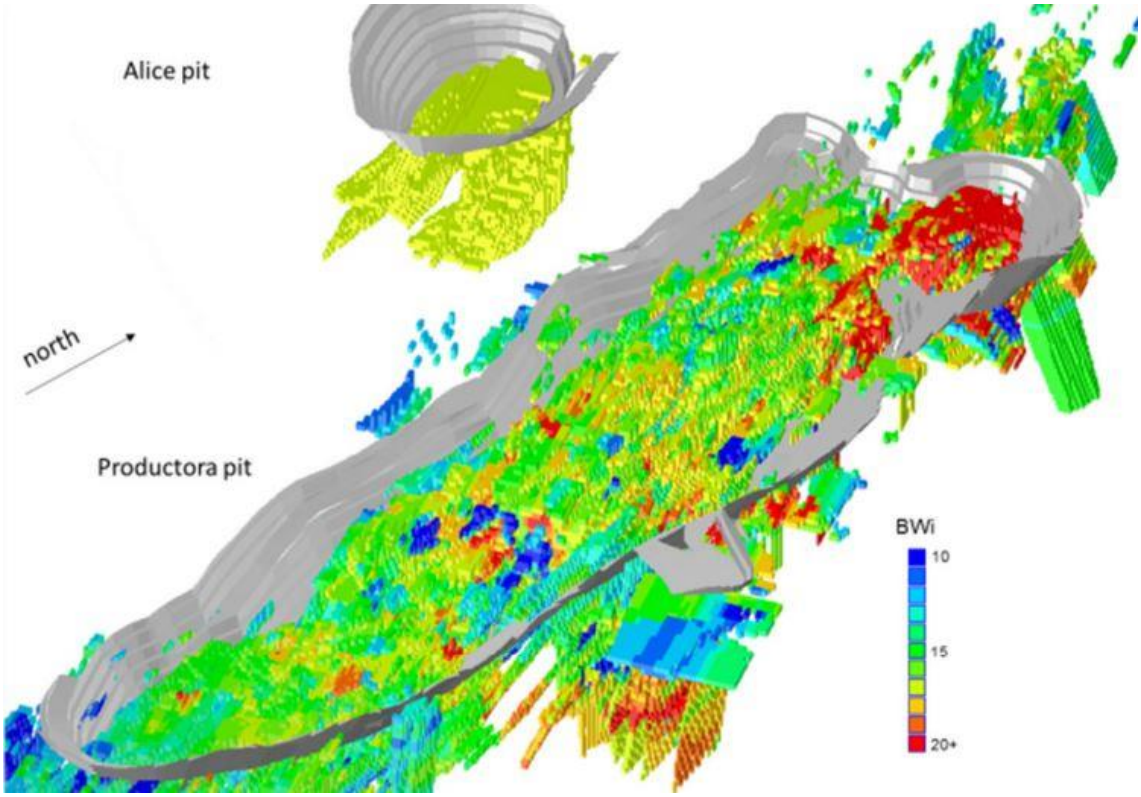

Figure 3. 3D Block model of Chilean deposits, including Bond Work Index of each block. (King and Macdonald, 2016)

Geological 3D block model can tell what the grade of valuable metal is and how much there are valuables in kilos or tonnages. This way it is easy to calculate the value of each block and later, the value of orebody. When these block models are developed further, they could be called a geometallurgical model. Geometallurgical model will be more useful because it gives an estimation of the operational costs of each block. Factors affecting operational costs and overall costs are especially the concentration of penalty elements, throughput rates, processing costs of a certain block and metallurgical recovery. Concentrator throughput rates are dependent on mostly the hardness and grindability of the ore in each block. If the ore is hard or resilient the grinding residence times are longer and throughput rates lower. This means that ore will stay longer in the grinding circuit and throughput rates are lower. When this is happening also concentrate mass flow is lower and temporal cash flow decreases. When grinding energy stays at the same level but grinding circuit throughput decrease that means grinding energy per

processed ore (kWt/h) increase. It also has a negative impact on processing costs. (Dunham and Vann, 2007)

Geometallurgical units can be used to define the variability in ore feed and process design will be based on those units. If orebody includes many different ore types which are behaving differently in process, flowsheet possible needs to the blending of different ore types. Processing is very complicated to control if ore type changes a lot. It is possible to design a flowsheet that can process different kind of ores, but capital costs usually increase higher. There are different solutions for this problem, for example at Outokumpu mine in Kemi, there are two different concentrate types, lumpy and fine concentrate. If processed ore is hard, grindability is low and chromite grade is high it is economic to do lumpy concentrate because there is no reason to grind ore too fine. If chromite grade is lower and ore is softer, they will grind it more and mass flow of fine concentrate will increase. Geometallurgical model is based on data from drill core and variables are host rock type, alteration, grain sizes, sulfide grades, metal ratios, texture of minerals, metal grades and structural geology. The list is long about what is affecting to metallurgical performance, but the recovery of each ore type is one of the biggest impacts to cash flow. (Lotter, 2011)

Accuracy of a geometallurgical model depends on two major aspects. Representative sampling is first because all mineralogical and geological data are based on drill core samples. Sampling is expensive, so geometallurgy team should calculate how many samples are needed and how samples are used as beneficial as possible. If a model is made for a Brownfield project, samples from the existing process are used. In cases where random sampling is required, Gy´s sampling models are often used. Different sampling methodologies are used to estimate the minimum amount of sampled ore. (Lotter, 2011)

Geometallurgical model development work starts with the sampling campaign plan. The plan includes how drilling is performed and how many drill holes are required to cover the whole orebody. The sample should cover representative chemical and mineralogical composition. Thus, ore units vary in different locations of the orebody, the drilling should be extensive containing ore from all parts of the deposit. Considering the test

work, drill core samples should represent variations within the ore body. Then each sample should be tested separately and so cover all variations in metallurgical performance. (Wills and Napier-Munn, 2006)

Collahuasi´s geometallurgical model for grinding circuit is a good example of succeeded model design for existing concentrator plant. During Collahuasi´s project, the team used two different drill core types (diameters of 85mm and 65mm). Core logging and sample description were done in every two meters of each drill core. During core logging, geologists gathered data package that included, logging lithology, alteration, structures, mineral zonation and geotechnical parameters. Conclusion and feedback of this geometallurgical model were very positive. They were able to forecast accurately production rates of the grinding circuit. Modelled and observed treated ore throughputs were close to each other with only 5.2% relative error calculated. This verifies how precise the model was and it can be used as a reference during model development projects. (Alruiz, O *et al.*, 2009)

Like it is said drilling is expensive, so it should be optimized. Metallurgical test work is also expensive and often mining companies save too much during test work campaign and it might become a fate for the company. Essential test work is needed to determine flowsheet and reagents, size of the plant and equipment for certain throughput. Designing the flowsheet and defining quantitative data is also required. Laboratory scale tests ensure the basics of process engineering to perceive the plant. If laboratory tests are confident, the next step is to carry out pilot scale tests to provide more data on continuous process and controlling parameters. Different companies like Outotec do such test works. During process design, comprehensive metallurgical test work is very necessary to find successful flowsheet. It depends how wide the geometallurgical model will be, does it cover only grinding or flotation circuit or both. (Wills and Napier-Munn, 2006)

Grinding circuit modelling requires information about ore hardness and grindability. Normally circuit design demands large-scale testing campaign that requires sample material of 5-200kg and testing is also a very time-consuming procedure. Typical tests used are Drop Weight Test, SMC Test, Rotary Breakage Test and Bond Work Index.

Because tests cost a lot and take time, the testing program should be optimized. In all comminution tests, the idea is to assess, how much the particle size reduction is occurring and how much it requires grinding energy. (Mwanga, Rosenkranz and Lamberg, 2017) developed small scale batch test, Geometallurgical Comminution Test (GCT) which requires only 220g of sample. GCT uses modified Bond equation together with a linear correlation factor. (Mwanga, Rosenkranz and Lamberg, 2017) pointed out that GCT is proofed with several different ores. (Andrea and Lopera, 2014)

When engineers and geologists created the geometallurgical model for Collahuasi deposit grinding circuit, they used JK Tech drop-weight test, SMC test and Bond Ball work index. The deposit was divided into six different geometallurgical units and tests were done with all methods. Different tests give different variables. JK drop-weight and SMC test give parameter A*b. A and b are ore breakage parameters. Parameter A means the maximum fragmentation of certain ore and parameter b represents the hardness of the ore (high value means softer ore). Bond work index output is in kWh/t so it performs straight how much grinding energy is consumed in certain unit. Unit or ore density is very usual measured variable in these test works. After the test work campaign, there are different values for geometallurgical units and it can be seen what unit consume most grinding energy or how much is theoretical throughput of the unit. When there is enough data from each unit it is possible to add geometallurgical information to the model. (Alruiz *et al.*, 2009; Saeidi, 2016)

2.2 Froth flotation

"No other single discovery made so much metal available", Frank R. Millikan in 1961.
Flotation is the most used beneficiation technology in the mining industry. Regarding to flotation, the earliest patented invention is from 1860 and today, there are still many researchers doing research on flotation. Mechanical, chemical and physical approaches are all important trends to develop the flotation process further. The economic significance is huge because in relation to other beneficiation technologies, it is a very feasible method. (Hukki, 1964)

Since flotation is a selective process, it allows separating different valuable minerals from complex ore. Sulfide and oxide minerals are the most commonly floated mineral groups. Both are possible to beneficiate with flotation, but processes differ from each other, especially from reagent side. (Wills and Napier-Munn, 2006)

Flotation is a physico-chemical beneficiation process and it is based on how different particle surfaces are behaving in complex liquid-solid-gas surroundings. Mineral particles are attached to air bubbles in an aerated pulp. Aim of flotation is that the particle containing valuable mineral get to the concentrate flow which is usually the overflow of the flotation cell (Figure **4**). Successful flotation of valuable material occurs if one or more of the following mechanisms is realized:

1. Selective attachment of material and air bubbles often is referred as “true flotation”
2. Material entrainment in the water which passes through the froth
3. Physical entrapment between particles in the froth attached to air bubbles often referred as “aggregation”

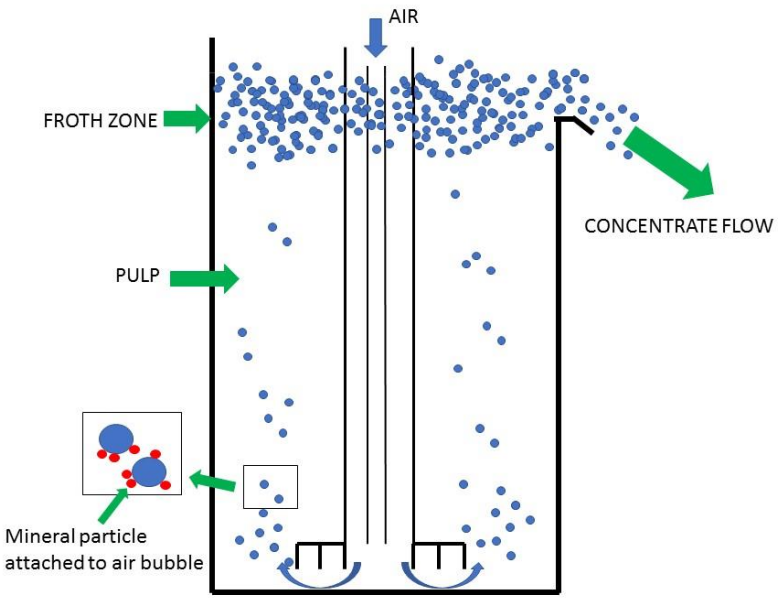

Figure 4. Principle of froth flotation. (Wills and Napier-Munn, 2006)

The selective attachment of particle containing valuable mineral is most often a manner to reach flotation target. But usually, all these three mechanisms are occurring partly. Gangue and valuable materials can both enter to concentrate because of entrainment or entrapment. Therefore, it is not possible to recover all gangue particles to tailings and all valuable particles to concentrate. Flotation depends on features of particles. If the particle surface is hydrophobic, it means it can be attached to air bubble. Some minerals are naturally hydrophobic but usually, *collector* chemicals are used to change particle surface from hydrophilic to hydrophobic. True flotation is expressly used to recover valuable minerals to concentrate. Reverse flotation is seldom used for sulfide ore, but more common for iron ores. It means that concentrate goes to underflow, this requires that gangue is hydrophobic, and it will go to overflow with air bubbles. (Wills and Napier-Munn, 2006)

2.2.1 Flotation reagents

Mining and hydrometallurgical industries use different inorganic, organic and synthetic organic reagents for flotation and solid-liquid separation processes. Many reagents are toxic and harmful for the environment but nowadays most of the reagents have a good response for technical and environmental requirements. Most of the reagents are added to flotation feed during the conditioning process. Conditioner is a tank where reagents and pulp are agitated strongly. Some reagents are added already to the grinding mill to have better adsorption to the mineral surface. Lime and sulphuric acid are the highest volumes used in the mineral processing industry. Lime is especially for pH adjustment, coagulation and heavy metal precipitation. Sulphuric acid is also for pH adjustments but also for leaching of heavy metals in hydrometallurgical processes. (Pearse, 2005)

2.2.2 Collectors

A collector is the most important reagent in flotation systems. Collector chemicals adsorb to the surface of the valuable mineral particle and chance the surface from hydrophilic to hydrophobic. Adsorption reduces the stability of the hydrated layer that is between the mineral surface and an air bubble, so attachment is possible when particle and bubble collide (Wills and Napier-Munn, 2006). The efficiency of flotation depends on the activity of minerals surfaces. Activities can be called as different forces like

physical or chemical forces. Both use the reduction of free energy of the system and the production of heat. Flotation reagents can change these forces to the wanted direction. These forces can be performed also with the contact angle between the mineral surface and bubble surface, Equation 1 present the equilibrium:

$$\gamma_{\frac{s}{a}} = \gamma_{\frac{s}{w}} + \gamma_{\frac{w}{a}} cos\theta \qquad (1.)$$

where γ values are surface energies and θ is the contact angle (Figure **5**).

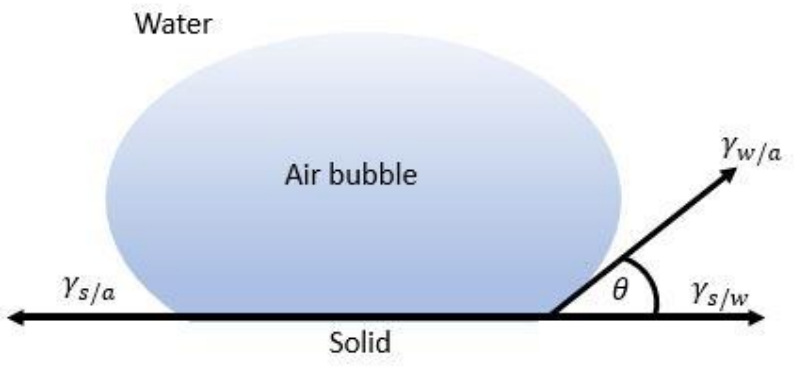

Figure 5. Contact angle between air bubble and particle. (Wills and Napier-Munn, 2006)

Collectors can be divided into ionizing and non-ionizing groups. Non-ionizing collectors are not soluble to water, so they create a thin film around the mineral particle. Ionizing collectors are mostly used and those can be divided into anionic and cationic groups. Anionic collectors can be divided again depending on the type of the polar group. Polar group adsorbs on the mineral surface and non-polar group adsorbs on the gas bubble. Polar group collectors are in some of the following groups: xanthate, cationic amine, phosphate, sulphonate, anionic sulphate, carboxylate or non-ionic oximes. Adsorption of mineral surface and collector is physical or chemical depending on the chemistry between them. Chemisorption is usually the wanted mechanism in flotation. Chemisorption is stronger and more stable than physical adsorption. (Lukkarinen, 1987; Wills and Napier-Munn, 2006)

The concentration of collectors is meaningful because if it is too low there is no reactive collector for all particle surfaces. If the concentration is too high, collectors can create multilayers reducing the particles hydrophobicity and decrease the recovery and selectivity. It is possible to use more than one different collectors because everyone has their own advantage. (Wills and Napier-Munn, 2006)

Xanthates (Figure **6**) have been used in flotation since 1923 and it is the most used collectors with dithiofosfates (Aerofloats). Xanthates are derivatives of carbonic acid. Xanthate is prepared by reacting an alkali hydroxide, an alcohol and carbon disulfide. The xanthates are mostly used for sulfide flotation processes. (Rao, 2004; Wills and Napier-Munn, 2006)

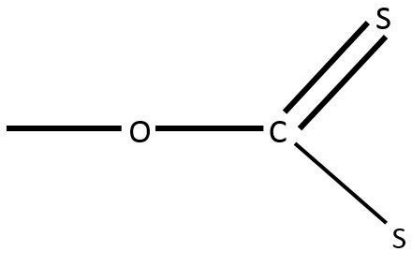

Figure 6. Chemical structure of Xanthate. (Wills and Napier-Munn, 2006)

Dithiofosfates (Figure **7**) are relatively weak collectors but they are often used with xanthates. However, they are effective and selective collectors for copper sulfide minerals. Dithiophosphates are prepared by reacting certain alcohols and sodium hydroxide with phosphate pentasulfide. (Wills and Napier-Munn, 2006; Rao, 2004)

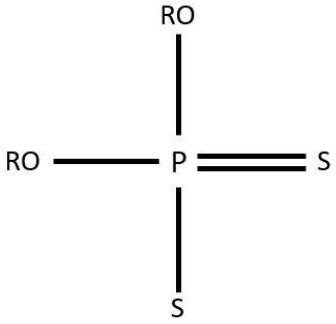

Figure 7. Chemical structure of Dithiophosphate. (Wills and Napier-Munn, 2006)

Fatty acid collectors (Figure 8) are carboxylic acids with a long hydrocarbon chain. Hydrocarbon chain is the hydrophobic element and polar carboxyl group is the hydrophilic element. Usually, fatty acid collectors have also the feature to create froth, so separate frothers are not necessarily needed. Phosphate and fluorite flotation processes are the main user of fatty acid collectors. Fatty acids require usually alkaline conditions, so flotation circuit or fatty acid are prepared by adding caustic soda. Fatty acids are mixtures of carboxylic acid which are extracted as raw materials, vegetable and animal fats and oils. (Pearse, 2005)

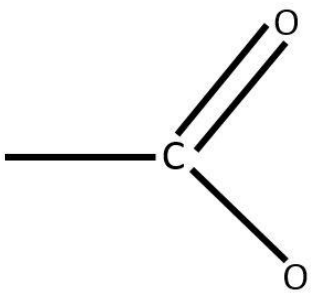

Figure 8. Chemical structure of Fatty acid. (Wills and Napier-Munn, 2006)

2.2.3 Frothers

Frothers are added to create stable froth to carry out hydrophobic mineral particles to concentrate flow. Stable froth occurs if air bubbles will not coalesce and stay separately. Weak froth stability can be the reason for inefficient flotation performance. A good froth is reached if it is strong enough to transfer mineral particles to launder but at the same time, it should last only until froth reaches the launder and the further handling, like pumping. (Wills and Napier-Munn, 2006)

Frothers are heteropolar organic reagents and those can be adsorbed on the air-water interface. The main mechanism is to reduce the surface tension of water to form a stable air bubble. It must be highly soluble to water unless it would distribute unevenly to slurry. Frothers consist of hydrocarbon and one or more polar groups. Frother includes

one carboxyl, carbonyl, amino, hydroxyl or sulfo group and alcohols (-OH) are mostly used. Alcohols have not collector features unlike carboxyls what can decrease collector dosage in selective flotation. Amino and sulfo group frothers have only weak collector features in flotation systems. (Wills and Napier-Munn, 2006)

Bubble size and froth stability have an impact on increasing flotation kinetics. When bubble size is decreasing, flotation rate constant increase. The reason is that smaller bubbles have a longer residence time in the cell and flotation probability will increase. Some frothers have a feature as being also a collector. The hydrophobic feature is not that strong to act alone as a collector, but the dosage of the collector can be lower if frother has a hydrophobic feature. (Rao, 2004)

2.2.4 Modifiers

Modifying agents are often used in flotation circuits. Modifiers are divided into several groups such as dispersants, activators, deactivators and depressants. Activators are compounds that promote the action of collectors. Collectors might not interact with the mineral surface if it is not pretreated with an activator. If adsorption with collector and some unwanted mineral surface is occurring, the mineral has to be treated with deactivator to offset adsorption. Depressants are reagents that prevent the action of collectors to adsorb within the mineral surface by changing hydrophobic surface to hydrophilic. Like deactivators, depressants can be organic or inorganic compounds. Rao (2004) listed the principle effects of modifying agents:

1. Control of the pH
2. Control of the competing ionic species concentration
3. Change the mineral surface by chemical reaction
4. Adjust the charge density
5. Modify the oxidation states
6. Metallic ions concentration controlling

Controlling pH value is possible to modify the charge density or zeta potential in the pulp. This way it is possible to control the adsorption of the surfactants in the flotation system. The challenge is to find a balance between, mineral surfaces, collector

concentration and concentration of ions in the flotation pulp. In dynamic flotation conditions, it is difficult to achieve a stable pH level. Ore feed is changing, and the concentration of ions is varying all the time. Usually, in concentrator plants, favorable pH range is determined, and it is controlled by using pH regulators (such as lime). This allows so called selective flotation that means individual minerals are possible to recover in different pH ranges. One common usage of pH control is depressing pyrite in sulfide flotation in ranges of high pH value >11. (Rao, 2004)

Dispersants are reagents which minimize heterocoagulation/aggregation between fine particles. Tackling this phenomenon, higher selectivity is reached. Sometimes fine particles are covering coarser particles and thus reduce their floatability. Dispersants are usually inorganic compounds. Some organic polymers are also used but those are not very efficient. These reagents are based on low molecular mass polymers of sodium polyacrylate. Besides flotation, applications for dispersants are the dispersion of kaolin, ceramic industry and modification of rheological properties. (Rao, 2004; Pearse, 2005)

Flocculants and coagulants are also reagents to improve (flocculant) improve or prevent (coagulant) agglomeration. Flocculant effect is based on long chain polymers to form bridges between particles to form agglomerates. Flocculant is usually utilized in thickening and filtration processes. Coagulant effect is based on the electrical charge of the particles. Coagulants have opposite charges than particles and thus neutralize charge density. When conditions are neutralized, particles may adhere to form agglomerates. (Wills and Napier-Munn, 2006)

2.2.5 Flotation technology

Concentrators are complex processes and can include unit processes which pre-treat grinding or flotation feed to simplify the flotation process. Desliming and sorting are both good examples of that. Successful flotation requires a relatively fine particle size of the ore (<150µm). Optimal particle size depends on the mineralogy and texture of the ore. Optimum particle size is usually studied with laboratory size-reduction tests and mineralogical characterization indicating the size of the particle providing the best degree of liberation and flotation performance. Particle sizes between 10 µm to 100µm

are usually target for flotation. Recovery losses to tailings are often caused by coarser or finer particles in the flotation feed. (Wills and Napier-Munn, 2006)

Suitable grinding provides an optimal particle size for flotation. The optimal particle size can be determined by knowing the size of particles after crushing and mineral liberation analyses. The optimal particle size after primary grinding should be enough to ensure acceptable grade, recovery and flotation time in the rougher stage. Re-grinding or secondary grinding are used for middling concentrate or tailings to increase liberation in certain flotation stage. Operational costs are highest in grinding, so optimizing all size reduction processes in concentrator provide savings of costs. (Wills and Napier-Munn, 2006)

Bubble-particle collision, attachment and detachment all are involved to proceed efficient flotation performance. There is a certain probability for each of these and particle and bubble sizes are variables for these probabilities. According to Schubert, (1999) it is not possible to determine optimal hydrodynamics for all particle sizes at the same time. Optimum flotation efficiency for coarse particles is the power input which must be minimized. Optimum flotation for fine particles means large collisions between particle and bubbles should be appearing. (Schubert, 1999)

Flotation machines can be divided into two groups, mechanical and pneumatic flotation machines. Mechanical is more used and pneumatic is possible to use only in few applications. Flotation cell is a container where reaction or process comes up. The major task of a flotation cell is to create gas-liquid dispersion and agitate flotation feed slurry through the entire cell. Air or some other gas is fed to the bottom of the cell where air bubbles and minerals get in touch with each other. Air bubbles with attached mineral particles, rise up and create froth layer on top of the cell. Froth or concentrate are then flowing to launder and then to pump sump. (Hukki, 1964; Kelly and Spottiswood, 1982)

A flotation circuit (Figure **9**) consists of multiple flotation machines and each of them have their own function. Term *flotation bank* means a series of flotation cells in a row. After grinding circuit, flotation feed is led to conditioner where reagents are added, and pulp is agitated strongly. From conditioner, flotation feed goes to the first bank called

rougher flotation. In this phase, the pulp contains many hydrophobic particles and mass pull to concentrate launder is high. Tailings of rougher bank enter to *scavenger* bank. In the scavenger stage, the pulp contains middling particles and the concentration of valuable particles is lower. The purpose of scavenger is to increase recovery of the flotation circuit. Tailings of scavenger are final tailings and valuable minerals recovery to final tailings should be as low as possible. Concentrate of scavenger bank is usually circulated again to rougher flotation. Concentrate of rougher flotation enters to *cleaner flotation* where the aim is to increase the grade of valuables in final concentrate. Commercial plant includes usually at least one or more cleaning stages to reach enough high-grade concentrate. Tailings of each cleaner banks are re-circulated to the rougher bank and earlier cleaner banks. (Wills and Napier-Munn, 2006)

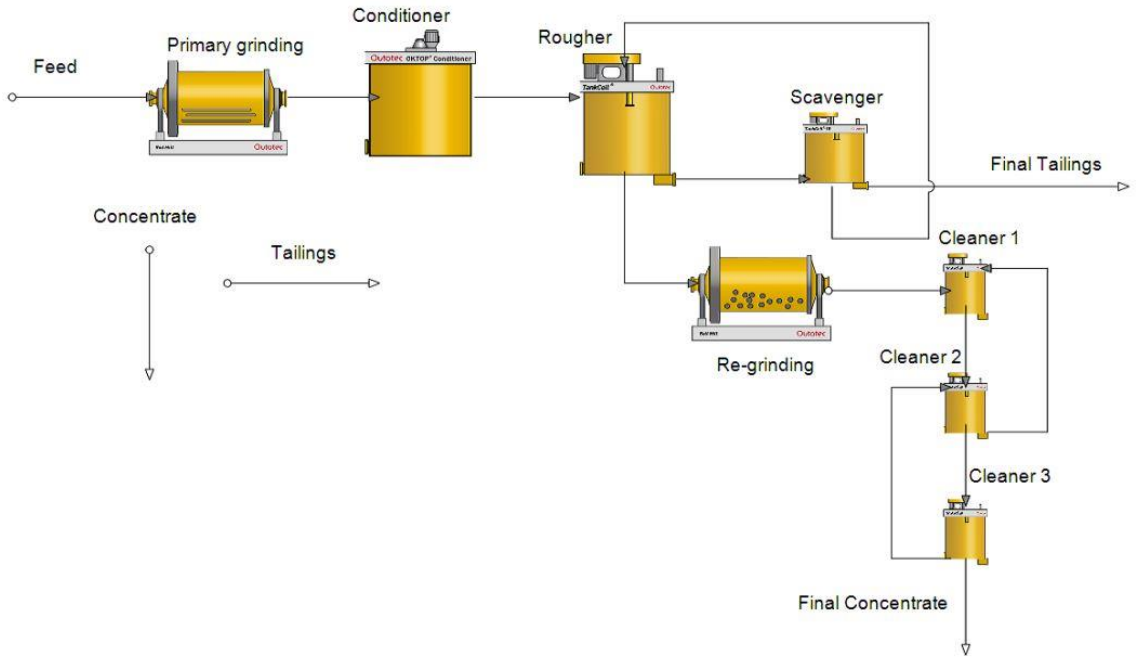

Figure 9. Example of a basic flotation circuit.

2.3 Copper sulfide flotation

Flotation of sulfide minerals is widescale and concentrate tonnages are largest in the metallurgical industry. One metallurgical challenge is to maximize the sulfide recovery while minimizing the recovery of gangue minerals. Selective collectors are selected to reach maximum flotation performance, but for example. Copper sulfides are floated using xanthates and dithiophosphates. Sulfide ores have multiple structures and those make complete utilization in their exploitation very difficult. All components should be extracted differentially for further processing. Sulfur, usually carried mainly by pyrite, may be presented in very large amounts in ores. Pyrite or pyrrhotite can be defined as a gangue mineral or it should be extracted to independent concentrate. (Wills and Napier-Munn, 2006; Glembotskii, Klassen and Plaksin, 1963)

There are over 170 copper-bearing minerals identified but only 10-15 are common and commercially exploited in the industry. Different copper minerals may occur together in the same ore. There are many similarities to float all these minerals, but differences affect the flotation of those. Differences are reaction with oxygen, collector and regulator chemistry and optimum pH value for flotation. Individual copper sulfide concentrates could be extracted by utilizing activators and depressants, creating appropriate alkalinity and producing slime peptization. Selective flotation is used for differential separation of copper, zinc, lead, pyrite concentrates and others. Copper ore flotation technology becomes even more complicated when ore contains oxidized copper minerals of various compositions. Pyrite often includes other precious metals such as gold, silver, cobalt and nickel but also impurities such as arsenic. These inclusions have also effect on the flotation performance and must be taken into account in the design stage. (Glembotskii, Klassen and Plaksin, 1963)

Chalcopyrite ($CuFeS_2$), chalcocite (Cu_2S), pyrrhotite (Fe_nS_{n+1}), arsenopyrite (FeAsS), pyrite (FeS_2), galena (PbS), sphalerite (ZnS), bornite (Cu_3FeS_3), covellite (CuS) and rare metal sulfides like molybdenite (MoS_2) are most important industrial sulfide minerals. (Glembotskii, Klassen and Plaksin, 1963)

Chalcopyrite is the most known copper mineral and it is usually a primary sulfide. Like chalcocite, chalcopyrite is sensitive for overgrinding. Pyrite, pyrrhotite, sphalerite and galena are all commonly associated with chalcopyrite. The chalcopyrite lattice breaks down at pH 10 value or more and it oxidizes at acidic pH value of 6 or less. Chalcocite alike, cyanide is possible to use for depressing of chalcopyrite. Covellite and bornite are both secondary copper minerals. Bornite flotation properties are close to chalcopyrite and chalcocite. Covellite is not extracted as an independent copper mineral because it is a minor copper carrier. (Glembotskii, Klassen and Plaksin, 1963)

Chalcocite could be primary sulfide but usually, it is secondary sulfide occurring with pyrite, chalcopyrite, bornite and covellite. Chalcocite may contain impurities like Ag, Fe, Co, Ni, As and Au. Selective chalcocite flotation is completed by depressing sphalerite and pyrite. Depression of chalcocite is possible by using caustic soda or cyanide. (Glembotskii, Klassen and Plaksin, 1963)

Collectors action with sulfide mineral is mainly similar for all minerals. Differences are occurring in chemical reactivities between minerals and nature of adsorbed species. All these variations are important to know while selecting conditions for selective flotation. For example, pyrite response for flotation is responsible for pH value of pulp (Figure **10**). For practical uses, pH levels above 10 enable the pyrite depression. Sodium cyanide is also used to depress pyrite by inhibiting the oxidation of xanthate. (Rao, 2004)

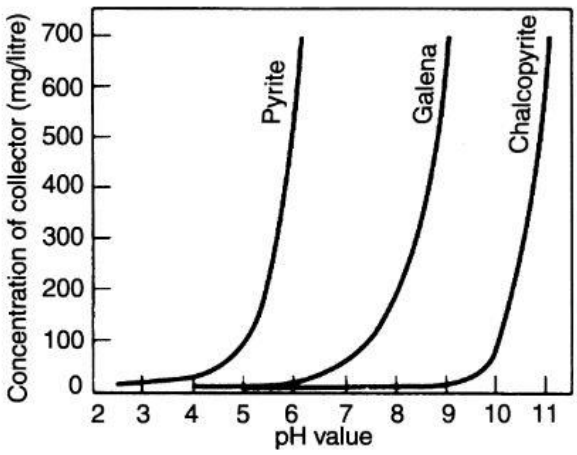

Figure 10. Critical pH value for pyrite, galena and chalcopyrite on the concentration of Aerofloat collector. (Wills and Napier-Munn, 2006)

2.4 Flotation of oxidized copper minerals

Besides copper sulfides, there are oxidized copper minerals such as malachite ($Cu_2CO_3(OH)_2$), crysocolla ($CuSiO_3xH_2O$) and cuprite (CuO) which could be extracted from ores. These minerals are not possible to recover easily like copper sulfide minerals. However, Glembotskii (1963) listed methods to float oxidized minerals:

- Sulfidising before flotation, carried out using suitable reagents like Na_2S or $(NH_4)_2S$
- Direct flotation, using carboxyl collectors. High recoveries, but weak selectivity.
- Flotation, using high consumption of xanthate. High operational costs and usually not feasible for production.
- Combination of hydrometallurgy and flotation treatment for oxidized and mixed copper ores, exploiting sulphuric acid solution to extract copper. Enable acceptable copper recoveries from difficult oxidized copper ores.

Extraction of oxidized copper minerals is challenging and often costs increase too high to implement a beneficiation project of certain ore. Regarding acid leaching, solvent extraction and electro-winning processes are working hydrometallurgical processes for oxidized copper minerals. The hydrometallurgical industry is developing and more such

as plants are built around the world. Again, we end up with the problem, that easy sulfide ore deposits are largely extracted, and industry must use more challenging ore deposits.

2.5 Flotation simulation

Laboratory test work is expensive, and it takes a lot of time. The simulation work will be more important and will be used more in the future because it is a faster and cheaper way to model flotation process. The simulation requires references from experimental tests, but a big work-load can be avoided with successful simulation and modelling. Even if flotation technology itself is well established there is still big work with quantitative predictive models that are used to simulate flotation process. Flotation includes many microprocesses that combines overall flotation unit process. Separation of different minerals and particles is challenging because of differential surface conditions of each particle. Next points should be filled to formulate quantitative flotation model (King, 2012):

- Correct chemical conditioning of slurry
- Differential hydrophobicity of all minerals
- Proportion of different mineral exposure on the surface
- Stable and mobile froth layer on the surface of the slurry

Almost all flotation models are based on that fact, flotation is a kinetic process. A model can be formulated in terms of flotation rate and based on the individual analysis of microprocesses in the flotation cell. Kinetic models for flotation are depended on several chemical and physical factors affecting to flotation rates of different minerals such as (King, 2012):

- Particle-bubble collisions
- Collision efficiencies
- Particle-bubble attachments
- Bubble loading during flotation
- Rise times of loaded bubbles

- Particle detachments
- Froth phase
- Breakage rate lamellar films
- Froth drainage through plateau borders

All these are possible to model but when approaching kinetics of batch flotation, simplified kinetic models are used. The following rate equations are describing homogeneous kinetics of flotation. Flotation rate is proportional to particle-bubble collision frequency and not relating to feed particle size distribution. This why first order model can be postulated (Gaudin, 1939):

$$\frac{dC_i}{dt} = -k_i C_i \qquad (2.)$$

where is C_i is the concentration of floatable mineral or element in the flotation cell at time t. The rate constant of floatable mineral k_i (1/min), also called floatability is in various time units. Integrating the Equation 2 to form the Equation 3. is used to calculate recovery, R as a function of time, (Lynch *et al.*, 1981)

$$R = 1 - e^{-kt} \qquad (3.)$$

this model assumes that maximum recovery will be 100%, so the Equation 3 was developed to the Equation 4 to be more realistic:

$$R = R_\infty(1 - e^{-kt}) \qquad (4.)$$

where R_∞ is maximum recovery and R is the recovery at the time t.

Equations 3 and 4 assume that flotation feed is homogeneous, and all particles have the same rate constant. Modifying these equations to be more realistic there should be the assumption that mineral particles have slow and fast flotation fractions to make a model of Two-component model. Three-component model counts that there are also non-floating particles in the flotation feed. When feed is distributed to fast, slow and non-floating particles Equation 5 is formulated for batch scale flotation:

$$R = m_f\left(1 - e^{-k_f t}\right) + m_s(1 - e^{-k_s t}) + m_n * 0 \quad (5.)$$

where m_f, m_s and m_n are representing mass fractions of fast, slow and non-floating material. Rate constants k_f and k_s represent floatability of fast and slow material. (King, 2012)

Klimpel model is assuming rectangular distribution and Equation 6 shown Klimpel model for batch scale flotation:

$$R = R_\infty \left[1 - \frac{1}{k_{max} t}(1 - e^{-k_{max} t})\right] \quad (6.)$$

where k_{max} is the maximum rate constant. Klimpel model assumes that rate constant is changing as a function of time, t.

Models above are based on batch scale and laboratory conditions. An added variable to the continuous model is the number of cells in a bank, n. Three-component model Equation 5 modified for continuous flotation is performed in Equation 7:

$$R = m_f \left(1 - \frac{1}{(1+k_f t)^n}\right) + m_s \left(1 - \frac{1}{(1-k_s t)^n}\right) + m_n * 0 \quad (7.)$$

Klimpel rectangular distribution model for continuous flotation is shown in the Equation 8:

$$R = R_\infty \left(1 - \frac{1-(1+kt)^{1-n}}{kt(n-1)}\right) \quad (8.)$$

2.6 Concentrator process design

Process design in mineral processing aims to create a plant with minimized capital costs and maximized long term profits. Also, minimization of project risks is an important aspect. Mining projects are known for high overruns of capital costs. A reason for overruns includes difficulties to evaluate how the true ore is behaving in the chosen process circuit, meaning how well the tested ore sample represents the true mill feed.

Another reason is the fluctuation of metal prices, this has straight effect to cash flow. Plant design project starts by engineering work and engineers design documents like process design criteria, flowsheets and many different drawings about plant and equipment. Process design criteria, mass balances and flowsheets are based on test work that has been done. Often this engineering work is based on experience of engineers and previous references. (Harbort and Quan, 2017)

Mining projects have faced historically plenty of errors and misinformation during the exploration phase. Inadequate evaluation of mineral resources and reserves is a very general topic in the mining industry. Flowsheet development for concentrator plants has evolved at laboratory and operation scales. The bases for a good process design are process mineralogy and representative sampling. Especially process mineralogy is key to find energy efficient grinding circuit and helps with flotation challenges. Also, successful scale-up requires comprehensive metallurgical test work program. Although limited budgets and demanding schedules worsen often the situations. The confidence of the sampling system must be clear, something that everyone in this industry field can agree with. Gy´s sampling model (Equation 9) is usually used when it comes to small amount of samples. (Lotter, Whiteman and Bradshaw, 2014)

$$\frac{ML}{L-M} = \frac{Cd^3}{s^2} \tag{9.}$$

where M is the minimum weight of sample required (grams), L is the gross weight of material to be sampled (grams), C is the sampling constant for the material to be sampled (g/cm^3), d is the dimension of the largest pieces in the material to be sampled (cm) and s is the measure of statistical error. The constant C is calculated using four factors which are shape (f), granulometric (g), mineralogical composition (m) and liberation (l). (Wills and Napier-Munn, 2006)

Geometallurgical model can be used for operating concentrator plant to have better results by optimizing process parameters according to the flowsheet. If concentrator start processing ore from other deposit they should survey how process parameters should be optimized to process ore blends or different ores. Soon concentrators are more and more exploiting ores from variable and smaller deposits. Deposits are getting more

complex regarding mineralization, lower grades, geology and more expensive mining and extracting. Another idea is to blend good and bad ore, that is why ore blending modelling is important to study more. When geometallurgical models are successfully used in an industrial plant, it is possible to forecast cash flow even more precisely. (Singh, 2017)

Outotec vision of geometallurgical test work procedure is presented in Figure **11**. This vision presents all important steps from sampling to ready-made geometallurgical model. The geometallurgical approach of process design and optimization should combine an operational model of each unit processes. Successful modelling tool provides the necessary flexibility to cover all kind of ores with any mineral composites. Models used, should include limitless amount of details and physical properties appearing in mineral processing.

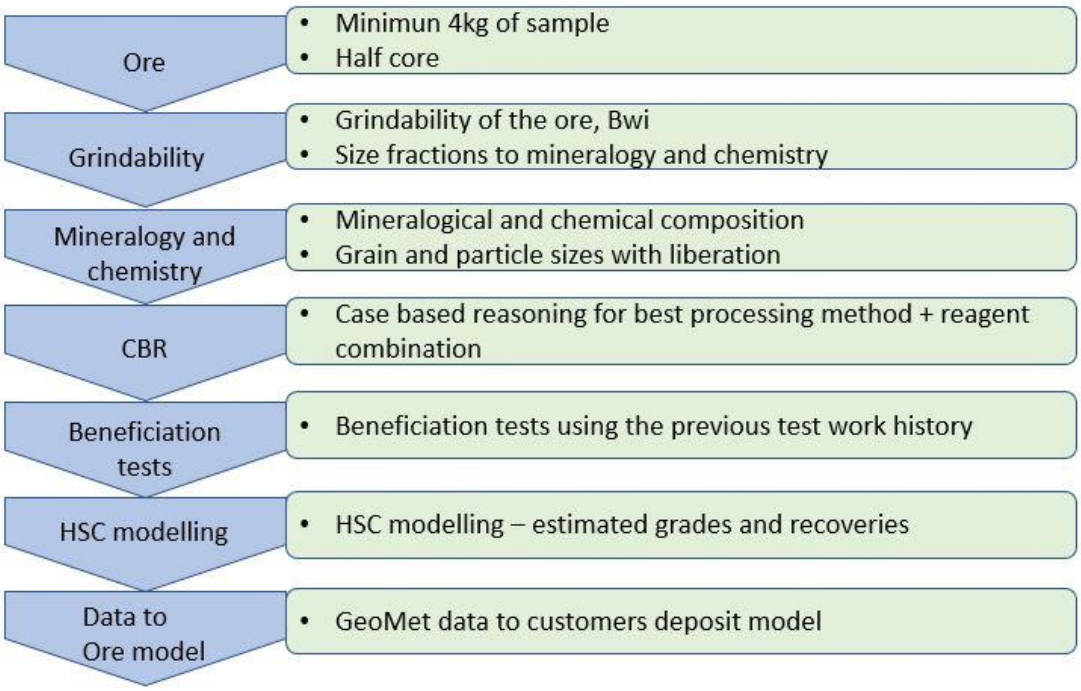

Figure 11. Outotec geometallurgical test work vision.

Figure **12** shows a simplified phase description of collected details for the model. Simulators are based on mathematical models of each unit processes they can manage diversities of material. In recent years, modelling in mineral processing is developed

from ore metal grades to modelling of different particles. Particles, including mineral grains, give a more accurate model to work with. To make the model more accurate, it's possible to add grain sizes to the model. This detailed data is not necessarily available if grain sizes are not determined. Models include a lot of data so creating and upholding one model needs plenty of working hours. Digitalization is developing every day so this aspect will easier the development of models. (Brochot, Gonzalez Fernandez and Durance, 2018)

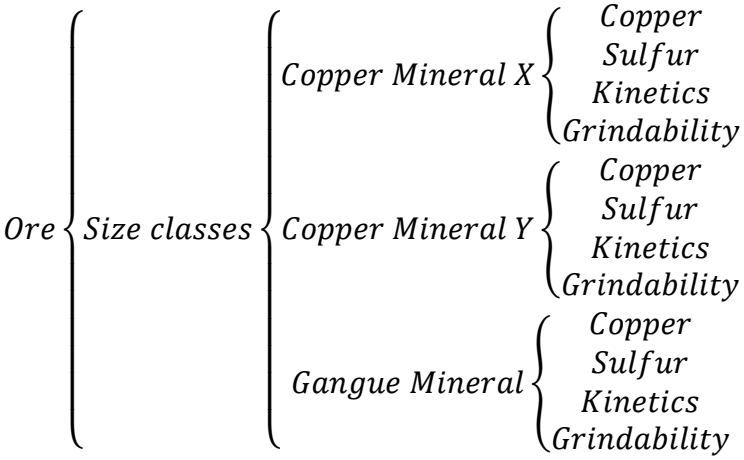

Figure 12. Ore advanced phase description. (Brochot, Gonzalez Fernandez and Durance, 2018)

2.7 Validation and verification of simulation models

Simulation models are becoming more used all the time. Models are used in problem solving and decision making, to make people´s life easier. People and stakeholders who are making decisions or are otherwise affected by model results keep asking if the model results are correct or not. At this point, the concern is the verification and the validation of a certain model. Commercial models need to be credible and developers want to be sure that confidence of the model is enough. If the model is answering various questions, the validity of the model has to be determined. (Sargent, 1998)

Conceptual model performance should be compared to real world system output. If the comparison is at an acceptable level, the comparison is valid. But if the comparison is false, it is invalid. Verification is another important term and it means that two or more results can be used to verify the accuracy level of real-world system or model results. Accepting the verification, results should be enough accurately to valid the model. Validation and verification (V&V) are two important steps in any model development. Graphical performance of model validation and relations between terms are shown in Figure **13**. The conceptual model meaning is all mathematical modeling data and equations to model processes. Meaning of the computerized model is an operational computer program that exploits the conceptual model for simulation process. (Oberkampf, Trucano and Hirsch, 2002)

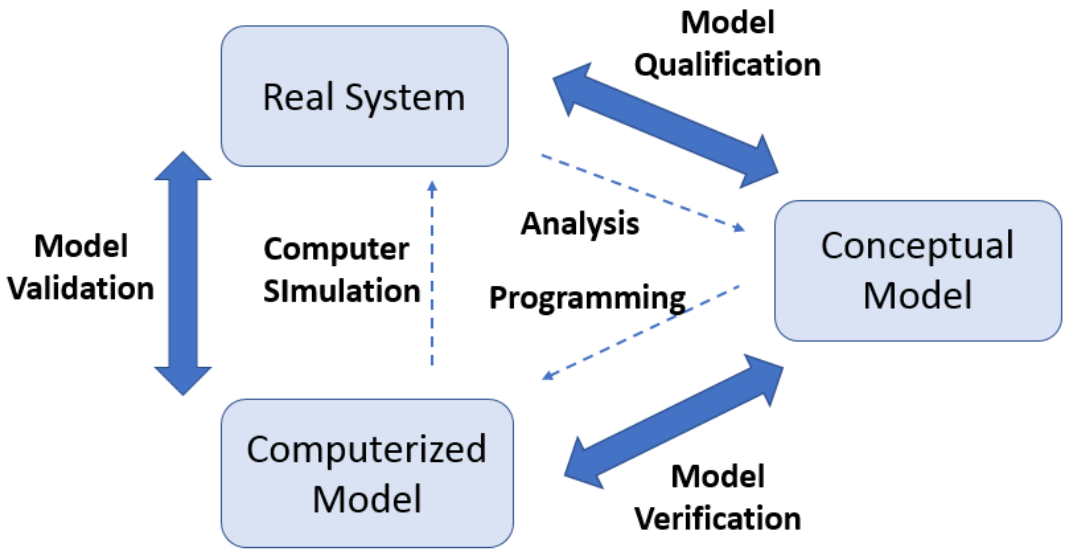

Figure 13. Phases of modeling and simulation validation and verification. (Schlesinger, 1979)

Sargent (1998), listed several validation techniques for different needs;

- *Animation,* model´s operational behavior is presented graphically as the model moves through the time

- *Comparison to other models,* using the same input for other models that have already validated
- *Degenerate tests,* model´s degeneracy testing by selecting appropriate values of input and internal parameters
- *Event validity,* events occurrences of the simulation model are compared to the real system to determine if they are similar
- *Extreme condition tests,* model structure and output should be workable for any unlikely combination of inputs though
- *Face validity,* exploiting knowledgeable people and asking if the model behavior is reasonable, for example, is the model input-output relation correct
- *Fixed values,* the method uses various model input and internal variables and parameters. Checking model results against calculated values.
- *Historical data validation,* if data is existing, it can be used for the model building or determine how model works
- *Historical methods,* these used methods are rationalism, empiricism, and positive economics
- *Internal validity,* many runs of a stochastic model are run to determine the amount of stochastic variability of the model
- *Multistage validation,* is a combination of historical methods, rationalism, empiricism and positive economics
- *Operational graphics,* values of variable performance measures
- *Parameter variability-sensitivity analysis,* different values of input and internal parameters to evaluate model behavior and output
- *Predictive validation,* comparison of system behavior and model's forecast
- *Traces,* behavior of different specific entities in the model is determined
- *Turing tests,* knowledgeable people discriminate operations between system and model output

So, there is a long list of specific methods named. Many times, more than one method is used for validation. Next, there are important steps that should be done notwithstanding the technique used in the validation. First, it is important to familiarize with the model, how it is working and what calculations it is based on. There should be a system

developer or expert who supervise the use of the model. Next step is to use the model with different input assumptions. Quantitative testing of the model is important to learn how it responds to variation in inputs. There should be specified accuracy required to have a successful validation. Accuracy must be determined with the model development team and sponsors. (Tutorialspoint, 2019; Sargent, 1998)

Next step is to determine how representative the output of the simulation model is. Real system output and simulation model should be on the same page or in a diagram to evaluate how close results are from each other. Comparison can be done using the Turing test, that means knowledgeable people can discriminate results to validate the model. Also, statistical methods can be used to compare both results. (Sargent, 1998)

3 EXPERIMENTAL WORK

The experimental work for this Master´s thesis was carried out at Outotec Research Center (later ORC) in Pori during January, February and March 2019. ORC is an important part of Outotec research and development work. Clients and internal R&D projects are general users for ORC services. Test work is a major part of the designing of industrial plant for Outotec clients. Process research, innovations and product development belong also in ORC scene. ORC includes pyro- and hydrometallurgy laboratories and mineral processing laboratory where the experimental work for this thesis was done. The mineral processing laboratory develops processes and equipment for grinding, dewatering and beneficiation technology.

During the experimental test work, also the services of the analytical laboratory were used. After the grinding and flotation tests, the results were utilized in following HSC simulations.

3.1 Aims

The experimental work of this thesis includes two stages. First, laboratory flotation tests and then HSC modelling and simulation. Samples for this work came from Rich Metal Group, (later RMG) from Southern Georgia, for it, Outotec has done research work. The aim of the experimental work was to do kinetic tests for rougher (RF) and cleaner (CF) flotation using these ore samples from RMG's Madneuli deposit. Firstly, grinding and kinetic flotation test for each geometallurgical was carried out. Next, a matrix for different blends was created (Table 1). When all the flotation tests were successfully completed, the results were modelled and simulated with HSC Sim. This enabled the comparison of results from flotation test work and simulations.

Before starting test work in the matrix (Table 1) is possible to see the ore blends used in each flotation test. ORC tested these ores before and defined the flotation variables, such as reagent dosages and grinding times. All details from the test work are introduced in chapters below.

Table 1. Flotation test procedure matrix for all four ore (XI, V, VIII-C1, VIII-C2) used in rougher (RF) and cleaner (CF) flotation test work.

RMG test	1	2	3	4	5	6	7	8	9	10	11	12	13	14	15	16
Rougher/Cleaner	RF	RF	RF	RF	CF	CF	CF	CF	RF	RF	RF	RF	RF	CF	CF	CF
XI	100				100				75	50	25	50	25	75	50	25
V		100				100			25	50	75		25	25	50	75
VIII-C1			100				100					25	25			
VIII-C2				100				100				25	25			

3.2 Geometallurgical units

Experimental work of this thesis uses four different geometallurgical ore types or ore blocks from RMG Madneuli copper-gold ores from Bolnisi mining district from Southern Georgia. These units represent different end-member ore types, including different composites, which are defined by different ratios of chalcopyrite, chalcocite and oxidized copper minerals. The average element composition is 0.28% to 0.52% copper and 0.19 to 0.56 ppm gold. In this thesis, the study of behavior of gold is excluded. Copper minerals are divided into three different minerals. Chalcopyrite, chalcocite group which includes chalcocite, digenite, anilite and geerite, all these have the general formula $Cu_{2-x}S$ and copper oxides/sulfates. The distribution of copper between different copper minerals are presented in Figure 14. Main gangue minerals are quartz, muscovite, sericite and pyrite. Some Madneuli samples include also chlorite and kaolinite, minerals which cause slimes during grinding and it is problematic for flotation. Chalcopyrite (Ccp), chalcocite (cc), cuprite (cupr), pyrite (py) and non-sulfide gangue (NSG) are minerals that are used for calculations of mass balances and simulations. These five minerals cover accurately all main and valuable minerals. (Liipo *et al.*, 2018)

The Madneuli ores are hosted by an upper Cretaceous sequence of volcanic-sedimentary rocks. Madneuli deposit is lying at northeast-trending dome and limbs of the dome are dipping between 10 and 40 degrees. Madneuli host rock is created by silicification, chloritization, sericitization and sulphidization. Madneuli deposit covers three different

mineralization styles: vein-disseminated, breccia and massive stockwork mineralization. A large part of Cu-Au mineralization is confined to areas of silica-rich alteration. (Talikka *et al.*, 2018)

Sample batches were already prepared, thanks to earlier test work at ORC with these RMG ores. Mineralogical and chemical analysis were also carried out in ORC and additionally locked cycle flotation tests were done in RMG´s laboratory in Georgia. ORC did simultaneous flotation test work and geometallurgical classification is based on those flotation results. (Talikka *et al.*, 2018)

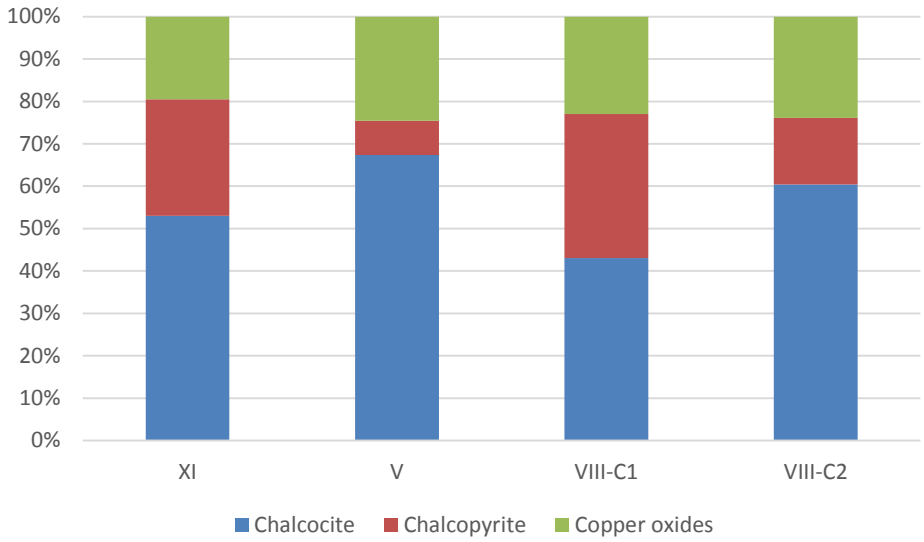

Figure 14. The distribution of copper between different copper minerals. (Liipo *et al.*, 2019)

3.2.1 Madneuli Block XI Ore

Madneuli XI (former XI-C1) is a medium-hard ore and it contains 0.45% copper, 5.95% iron, 3.36% sulfur and 0.56 ppm gold. Based on Outotec mineralogical studies, primary sulfides of the XI sample are pyrite, chalcopyrite, chalcocite and minor amounts of covellite and bornite. Major gangue minerals are quartz, chlorite and muscovite. Pyrite is common and widespread. Pyrite may cause losses of copper because sometimes it is rimmed by chalcocite and sometimes chalcopyrite occurs as an inclusion in pyrite.

Additionally, copper is appearing in covellite, bornite and in grain of metallic copper but amounts are minor comparing to chalcocite and chalcopyrite. Copper occurs also in delafossite, Cu-Fe oxide phases and sulfates. (Liipo *et al.*, 2018)

Copper is mainly carried by copper sulfides (80.5%) and chalcocite is the more dominant carrier. Pyrite is the primary carrier of iron and sulfur. Copper oxides and sulfates carry 19.5% of total copper, mostly in -20µm fractions. (Liipo *et al.*, 2018)

3.2.2 Madneuli Block V Ore

Madneuli V (former V-C1) ore can be classified to medium-hard ore. Sample V contains 0.52% copper, 6.25% iron, 3.15% sulfur and gold grade are 0.56 ppm. Sample V is containing 58.39% quartz, 17.5% micas, 14.49% chlorite, 5.58% pyrite, 2.27% kaolinite, chalcopyrite (0.49%), chalcocite (0.12%) and copper oxides/sulfates (0.20%). Copper is primarily found from copper sulfides, 75.5%. The rest of the copper are in copper oxides and sulfates, 24.5%. (Liipo *et al.*, 2018)

3.2.3 Madneuli Block VIII-C1 Ore

Madneuli VIII-C1 sample had higher hardness compared to XI and V samples. The sample contains 0.31% copper, 5.89% iron, 5.13% sulfur and gold grade are 0.19 ppm. Mineralogical characterization shows that copper minerals are occurring in quite difficult relationships with gangue minerals. Chalcopyrite occurs in particles with silicates and combination with chalcocite-covellites. Chalcopyrite is also found in inclusions within pyrite. Chalcocite is appearing within fractures of pyrite as it occurs in Madneuli XI and V samples. (Liipo *et al.*, 2018)

Mineral composition in VIII-C1 sample consists of 68.81% quartz, 11.73% micas, 6.9% chlorite, 9.44% pyrite, 3.23% kaolinite and 0.13% carbonates. Copper in this sample are occurring in 0.25% chalcopyrite, 0.17% chalcocite and 0.11% copper oxides/sulfates. Major copper carriers are chalcocite with 43% and chalcopyrite 33%. Rest of the copper is carried in oxides (23%), this has a clear effect on copper flotation performance. (Liipo *et al.*, 2018)

3.2.4 Madneuli Block VIII-C2 Ore

Madneuli VIII-C2 sample contains 0.28% copper, 5.56% iron, 5.53% sulfur and gold grade is 0.43 ppm. Pyrite-chalcocite relations are quite challenging and will have a negative impact on flotation. Chalcopyrite is often found with pyrite or silicates and it will affect recovery. Compositions between covellite and chalcocite are common in this sample. Mineral composition of VIII-C2 sample is following, 74.16% quartz, 10.32% micas, 2.95% chlorite, 9.92% pyrite, 1.26% kaolinite, 0.11% carbonates, 0.19% chalcopyrite, 0.11% chalcocite and 0.14% copper oxides/sulfates. (Liipo *et al.*, 2018)

Copper is primarily found in copper sulfides (60% in chalcocite and 16% in chalcopyrite) and rest (24%) is carried by copper oxides and sulfates. Dominant copper sulfide carrier is chalcocite. Copper oxides and sulfates are not amenable to flotation so copper efficiency will not be high regarding to high amount of oxides and sulfates. (Liipo *et al.*, 2018)

3.3 Materials

3.3.1 Laboratory equipment

ORC mineral processing laboratory provides opportunities for studying numerous unit processes. There is possible to treat big samples representatively and efficiently. In this chapter, all equipment, used during the experimental work are described.

Ball mill

The grinding procedure was carried out with laboratory ball mill presented in Figure 15. Grinding was conducted with grinding media including 27 mm (3,3kg) and 19 mm (8,7 kg) balls. The material of grinding media and mill was mild steel.

Figure 15. Laboratory ball mill and Sample divider.

Sample divider

A slurry divider was used, and it is shown in Figure 15. It divides slurry samples to two 1/12 portions and the remaining 10/12 was third individual portion. This divider was used during sieving tests. Ground sample was ground to smaller portions, that was used in sieving tests.

Wet-sieve machine

The experimental work started by doing fixed grinding and wet-sieving tests for each ore unit. The wet-sieve machine separates all particles from each other that enables a reliable sieving result. Grinding times were evaluated from Outotec test report and P80 values of ore samples were confirmed with sieving and creating particle size distributions from samples. The used sieves were 300, 212, 150, 106, 75, 45 and 20µm sieves.

Flotation machine

Outotec-GTK laboratory flotation machine (Figure 16) was used for flotation. It works with automated scrapers with adjustable air, water, nitrogen, rotor speed and scraping

frequency. Flotation cells sizes are 2, 4, 8 and 12 liter volumes with three different size of rotors; 45, 60 and 75 mm. It is possible to use pH/Eh-measurement devices during the flotation process.

Figure 16. Outotec GTK laboratory flotation machine.

3.3.2 Reagents

Aerofloat 208

Outotec studied different collectors with these ore samples and Aerofloat 208 iterated to give the best metallurgical performance for flotation. This is a collector including dialkyl dithiophosphate and diethyldithiophosphoric acid is produced by Cytec. Aerofloat 208 is selective Cu-collector. Based on Outotec report, pyrite rejection is efficient and giving lower pyrite recovery to rougher concentrate. In addition, good enrichment ratio and stage recoveries of copper are achieved.

Dowfroth 250

Dowfroth 250 ($CH_3(PO)_{6.3}OH$) was used as a frother (based on Outotec previous test work). This frother is polypropylene glycol methyl ether.

Calcium hydroxide ($Ca(OH)_2$)

Calcium hydroxide was used as a pH modifier to reach the target pH value of 12 after conditioning. Ores included pyrite to be depressed and that is why pH was set to 12. Madneuli VIII-C1 and VIII-C2 included approximately 9-10% of pyrite and Madneuli XI and V included 4-6% of pyrite. High amount of pyrite in Madneuli VIII-C1 and VIII-C2 required higher consumption of calcium hydroxide during flotation.

3.4 Grinding test work

One 1,5 Kg batch was used for each ore type, so a total of 6 Kg was used. Ore batches were crushed to particle size under -1mm with the crusher. Crushed ore was classified with vibrating screen and screen size of -1.14mm. Screen underflow was distributed to 1.5 Kg batches for grinding and flotation test work. Flowsheet of crushing and classification are shown in Figure 17.

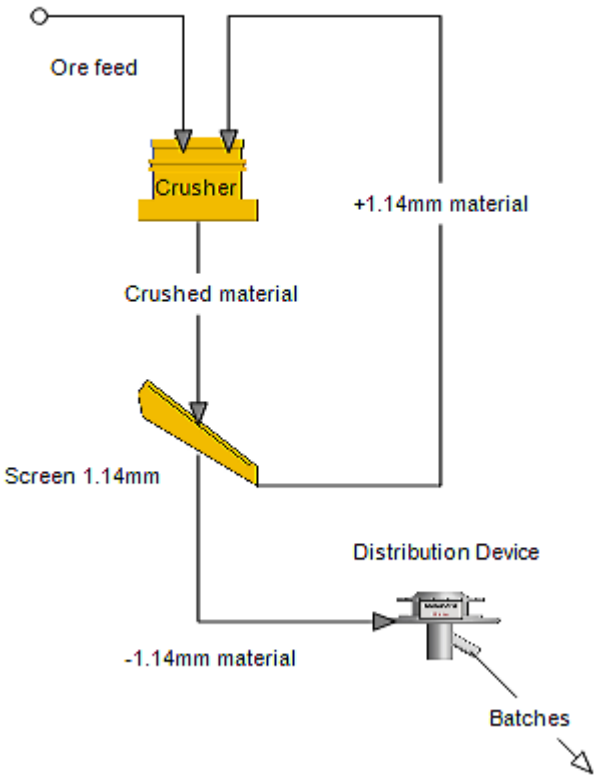

Figure 17. Crushing flowsheet.

Grinding was conducted during 5, 15, 20 and 30 minutes. Results and particles sizes of these grindings are possible to find from Appendix 1. Particle size distributions and grinding time analyses are justifying grinding residence times for thesis grinding phase. Target particle size for flotation was set to 55 µm and grinding times were chosen using Grinding time vs. P80 curves (Appendix 1). Grinding times are calculated from curve equations.

A mild steel laboratory ball mill was used for grinding. A grinding ball media of 12 Kg used and was also mild steel. Solids-% was carried out with 65 percent solids content. When grinding was done the mill and balls were washed with tap water to recover all ground ore to vessel. Next ground ore was divided with sample divider to 1/12 sub-samples (125g) and then again to 1/12 sub-samples (10g). Because each grinding ore batch was 1,5 Kg the resulted sub-samples were approximately 10 g. Then two sub-

samples were combined to go through sieving process. Approximately 20 g of each sample were wet-sieved.

3.5 Rougher Flotation test work

Rougher flotation tests were conducted for each ore type. First, the ore sample was ground in a laboratory ball mill with 65% of solids-%. Calcium hydroxide was added in the grinding mill to increase the pH value before the conditioning phase. Grinding times of each unit was set to reach P80 value of 55µm. Because of the similarities of Madneuli XI and V, the reagent recipe was the same for both of those ores. Also, the addition of reagents for flotation of Madneuli VIII-C1 and VIII-C2 were also the same in those flotation tests. Flotation cell volume was 4-liter, rotor speed was set to 1800 rpm and air flow rate were 3 l/min in each test. Tap water was used in each test. Target was to investigate flotation kinetics, so four points were selected for each test. Flotation times were RF1 = 1min, RF2 = 2min, RF3 = 4min and RF4 = 8min, totally 15min of flotation of each unit to determine infinite recovery, R_{max}. The flotation flowsheet is shown in Figure 18.

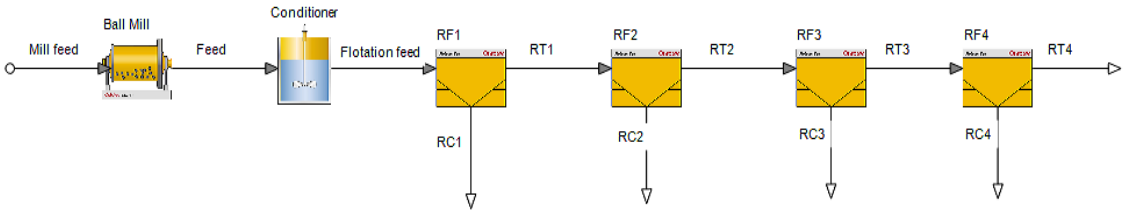

Figure 18. Flowsheet of rougher flotation.

In conditioning phase first, water was added to reach the target liquid level in the cell. The line was drawn in the side of the cell. The was to add enough tap water to reach the same liquid level in every flotation. There was no target solids-% in the flotation. Next, more calcium hydroxide was added to reach a pH value of 12. The collector and frother were added with two and one minute conditioning times respectively. The reagent

dosages can be found in Table **2**. More collector was added before RF3 and RF4 to enhance mass pull of later flotation phases.

Table 2. Rougher and cleaner flotation procedure.

RMG test	1	2	3	4	5	6	7	8
Rougher/Cleaner	RF	RF	RF	RF	CF	CF	CF	CF
XI	100				100			
V		100				100		
VIII-C1			100				100	
VIII-C2				100				100
Grinding time, min	17	15	23	23	17	15	23	23
Re-grinding time, min	-	-	-	-	2.5	0.5	4	4
CaOH2 addition mill, g/t	2000	2000	3400	3400	2000	2000	3400	3400
Collector dosage g/t	100	100	130	130	130	130	150	150
Frother dosage g/t	20	20	30	30	30	30	30	30

3.6 Re-grinding test work

In order to increase the selectivity re-grinding test work of the ore was required. First, rougher flotation was done with two times five minutes of flotation. Then rougher concentrate was filtered and silted to target solids-% which was 50%. Re-grinding was done with special re-grinding mill and media (Figure 19). Mill volume was smaller as was the amount of grinding media though. The weight of balls was 4,33 Kg, including 19 and 10 mm balls. The rougher concentrate was ground for two minutes and a sample was taken from the slurry. The slurry sample was evaluated with laser diffraction particle size analyzer. Then two minute grinding was repeated as many times as needed to reach P80 value of 25-30µm.

Figure 19. Re-grinding mill and ball batch.

3.7 Cleaner flotation test work

Cleaner flotation test work was conducted for each four ore type. Primary grinding was carried out like in rougher flotation, with the same grinding times (Table 2). Rougher flotation times were two times five minutes with two-minute collector conditioning between two flotation stages. The reason was to increase mass pull to rougher concentrate by adding collector during middle conditioning. The rougher concentrate was filtered and then silt to target solids-% for re-grinding.

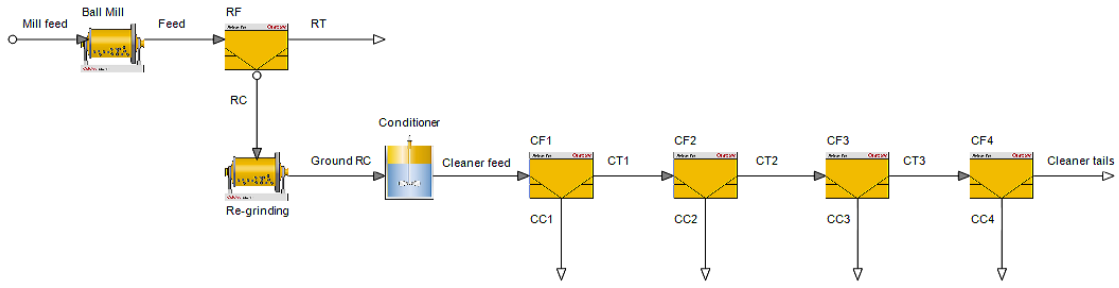

Figure 20. Cleaner flotation flowsheet.

After re-grinding, the slurry was recovered into 2 liter flotation cell. Condition was similar as it was in the rougher stage, but reagent dosages were smaller because there was 5-25% mass pull to rougher concentrate from the feed. Target pH value was again 12 and $Ca(OH)_2$ was added enough to reach that value. Conditioning for reagents were two minutes for the collector and one minute for the frother. Airflow was set to 2 liters/min and rotor speed to 1300rpm. The aim was to investigate cleaner kinetics, so flotation times were; CF1 = 1min, CF2 = 2min, CF3 = 3min and CF4 = 6min, totally 12min to reach infinite recovery, R_{max}. Cleaner flotation flowsheet performed is shown in Figure 20 and the flotation reagent dosages used in Table **3**.

3.8 Blend flotation test work

Blend flotation test work included rougher and cleaner flotations. Table **3** presents the percentage of ore blended in certain flotation test. Madneuli XI and V were chosen to examination that is more detailed. Three rougher and three cleaner blend flotations were done for these two ores. The ore ratios of blending are 75/25, 50/50 and 25/75 those were chosen to provide enough data for validation.

Flotation reagents dosages were similar for both ores so also during blend flotations dosages are specified in Table 3. Madneuli XI and V had grinding times 17 and 15 minutes, so in blend tests grinding times were weighed averages. Grinding and sieving tests were only done for reference tests for each ore type. Because ore harnesses were very close to each other it is assumed that the particle size of flotation feed was optimal for flotation in each blend test. Grinding times and reagent dosages are presented in Table **3**.

Besides blending Madneuli XI and V ores, also two extra flotation tests were carried out. In RMG12 flotation there were three different ores and in RMG13 four different ore. Grinding times and reagent dosages in these flotations were weighed averages. Particle size is assumed to be optimal because all ores have quite similar mineralogy and grindabilities. Optimal pH value was 12 for all ores so it was optimal in these blend flotations though.

Table 3. Blend flotation procedure.

RMG test	9	10	11	12	13	14	15	16
Rougher/Cleaner	RF	RF	RF	RF	RF	CF	CF	CF
XI	75	50	25	50	25	75	50	25
V	25	50	75		25	25	50	75
VIII-C1				25	25			
VIII-C2				25	25			
Grinding time, min	16.5	16	15.5	20	19.5	16.5	16	15.3
Re-grinding time, min	-	-	-	-	-	2	1.5	1
CaOH2 addition mill, g/t	2000	2000	2000	2700	2700	2000	2000	2000
Collector dosage g/t	100	100	100	120	120	130	130	130
Frother dosage g/t	20	20	20	30	30	30	30	30

3.9 Analysis equipment

Inductively coupled plasma optical emission spectroscopy (ICP-OES) was the method used in chemical analysis for concentrate and tailings samples. ICP-OES is widely used in mineral processing industry and laboratories. Aerosol which includes sample is heated by plasma and in high temperature it produces excited atoms. Excited atoms emit light and wavelengths intensities are measured. Different elements give different intensities and so on grades can be calculated from each sample. (Kakko, 2016)

Copper phase assays consist of sequential copper analyses after four stage leaching. Leaching stages are water (P1), sulphuric acid (P2), cyanide (P3) and nitric acid (P4). This method provides a way to determine copper content divided in copper sulfates, copper oxides and silicates, secondary copper sulfides and primary copper sulfides. Then element to mineral conversion was made using HSC Chemistry® 9 Geo module. Copper phase assays are converted to minerals with HSC Geo module and certain mineral matrix (Table **4**). Ore samples contain three different copper minerals which are: chalcopyrite (primary copper sulfide), chalcocite (secondary copper sulfide) and cuprite (copper oxides). Pyrite is a sulfide gangue mineral and quartz cover all silicate gangue minerals used in calculations (named non-sulfide gangue, NSG). Element to mineral conversion calculation uses stoichiometric ratios of each mineral. Sulfur was

determined using by combustion analysis which is used for carbon and sulfur assays. (Liipo *et al.*, 2019)

Table 4. Mineral matrix for element to mineral calculations.

	Chalcopyrite	Chalcocite	Cuprite	Pyrite	NSG
Si %					46.74
Fe %	30.43			46.55	
O %			11.18		53.26
Cu %	34.63	79.85	88.82		
S %	34.94	20.15		53.45	

3.10 HSC Sim Simulations

Mineral conversion from chemical assays was made first. Mineralogy is simplified to five minerals which are chalcopyrite (ccp), chalcocite (cc), cuprite (cupr), pyrite (py) and non-sulfide gangue (NSG). Cuprite covers copper oxide minerals and non-sulfide gangue covers all gangue minerals besides pyrite. In this case, pyrite is defined as a gangue mineral and it has a major effect on flotation performance. Chalcopyrite is a primary copper sulfide and chalcocite is a secondary.

After mineral conversion and definition, mass balances were calculated including grades and recoveries for each mineral in each stream. In addition, elemental copper and sulfur grades and recoveries are given in mass balance calculations. Stage and cumulative recoveries are expressed in mass balances. Kinetics curves of each mineral and element are drawn by using excel. Chemical compositions based on analyses are converted to minerals using the non-negative least square method. Sometimes chalcopyrite grade is negative in these calculations it is defined to be zero.

Next mass balances were added to HSC Sim mass balance tool and streams were evened. HSC Sim mass balance tool calculates again stage recoveries to flowsheet and it is easy to make proof that input-output comparison matches. HSC Sim model fit tool is used to define kinetics parameters for each flotation. Rectangular distribution equation

(Equation 10) for laboratory flotations was used to calculate maximum rate constant (k_{max}) and infinite recovery (R_∞).

$$R = \left(\frac{R_\infty}{b}\right)\sum_{i=1}^{b}(1-(\exp(-k_i t)), k_i = \frac{k_{max}}{b}, k_{i>1} = k_{i-1} + k_1 \quad (10.)$$

where, t is the cumulative residence time, $b = 15$ and $R_\infty \leq 1$.

After kinetic curve is fitted to kinetic points, the tool defines kinetic values for k_{max} and R_{max}. HSC Sim model fit tool draws kinetic curve and grade-recovery curves for each mineral and element wanted (Figure 21). Based on a rectangular distribution equation, HSC Sim calculates kinetic values and those can be picked up for modelling. Kinetic curves fitted on kinetic points are shown in Appendix 2.

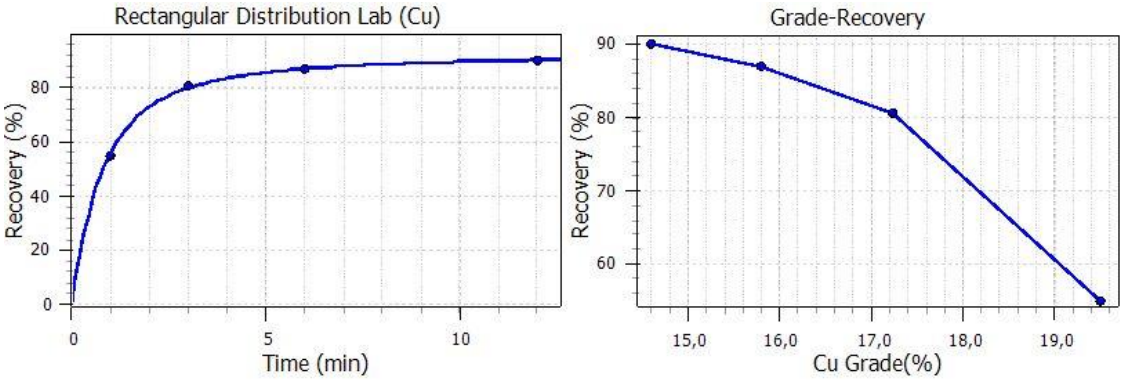

Figure 21. HSC Sim model fit tool represent kinetic curve and grade-recovery curve for each mineral and element.

The next step was to create a simplified flowsheet for blend model (Figure 22). The model has two inputs feeds so there are two separate conditioners for both feeds. Two different ores were added to the same flotation circuit. Kinetics for both reference ores were calculated with HSC Sim model fit tool and then added to model conditioners (Figure **23**). Feed setup included the define composition of minerals from reference mass balances. Flotation residence times were defined to cell parameters. A simulation model was created also for three and four ore blends. This model included naturally four conditioners for all different ore types.

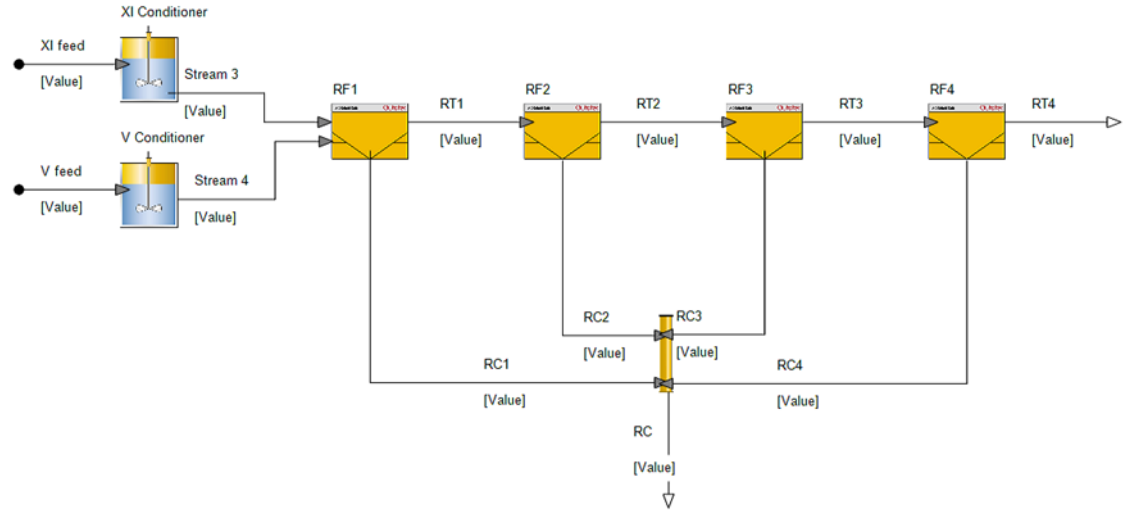

Figure 22. Flowsheet for blend model.

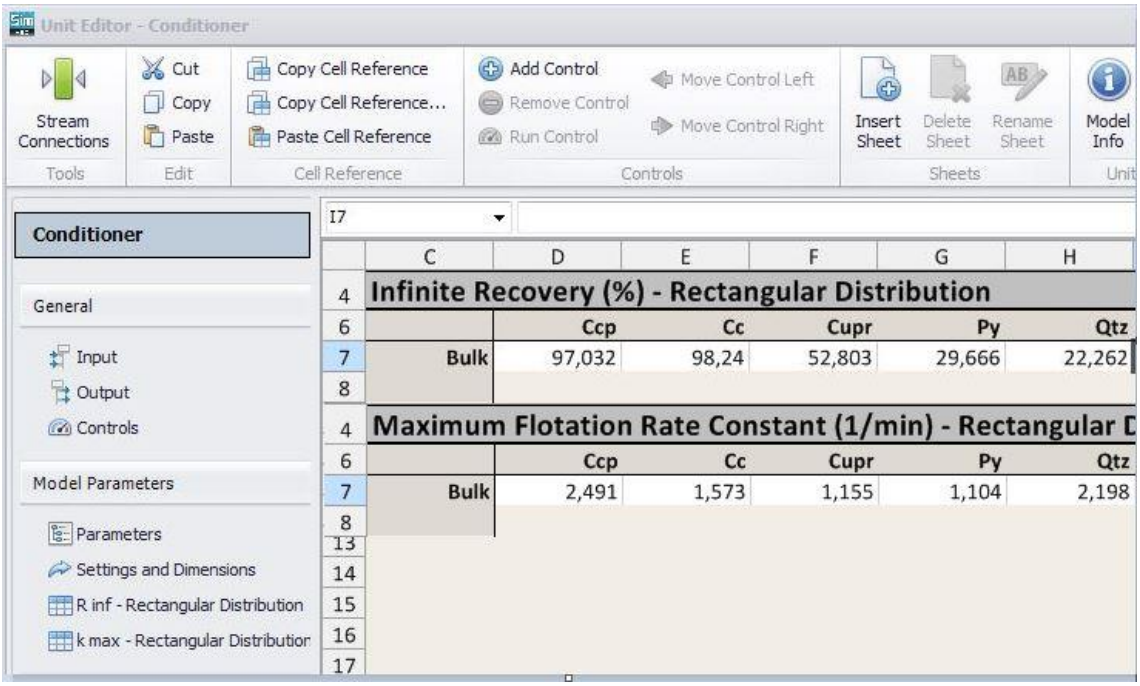

Figure 23. Kinetics for conditioner unit model.

When the model was ready, HSC Sim scenario editor tool was used to calculate results for different blends. Two reference ores were added to the model with different portions and combined flow was always 100%. It is possible to choose what parameters tool calculated and Cu-grade in rougher concentrate, Cu recovery to rougher concentrate and

mass flow of rougher concentrate was chosen to be determined. In addition, kinetic curves for separate copper and gangue minerals were determined. HSC Sim scenario editor tool can also calculate grades of minerals in each stream wanted.

Flowsheet model was done also for cleaner flotations (Figure 24). Blend flotation tests were done with similar blends for cleaner flotations though. Model flowsheets were different because there was kinetics for rougher and cleaner flotations for both ores.

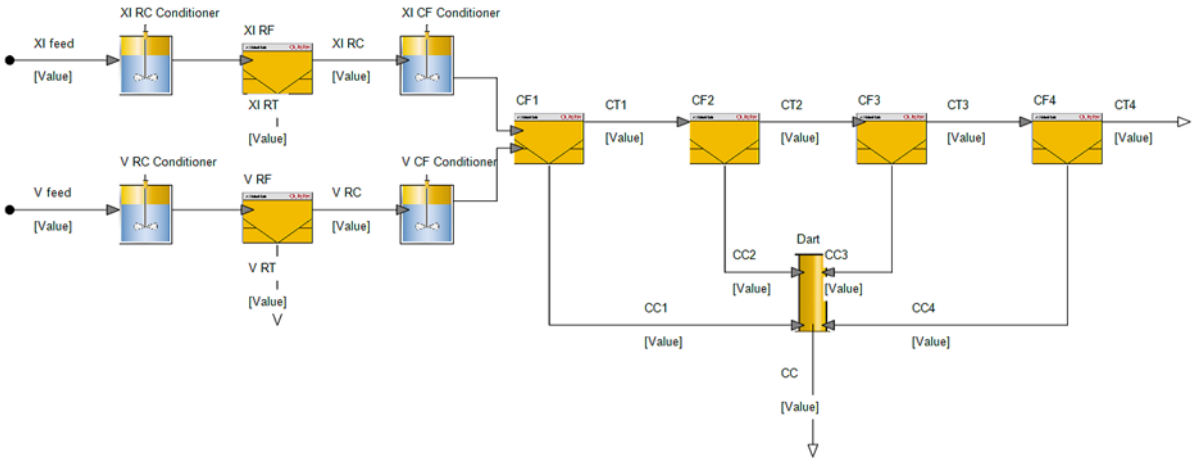

Figure 24. Model flowsheet for cleaner flotation.

4 RESULTS AND VALIDATION

4.1 Grinding and sieving

The aim of grinding and sieving tests was to confirm the grinding times for all four ore types. Primary grinding times were selected from previous test report. The optimal particle size for flotations was P80 = 55-60 µm and that was reached with all ores. Grinding times and P80 values in grinding tests are shown in Table 5. Particle size distribution charts are shown in Appendix 1.

Table 5. Grinding time of each ore type.

Ore	Grinding time, min	P80, µm
XI	16	59
V	15	55
VIII-C1	21	58
VIII-C2	23	55

4.2 Rougher flotation results

Flotation test work results are based on chemical analysis done in ORC analytical laboratory. Mass balances calculated from the analysis are shown in Appendix 3. Mass balances perform stage and cumulative grades and recoveries of five minerals. Elemental copper and sulfur recoveries and grades are calculated to mass balances though. Madneuli units were determined and kinetics of each four ores are shown in Figure **25**.

When the chemical composition is converted to minerals, the adjustment of the grade of chalcopyrite could be negative. Therefore, the calculation is made using non-negative least square method and the grade is defined as a zero. Practically 100% recovery is not possible, because the detection limit of chemical analysis is >0,05% Cu the (ICP-OES method). There is a small error in chemical analysis when a back-calculation is done which is considered as no-significant.

Figure **25** shows the elemental copper and copper mineral kinetics for different ores. As expected, the highest copper recovery (86,0%) was obtained from Madneuli XI ore. Other ore types had relatively low copper recoveries (Madneuli V = 68,4%, Madneuli VIII-C1 = 73,8% and Madneuli VIII-C2 = 65,0%).

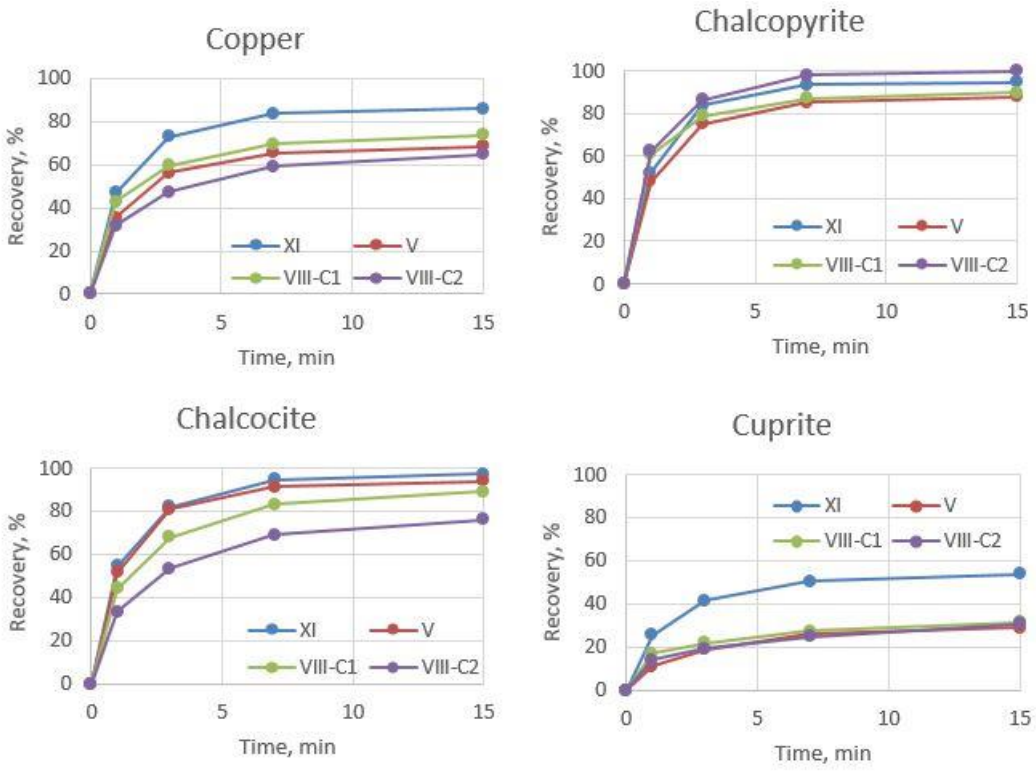

Figure 25. Recovery versus time of elemental copper and copper minerals for each type of ore.

Figure **26** represent rougher copper concentrate copper grade and recoveries of each unit. Madneuli XI and V have closely same grindability (Bond work index) and proportions of gangue minerals are similar. But grades and recoveries are very different from each other. Madneuli XI have high recovery (86%) and quite low copper grade (1.75%). Conversely Madneuli V have low recovery value (68.4%) but high copper grade (5.75%). These two units are selected for blend flotation test for the reason, that metallurgical performance differs from each other remarkably. Reason for this is the difference between distribution of copper in copper minerals.

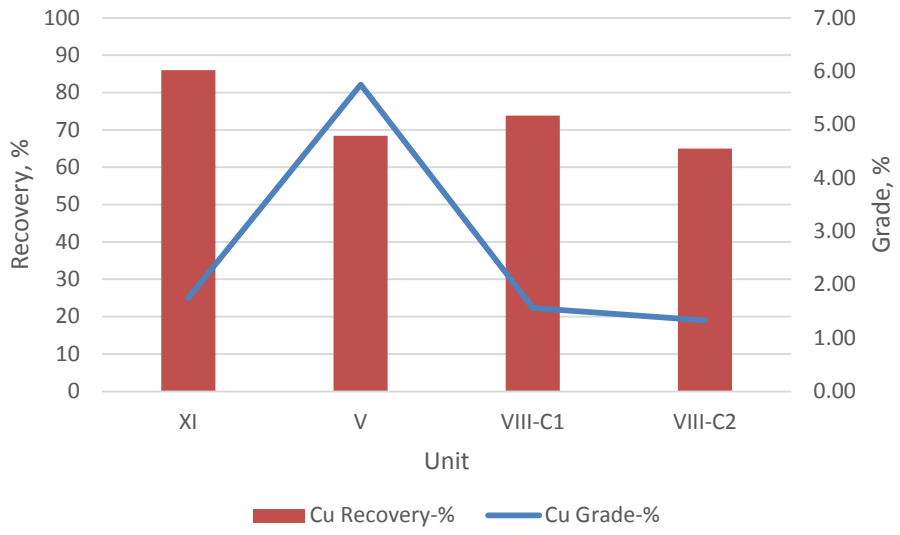

Figure 26. Copper grade and recovery for rougher concentrate on each unit.

Figure **27** shown copper grades and recoveries of each blend and Madneuli XI&V references. There is a marked trend when XI/V ratio changes. The grade is increased when there is more Madneuli V ore. Copper recovery is increased when there is more Madneuli XI ore.

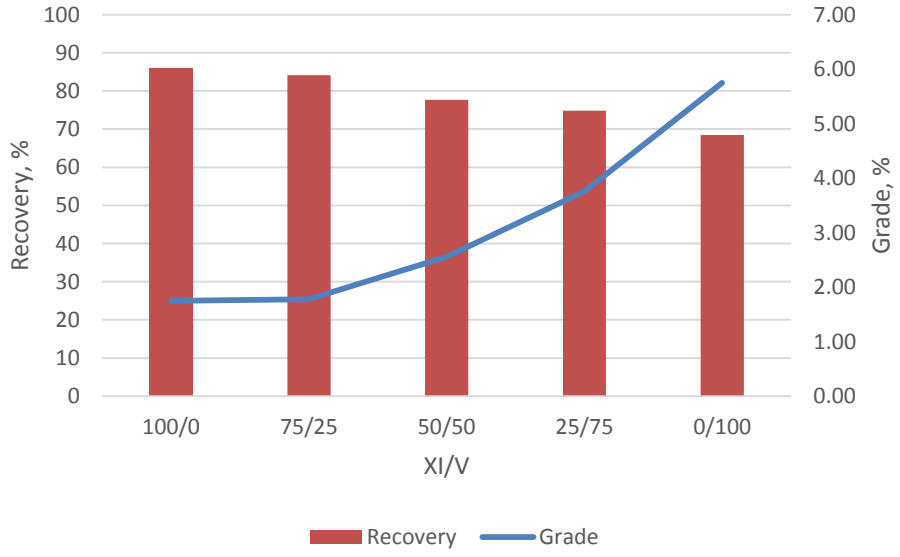

Figure 27. Copper grades and recoveries in flotation test for each ore blend (XI/V).

Figure **28** shows how copper is distributed between three copper minerals in each blend. Around 50% of copper is in chalcocite in every blend. In Madneuli XI, there is around 30% of copper in the chalcopyrite and the rest is in copper oxides/sulfates (cuprite, 20%). In the ore Madneuli V there is more copper in copper oxides/sulfates (37%) than in chalcopyrite (13%). This is the reason for copper recoveries and rougher concentrate mass pull results in blend flotation tests.

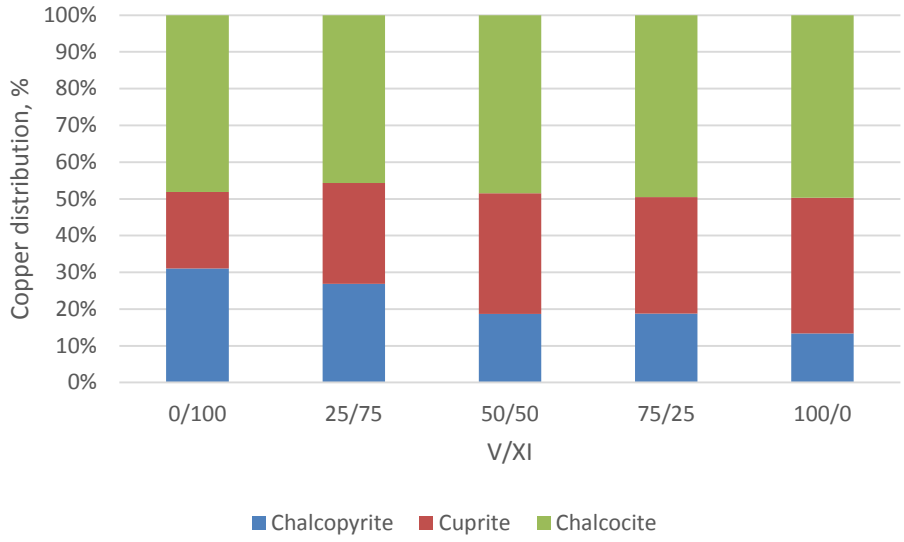

Figure 28. Copper distribution between copper minerals in the blending V/XI ores.

Comparing these units by copper mineral recoveries, all have similar kinetics. Except biggest deviation is cuprite recovery in Madneuli XI. Cuprite recovery in Madneuli XI is 53.9% when it is only 30-31% in other units (Figure **25**). This is one reason for Madneuli XI high total copper recovery. Figure **25** shown that chalcocite recoveries in Madneuli XI and V are higher than in Madneuli VIII-C1 and VIII-C2. The reason for this is the relation of chalcocite and pyrite as these two are appearing together, so unliberated chalcocite is recovered to tailings with pyrite. While Madneuli VIII-C1 and VIII-C2 have a high pyrite recoveries, chalcocite recoveries are lower because of the mentioned relation of chalcocite and pyrite.

Figure **29** represents the kinetics of gangue minerals, pyrite and NSG. In the flotation test of Madneuli XI ore, both pyrite and NSG have high recoveries. Because there was

the high recovery of copper minerals to Madneuli XI concentrate it is possible to deduce the association of copper minerals with gangue in Madneuli XI. Rougher concentrate mass pull was around 25% in Madneuli XI rougher reference flotation test. Madneuli V have lowest recoveries of gangue minerals. Rougher concentrate mass pull at Madneuli V rougher flotation test was only 6 %.

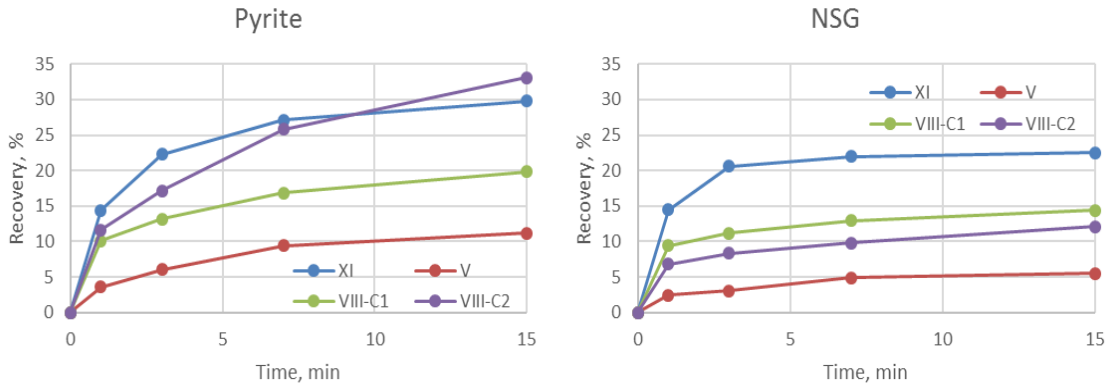

Figure 29. Gangue minerals kinetics of each unit.

Madneuli VIII-C2 reach the highest pyrite recovery (33.1%) after 15 minutes of flotation test. Cumulative pyrite recovery profile in Madneuli VIII-C2 is not similar because, after 7 minutes of flotation, pyrite is activated through flotation test. This could be reason for the weaker association of pyrite and NSG in VIII-C2 ore. Pyrite content in Madneuli VIII-C2 is also high (9.3%) so it can be concluded that rougher concentrate quality is weak because of activated pyrite. Pyrite content in Madneuli VIII-C1 feed was high (9.3%) and recovery was 19.9%. VIII-C1 has relatively high NSG recovery (14.4%) to concentrate so these two aspects are reasons for weak quality of concentrate in Madneuli VIII-C1 flotation.

4.3 Cleaner flotation results

Figure **30** presents the cumulative copper mineral recoveries obtained in the cleaner stage. The copper sulfide chalcopyrite shows the highest flotation rate in the first minute

reaching around 80% of recovery in XI and more than 60% for V, VIII-C1 and VIII-C2. Comparing to rougher flotation tests, cuprite recovery is the highest again in Madneuli XI, also the elemental copper recovery is highest in Madneuli XI as it was in rougher flotation test. Chalcocite was well activated, and its flotation was high in the Madneuli V ore (92,1%).

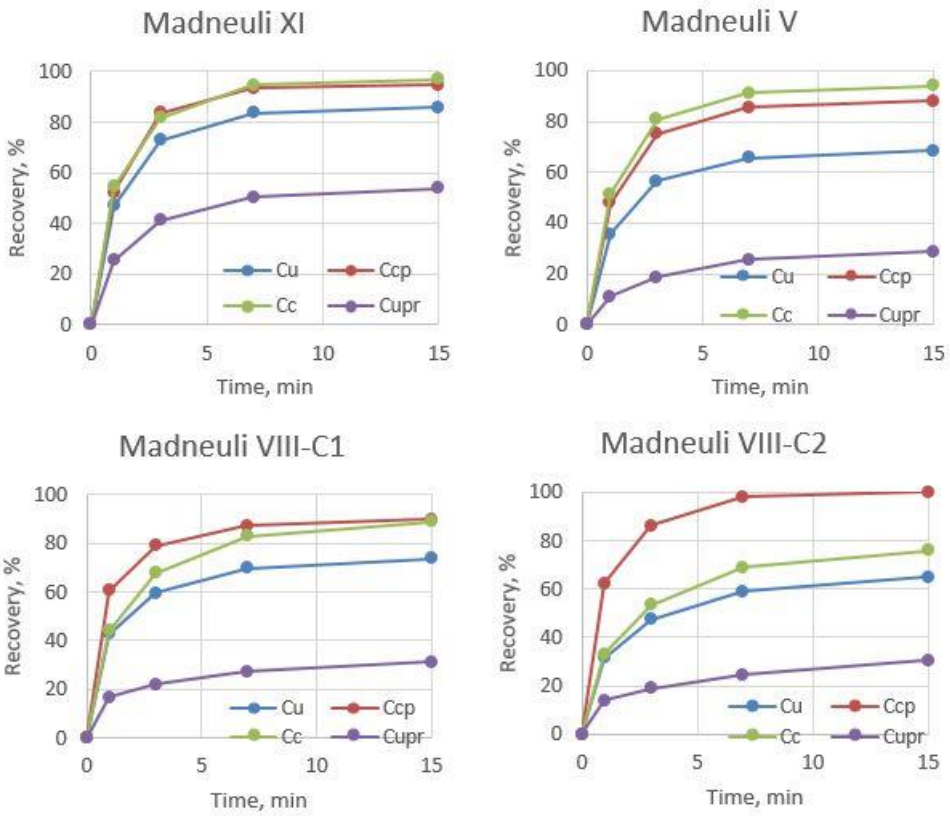

Figure 30. Elemental copper and copper mineral kinetics of Madneuli sample flotation tests.

Figure **31** represents pyrite and NSG kinetics to cleaner concentrate. Madneuli V have again lowest gangue recoveries and so it has the highest copper grade in cleaner concentrate (26,0%).

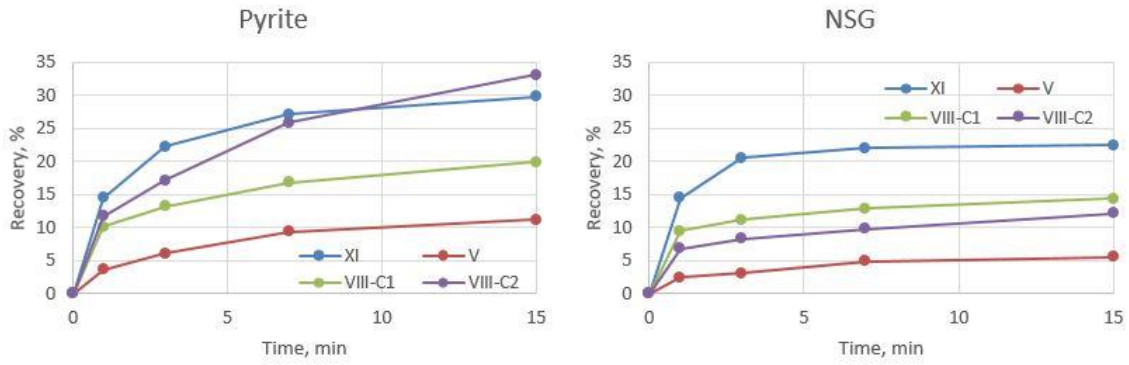

Figure 31. Gangue mineral kinetics in cleaner flotation test for each unit.

Figure **32** shows copper grade and recovery in cleaner concentrate and the pattern is similar as it was in rougher flotation stage (Figure **26**). Madneuli XI have the highest recovery but a low grade and vice versa Madneuli V have the highest grade, but the recovery is low. This confirms the differences in metallurgical performances between the two units. Madneuli VIII-C1 and VIII-C2 have lowest copper grades and recoveries. These two ores give relatively poor results and the concentrate quality is poor in both cases.

Madneuli XI cleaner reference flotation test was not successful because of overflowing during rougher flotation. In simulation work kinetics are from separate reference test done for Madneuli XI ore with similar flotation conditions. Only except was flotation time which was 8 minutes, so cumulative recoveries are not comparable with blend tests.

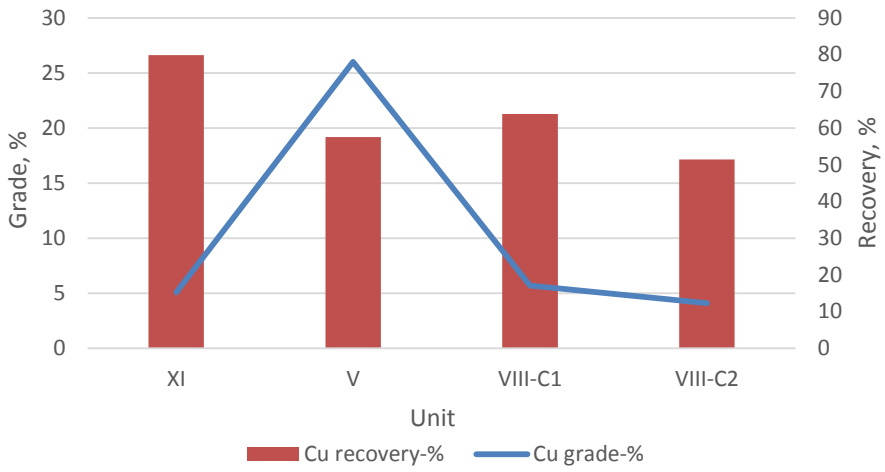

Figure 32. Copper grade and recovery in cleaner concentrate of each unit.

4.4 Blend rougher flotation results

Madneuli XI and V were blended together in blend flotation tests. Besides four reference tests, six blend flotation tests were carried out for better examination. Madneuli XI and V were blended with the following shares: 75/25, 50/50 and 25/75 percentages of these two ores. Reference flotation tests are executed with 100% of each ore. Mass balances for each flotation test are found in Appendix 3. Each mass balance includes cumulative recoveries and grades of elemental copper and sulfur. Recoveries and grades are calculated also for three copper and two gangue minerals. Kinetic curves of each flotation test are presented in Appendix 4. Figure **33** shows that chalcopyrite is recovered remarkably well in each flotation test. Chalcopyrite recoveries are between 86 and 96% in all flotation tests.

Chalcocite recoveries are also good being between 93 to 97% (Figure **34**). Biggest differences occur in copper oxide mineral (cuprite) recoveries with highest 54% and lowest 30%. Figure **35** resents both copper and cuprite cumulative recoveries in rougher flotation tests. Correlation is clear in both pictures Madneuli XI reference gives highest and Madneuli V yield the lowest recovery. Blends between references present a good agreement within the two references. A higher percentage of Madneuli XI ore, the

higher copper recovery is. This is an important point to explain results in all flotation tests.

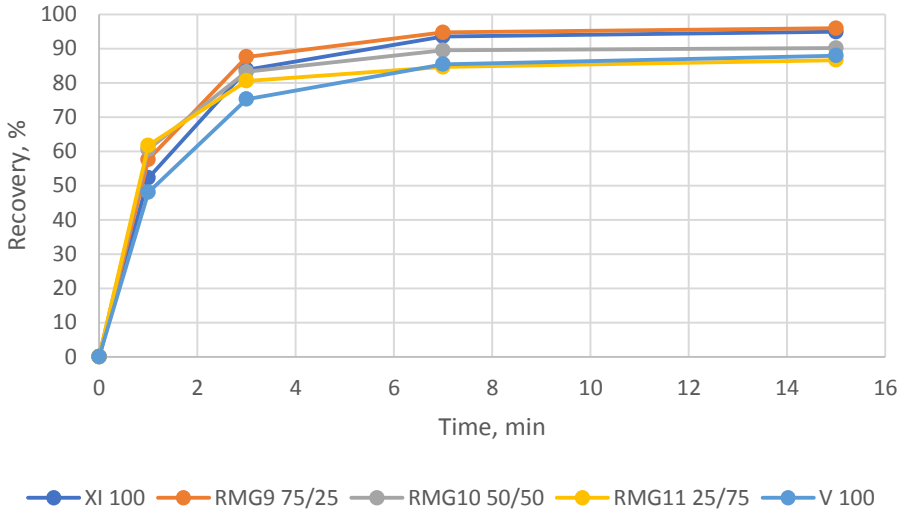

Figure 33. Chalcopyrite cumulative recoveries in rougher blend flotations.

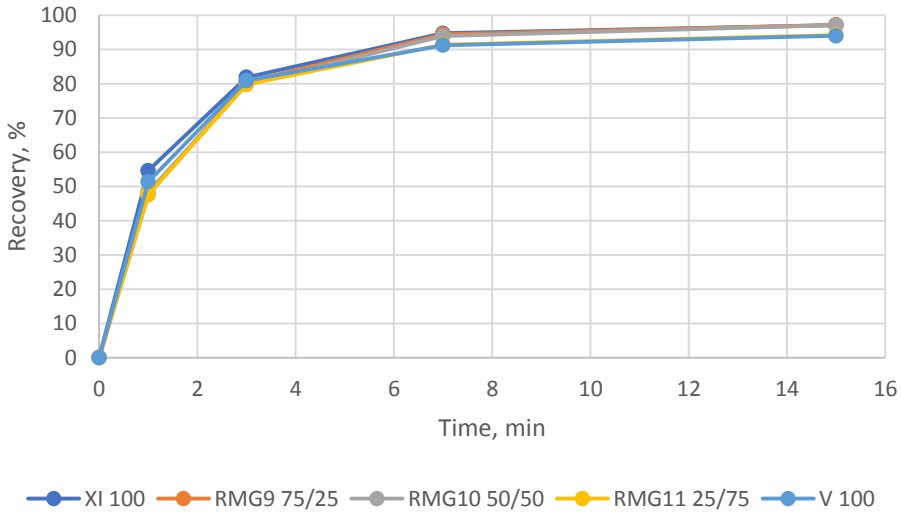

Figure 34. Cumulative recovery of chalcocite in blend flotation tests.

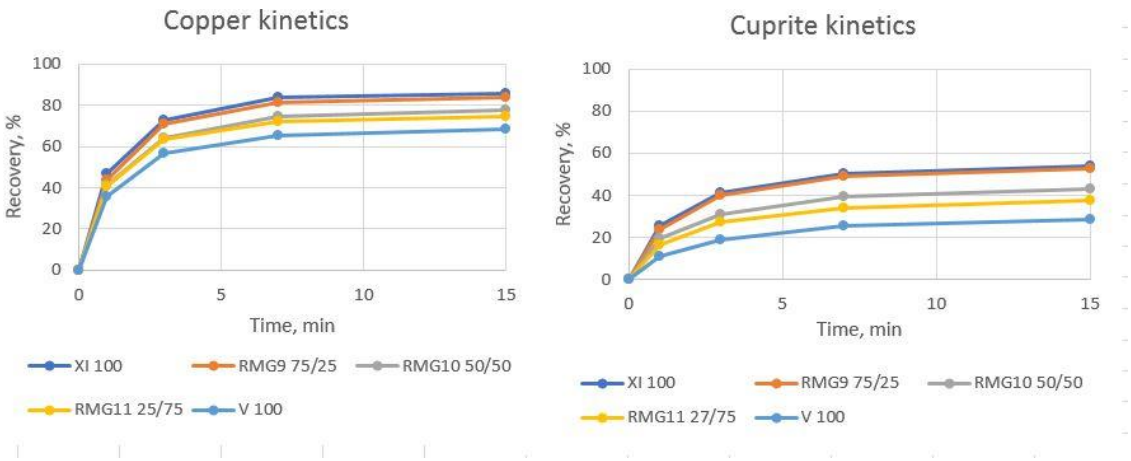

Figure 35. Elemental copper and cuprite kinetics in rougher blend flotations.

Figure 36 shows cumulative recoveries of both gangue minerals, pyrite and NSG. Pyrite and NSG recoveries are close to together in XI 100 and XI/V 75/25 flotations. In XI/V 75/25 flotation test, froth was slightly overflowing which is the reason for a bit increased recovery for total copper, cuprite, pyrite and NSG.

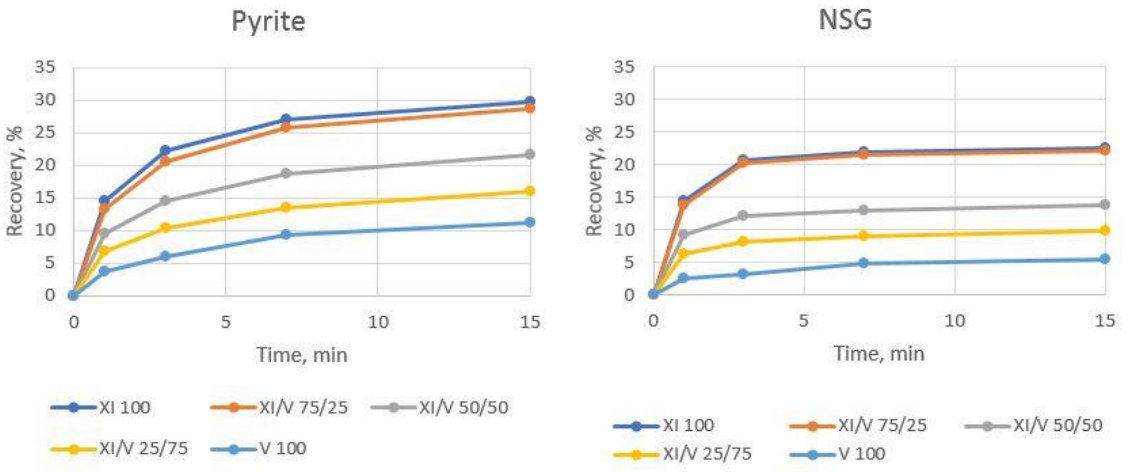

Figure 36. Gangue mineral kinetics in rougher blend flotation tests.

HSC Sim simulation results are based on Scenario editor tool calculations. Reference kinetics were fed to HSC and Scenario editor calculated the results for different blends. In the feed definition, mineral grades are picked from back-calculated values of

reference mass balances. Experimental and simulated results can be seen in Appendix 5. Figure 37 shows the correlation between simulated and experimental copper recovery results. Appendix 6 (Figure 47-Figure 49) presents the parity charts where is possible to see the correlation between simulated and experimental results. Coefficient of determination (R^2) value for copper recovery results was 0.97.

Figure 37 presents simulated and experimental results of copper grade in rougher blend flotation tests. Rougher concentrate mass pull in flotation tests are presented in Figure 39. Copper grade results can be seen in the parity chart and coefficient of determination value is 0.99. Same R squared value for the mass pull is 0.95.

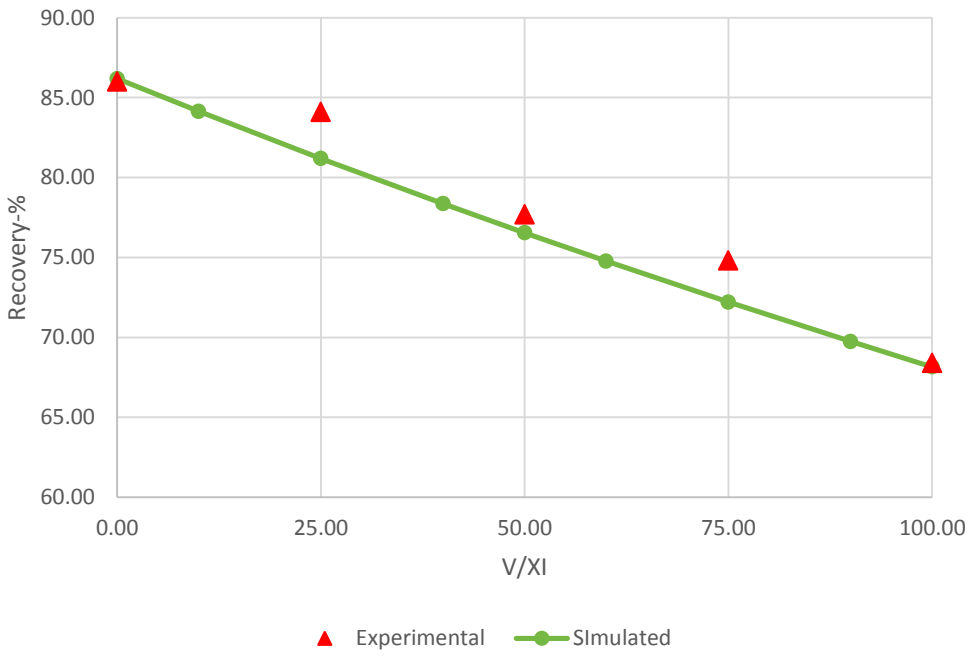

Figure 37. Simulated and experimental copper recovery results from rougher flotation tests for various blending ratios of V/XI ores.

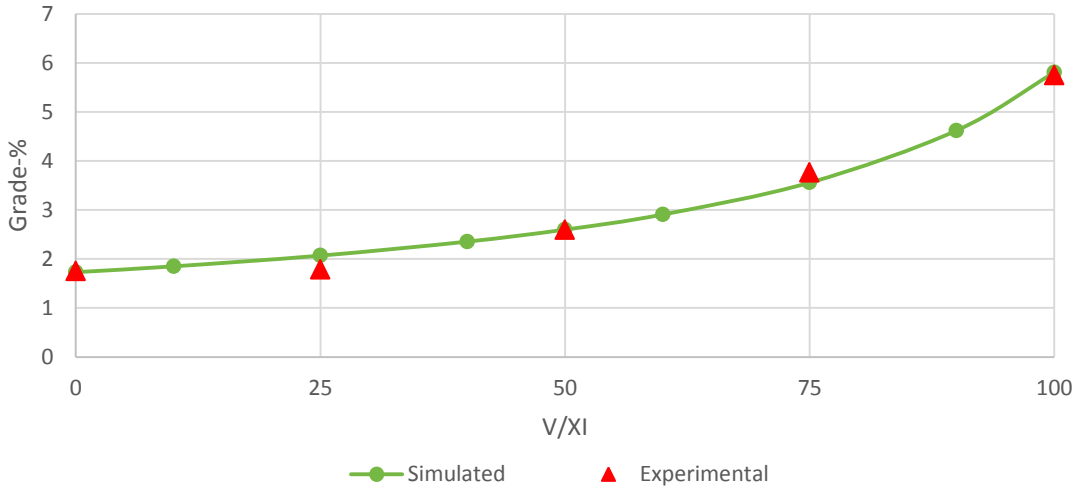

Figure 38. Simulated and experimental copper grade in rougher concentrate for various blending ratios of V/XI ores.

Figure 39. Mass pull to rougher concentrate (the arrow shows the overflowing in one blend flotation giving a high mass pull in one experimental point).

Experimental and simulated results are calculated also for all five minerals separately. Copper mineral grade curves have the same shape than elemental copper grade has

(Figure 40). Curve steepens when blend includes more Madneuli V ore. Appendix 7 presents more results of individual mineral grades. It includes grades and recoveries for copper minerals and both gangue minerals. Pyrite grade follows the copper mineral grades, getting higher when the amount of Madneuli V ore is increasing. Non-sulfide gangue grade decrease when the amount of V ore is increasing. Pyrite and NSG recoveries are decreasing linearly when the amount of Madneuli V ore is decreasing. RMG9 flotation test (V/XI – 25/75) stands out on almost every curve because of little over flowing during flotation test.

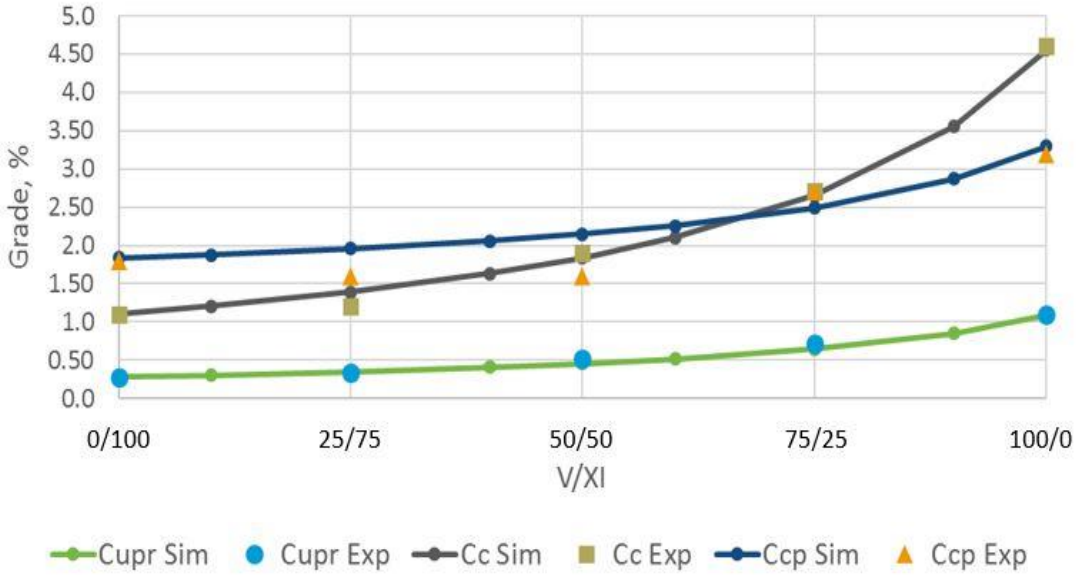

Figure 40. Copper mineral grades in rougher concentrate.

Results show mostly differences in concentrates final grade and recovery. Also, cumulative recoveries are calculated in mass balances and simulated with HSC. Figure 41 shown simulated kinetic curve for RMG10 XI/V 50/50 blend flotation test. Red dots present experimental cumulative recoveries. This figure ensure gives very promising result for ore blend modelling and simulation.

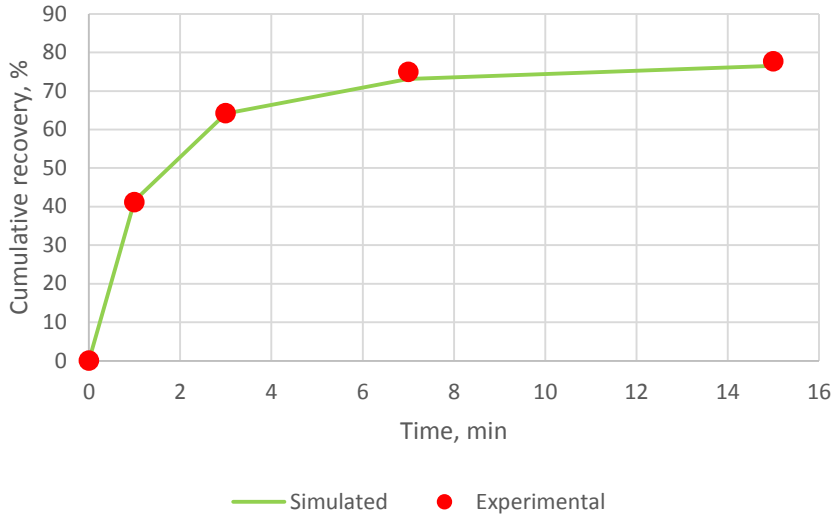

Figure 41. Simulated kinetic curve and experimental cumulative recoveries in RMG10 flotation test.

RMG12 and RMG13 flotation tests were special tests because three and four ores were blended. Reagent dosages and grinding times were weighed averages so it is impossible to proof were the conditions completely correct but however, particle size was optimal because it was measured with laser after grinding. Also, reference tests for Madneuli VIII-C1 and Madneuli VIII-C2 were not successful because of overflowing, during the first minute of flotation tests. Results are promising and show that it could be possible to simulate blends including more than two ores. Experimental grades are lower than simulated and comparably recoveries are higher. These two aspects are probable reasons for overflowing in two reference tests. In addition, higher mass pulls in the experimental tests is analogous reason for that.

Table 6. Simulated and experimental results from RMG12 and RMG13 tests.

Test	XI/V/VIII-C1/VIII-C2	Cu grade %	Cu grade %	Cu Rec %	Cu Rec %	Mass pull %	Mass pull %	Py grade %	Py grade %
		Sim	Exp	Sim	Exp	Sim	Exp	Sim	Exp
RMG13	25/25/25/25	2.02	1.64	73.52	77.80	14.84	19.0	11.73	10.40
RMG12	50/0/25/25	1.62	1.31	79.19	81.20	19.11	23.80	10.21	10.0

4.5 Blend cleaner flotation tests

Blend flotation tests for cleaner phase were conducted with similar blends than in rougher flotation tests. Madneuli XI and V were blended with 25% steps and XI/V ratios were; 100/0, 75/25, 50/50, 25/75 and 0/100. Simulated and experimental copper grades and recoveries to cleaner concentrate are shown in Appendix 5. In the simulation, the used feed definition is back-calculated mineral grades from cleaner flotation tests. Simulation flowsheet includes individual conditioners for rougher and cleaner flotation (Figure 24). Kinetics for rougher conditioner is the same as used in rougher reference flotation simulation. Kinetics for cleaner flotation is defined from cleaner reference flotation tests. Because rougher kinetics are from different flotation tests than cleaner flotation, the end member points are not exactly the same.

The reference test for Madneuli XI cleaner has not succeeded due to overflowing during rougher flotation. Mineral kinetics from Madneuli XI reference test are determined from separate flotation test done earlier in ORC. Elemental copper and copper mineral kinetics from separate flotation test can be seen in Figure 42. Cumulative flotation time was 8 minutes when it was 12 minutes in other flotation tests. However, the kinetics are comparable and can be used in this thesis work. There are no experimental results from Madneuli XI cleaner flotation test because of the shorter flotation time. Comparison between simulated and experimental results is correlating quite well and cleaner flotation results look promising.

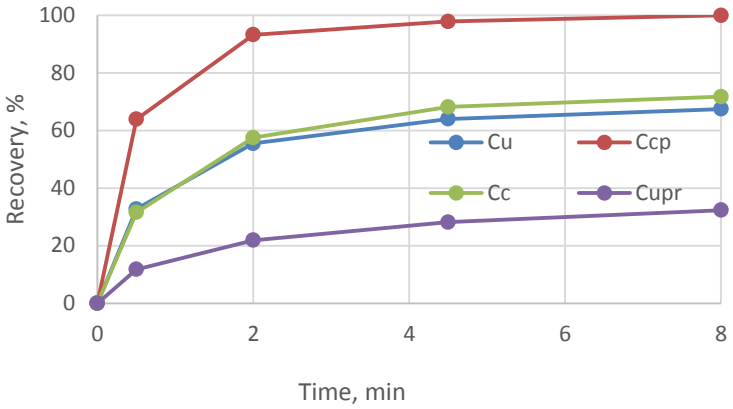

Figure 42. Elemental copper and copper mineral kinetics of Madneuli XI simulation reference flotation test.

Figure 43 and Figure 44 show kinetics from reference and blend cleaner flotation tests. It is easy to indicate that Madneuli XI reference test has failed because of overflowing and especially pyrite and NSG recoveries are clearly higher than in other flotation tests. This is the reason why this RMG5 reference test was no useful for simulation work of cleaner blends.

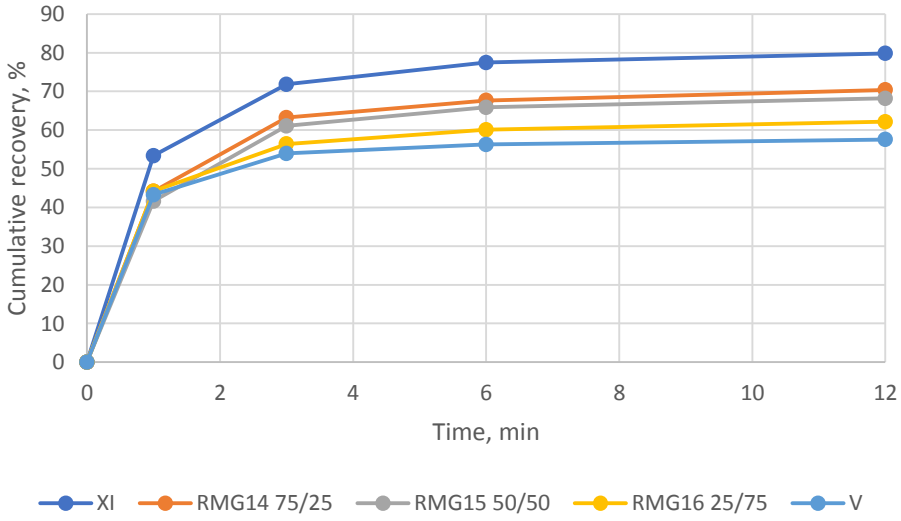

Figure 43. Kinetics of elemental copper in cleaner flotation tests.

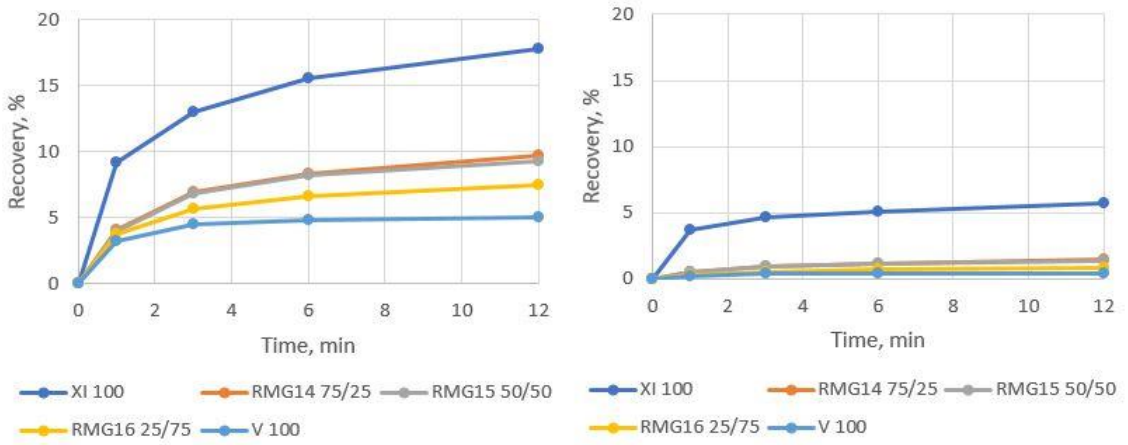

Figure 44. Kinetics of pyrite (left) and NSG (right) in blend cleaner flotation tests.

Simulated and experimental copper grade in cleaner concentrate is shown in Figure 45. Madneuli V reference points are matching. Madneuli XI experimental reference point is missing because, in reference flotation test, the used flotation time was 8 minutes, so it is not comparable with other flotations. The R^2 value of the experimental points of copper grades is 0,93. Simulated and experimental copper recoveries are shown in Figure 46. Simulated and experimental recoveries are responding each other's, and results look very promising. The R^2 value of experimental recoveries is 0,97. Figure 47 shown experimental and simulated results of cleaner concentrate mass pulls in cleaner blend flotation tests. The R^2 value is 0,94 for experimental mass pull results. Back-calculated mineral grades in rougher and cleaner reference tests are presented in Appendix 8.

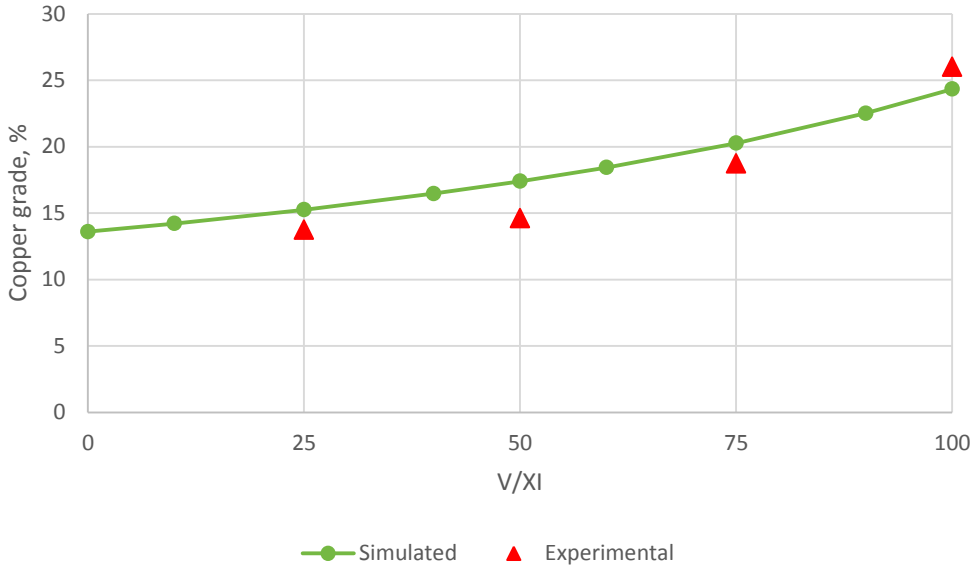

Figure 45. Copper grade in cleaner concentrate in cleaner blend flotation tests.

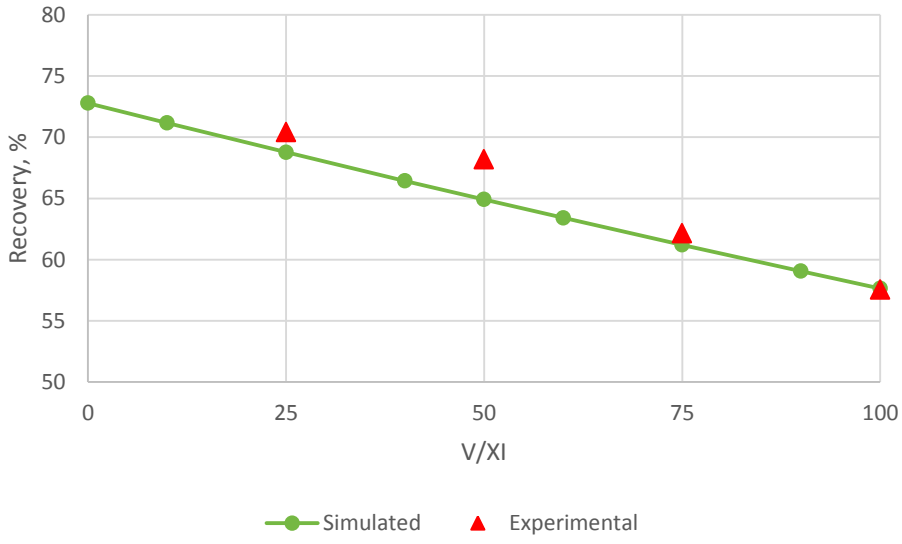

Figure 46. Copper recovery to cleaner concentrate in cleaner blend flotation tests.

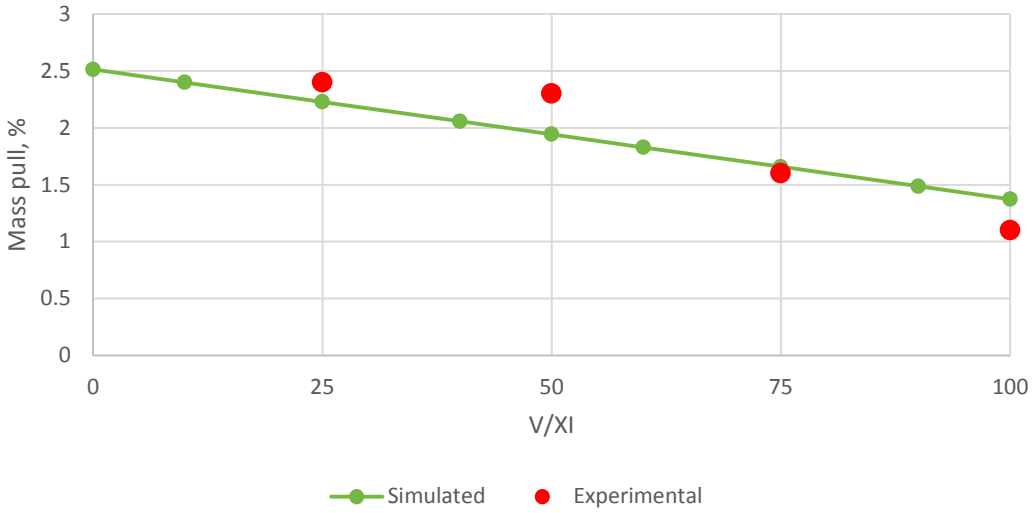

Figure 47. Cleaner concentrate mass pull in cleaner blend flotation tests.

4.6 Validation

During this thesis work, the used ores were pretty similar to each other. The validation has a margin of error because it would require more flotation tests with various blending and more different ores. But results of this thesis are very promising and blend the simulation can be made if ores have similar mineralogy together. The validation of simulation model was done by comparing the results of simulated and experimental results. In rougher flotation, results are close to each other. In cleaner flotation, the results are also looking very promising even if another reference kinetics are from older reference flotation test. Results of simulated and experimental rougher flotations are compared in parity charts. Actual correlations are possible to see in these graphs (Figure 48, Figure 49 and Figure 50). R^2 values are calculated for copper recovery (0.963), copper grade (0.989) and rougher concentrate mass pull (0.953) in rougher blend flotations.

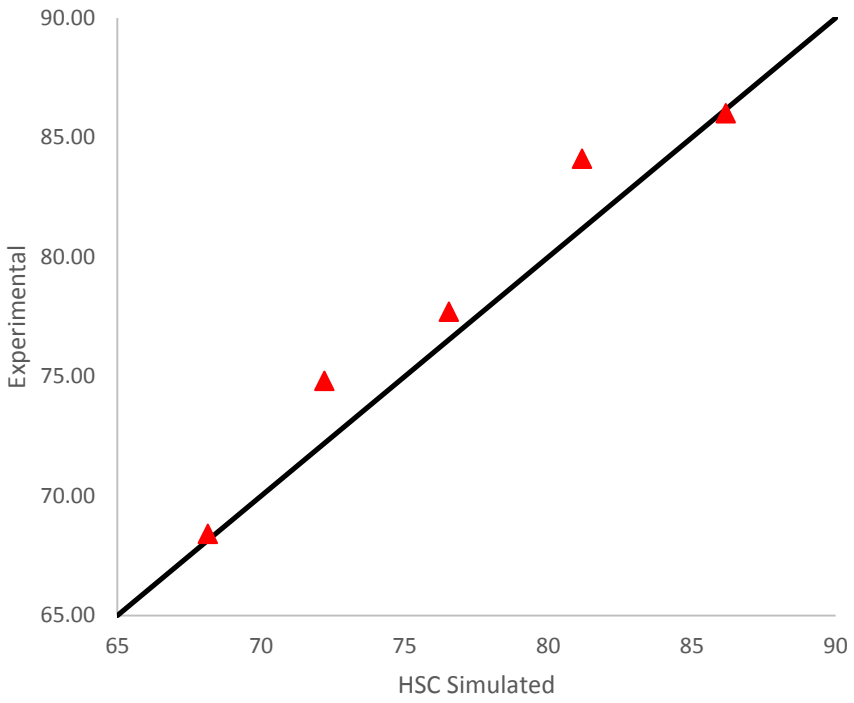

Figure 48. Copper recovery in rougher flotation tests - Parity chart.

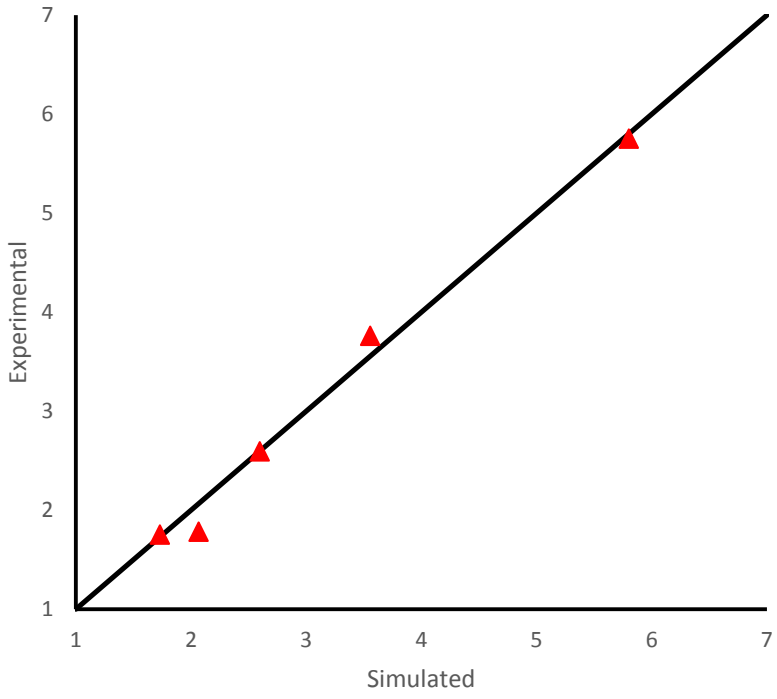

Figure 49. Copper grade in rougher concentrate - Parity chart.

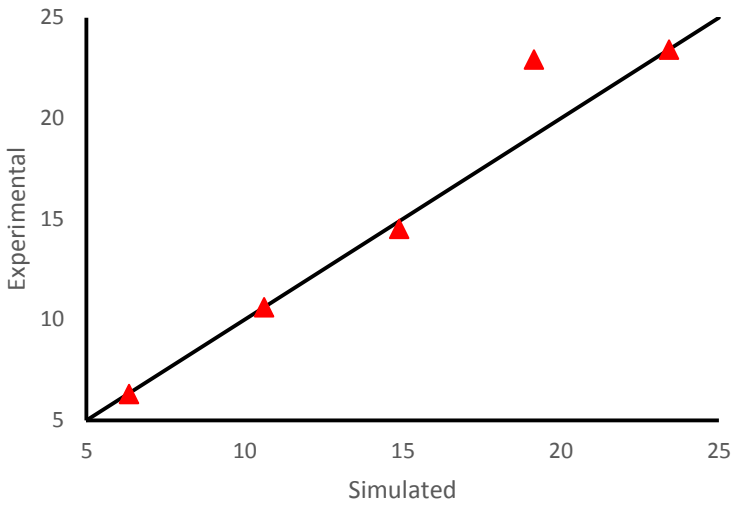

Figure 50. Mass pull to rougher concentrate - Parity chart.

Ore samples were analyzed earlier, and results are included in Outotec report. The report includes elemental copper and mineral grades for each ore. During thesis work, grades are back-calculated in mass balances. Mass balance calculations are based on chemical analysis results. Elemental copper and copper minerals (ccp, cc and cupr) grades are compared together with the previous report and back-calculated results. Comparison of these results is performed in parity charts which can be found from Appendix 8. Parity charts confirm that calculations are correct because results are close to each other.

4.7 Discussion

The main object of this thesis work was to study and validate the simulation and modelling of flotation behavior of different ore blends based on the experimental flotation tests done during thesis project. Existing literature is focused more into fundamental flotation modelling and phenomena of flotation into which the methodology and theory of this thesis are based on.

Madneuli XI/V ores were blended in different proportions. Findings in rougher flotation correlate with simulated results with good agreement given R^2 values of 0.96, 0.99, 0.95 for copper grade, copper recovery and concentrate mass pull respectively. Cleaner flotation results don't give same agreement than rougher flotation results but still the differences are not significant (R^2 values for grade (0.93), recovery (0.97) and mass pull (0.94)). Results suggest that finding of the thesis and future studies of the same topic could be applied in design work and could influence the design and optimization of the concentrator because of savings, both in time and costs, in experimental test work.

The similarity of the ore mineralogy can be considered as a limitation. All four ore included the same five minerals in modelling and simulations, and other ore variable (such as gangue composition, grindability, flotation behavior) were also similar to each other. However, there ores originate from the ongoing mining operation, and thus represent a true case.

The main important output of the thesis is the correlation between experimental and simulated test results. The R-squared values for copper grade, copper recovery and concentrate mass pull are >0,95 in rougher flotation showing the experimental results were close to the model trend line. The little differences can be explained by variations in independent variables such as a small overflowing during the beginning of flotation tests and difficulty for selecting the liquid line to start the flotation tests.

Correlation of both results was done based on elemental copper and mineral grades and recoveries. Elemental copper and copper mineral grades are increasing more when there is higher copper oxides/sulfates/chalcopyrite ratio in the feed. When the ratio is lower in the feed, grades will decrease which is correct as the copper is contributed by various Cu-minerals. The copper recovery value is linearly decreasing when there is more Madneuli V ore. The recovery is increasing when feed includes more Madneuli XI ore because it includes more Cu-sulfides in the composition (Figure 14 and Figure 28). Difference between grade and recovery is that the values of recovery increase/decrease linearly while the values of copper and copper mineral grades increase/decrease exponentially.

Validation chapter represents the correlation between the feeds mineralogy and back-calculated feed grades of mass balances. Correlation of back-calculated and analyzed mineral grades indicates that mass balance calculations are correct and, simulation inputs are right. This thesis is a good starting point for studying ore blend modelling and simulation.

5 CONCLUSIONS

The validation of the ore blend flotation simulation model was studied in this thesis work. The conducted experiments were rougher and cleaner flotation tests for four end-member ores. In addition to reference tests, 12 different ore blend flotation tests were made. HSC Chemistry Sim simulations were done for same ore blends and results were compared then together.

The main object was to create similar flotation conditions for each flotation test while only variable was the proportion of each ore type. First reference flotation tests were executed for pure ore types and then two ores were blended with different proportions. Madneuli XI and Madneuli V ores were selected to more precise examination because both of those were floated in same flotation conditions.

P80 values for grinding were almost the same (55-60 μm) and reagent dosages were the same. Even if both have similar processing requirements for flotation, the flotation performance differs from each other. In rougher flotation tests, Madneuli XI had high copper recovery (86%) and low copper grade (1,75%). Comparably Madneuli V had low copper recovery (68,4%) and higher copper grade (5,75%). Therefore, these two ore were reasonable ores for blending and this thesis work because of different metallurgical results of these two ores (Madneuli XI&V). Reason for different metallurgical performance is the distribution of copper between three copper minerals. Madneuli V had higher (copper oxide/sulfate)/(chalcopyrite) ratio comparing to Madneuli XI ratio. The amount of copper carried by chalcocite was same in both ore types.

The expectation for the experimental results was that results would be the same or similar what HSC Sim calculates. Experimental and simulated results of grades, recovery and mass pull are close with differences of less than 5% (R^2>0.95). Therefore, simulation of flotation of two blended ores with similar mineralogy as validated and works like in the real-life flotation test.

An important aspect is the repeatability of laboratory flotation tests. Flotation tests were executed with Outotec-GTK lab cell which uses automated scrapers and it allows maintain the flotation conditions better than the hand scraping. Each flotation test is carried out with the same convention but there was some overflowing in couple flotation tests. These can be seen as a too high recovery and low copper grade in individual flotation test and it explains differences in some cases. About repeatability of flotation batches, back-calculated copper and mineral grades in each flotation are not complete analogous between rougher and cleaner batch even if there are the same amounts of both ores (Appendix 8).

In summary, the modelling software HSC Sim is suitable to be used for simulation of different ore blends if ore types have similar mineralogical properties. Nevertheless, simulation requires metallurgical study and test work of each end-member ore type. Modelling work should be done for end-member ores based on experimental study. Modelling work output (R_{max} and k_{max}) is then used in simulation work. The output of this thesis shows that geometallurgical model development can exploit simulation tools like HSC Chemistry. The ideal situation is that mining companies can develop their mine plan or geometallurgical models and they can model the kind of concentrate they can produce using different ores from different deposits.

Recommendation for further test work is to blend more different ores. In this thesis, used ores were quite similar within their mineralogical perspective. For example, in each ore, there were the same five minerals used in modelling and simulations.

Another important thing is how to blend two ore with different grindability. What happens if hard and soft ores are blended? What will be the Bond work index for different blends? In this thesis work, two blended ore had almost the same grindability and Bond work index which makes blending much easier. Another recommendation is that future work should include locked cycle test work and simulation validation for accuracy. Locked cycle flotation tests are even more expensive and time-consuming projects, so simulation and modelling work would provide more savings in these cases.

6 REFERENCES

Alruiz, O, M. *et al.* (2009) 'A novel approach to the geometallurgical modelling of the Collahuasi grinding circuit', *Minerals Engineering*, 22(12), pp. 1060–1067.

Andrea, P. and Lopera, M. (2014) 'Geometallurgical Mapping and Mine Modelling - Comminution Studies : La Colosa Case Study , AMIRA P843A by'.

van den Boogaart, K. G. and Tolosana-Delgado, R. (2018) 'Handbook of Mathematical Geosciences', in *Handbook of Mathematical Geosciences: Fifty Years of IAMG*, pp. 673–686. doi: 10.1007/978-3-319-78999-6.

Brochot, S., Gonzalez Fernandez, M. and Durance, M. V. (2018) 'Fine Modelling of Ores for Geometallurgy - Based Process Simulation', in *XXIXX International Mineral Processing Congress*. Moscow.

Dominy, S. *et al.* (2018) 'Geometallurgy—A Route to More Resilient Mine Operations', *Minerals*, 8(12), p. 560. doi: 10.3390/min8120560.

Dunham, S. and Vann, J. (2007) 'Geometallurgy, Geostatistics and Project Value - Does your Block Model Tell You What You Need to Know?'

Gaudin, A. M. (1939) *Principles of minerals dressing*. New York: McGraw-Hill.

Geostat, S. (2018) *Geological services*. Available at: http://www.geostat.com/ (Accessed: 14 December 2018).

Glembotskii, V. A., Klassen, V. I. and Plaksin, I. N. (1963) *Flotation*. New York: Primary Sources.

Harbort, G. and Quan, K. (2017) 'Concentrator Design – Standard Engineering Practice versus Geometallurgy and Simulation', *Amec Foster Wheeler*.

Hukki, R. T. (1964) *Mineraalien hienonnus ja rikastus*. Helsinki: Teknillisten tieteiden

akatemia.

Kakko, K.-M. (2016) *Taustahäiriöiden ennakointi ja eliminointi ICP-OES:llä*. Jyväskylän yliopisto.

Kelly, E. G. and Spottiswood, D. J. (1982) *Introduction to Mineral Processing*. New York: A Wiley-Interscience Publication.

King, G. S. and Macdonald, J. L. (2016) 'The Business Case for Early-stage Implementation of Geometallurgy – an example from the Productora Cu-Mo-Au deposit', in *3rd International Geometallurgy Conference*. Chile, pp. 1–22.

King, R. (2012) *Modelling and simulation of mineral processing circuits*. 2nd edn. Englewood: Society for Mining, Metallurgy and Exploration.

Lamberg, P. (2011) 'PARTICLES – THE BRIDGE BETWEEN GEOLOGY AND METALLURGY', in *Conference in Minerals Engineering, Luleå*. Luleå: Luleå Tekniska Universitet. Available at: http://www.diva-portal.org/smash/record.jsf?pid=diva2%3A1013733&dswid=-6398.

Liipo, J. *et al.* (2018) 'Geometallurgical characterization of complex copper-gold ores', in *Geometallurgy 2018 Conference*. Cape Town: The Southern African Institute of Mining and Metallurgy, pp. 1–9.

Liipo, J. *et al.* (2019) 'Geometallurgical characterization of South Georgian complex copper-gold ores', *Journal of the Southern African Institute of Mining and Metallurgy*, 119.

Lotter, N. O. (2011) 'Modern Process Mineralogy: An integrated multi-disciplined approach to flowsheeting', *Minerals Engineering*. Elsevier Ltd, 24(12), pp. 1229–1237. doi: 10.1016/j.mineng.2011.03.004.

Lotter, N. O., Whiteman, E. and Bradshaw, D. J. (2014) 'Modern practice of laboratory flotation testing for flowsheet development - A review', *Minerals Engineering*. Elsevier

Ltd, 66, pp. 2–12. doi: 10.1016/j.mineng.2014.04.023.

Lukkarinen, T. (1987) *Mineraalitekniikka*. 2nd edn. Helsinki: Insinööritieto.

Lund, C. (2013) *Mineralogical, chemical and textural characterisation of the Malmberget iron ore deposit for a geometallurgical model*, *Lulea University of Technology*. doi: 10.1016/j.electacta.2012.07.002.

Lynch, A. J. *et al.* (1981) *Mineral and Coal Flotation Circuits*. Amsterdam: Elsevier Scientific Publishing Co.

Mwanga, A., Rosenkranz, J. and Lamberg, P. (2017) 'Development and experimental validation of the Geometallurgical Comminution Test (GCT)', *Minerals Engineering*. Elsevier, 108(April), pp. 109–114. doi: 10.1016/j.mineng.2017.04.001.

Oberkampf, W. L., Trucano, T. G. and Hirsch, C. (2002) 'Verification and Validation for Modeling and Simulation in Computational Science and Engineering', in *Foundations for Verification and Validation in the 21st Century Workshop*, pp. 1–74.

Outotec (2016) *HSC Chemistry*. Available at: https://www.outotec.com/globalassets/products/digital-solutions/hsc/ote_outotec_hsc_chemistry_eng_web.pdf (Accessed: 2 April 2019).

Pearse, M. J. (2005) 'An overview of the use of chemical reagents in mineral processing', *Minerals Engineering*, 18, pp. 139–149. doi: 10.1016/j.mineng.2004.09.015.

Rajabinasab, B. and Asghari, O. (2018) 'Geometallurgical Domaining by Cluster Analysis: Iron Ore Deposti Case Study', *Natural Resources Research*, October.

Rao, S. R. (2004) *Surface chemistry of froth flotation*. 2nd edn. New York: Kluwer Academic/Plenum Publishers.

Roy, I., Ground, C. and Board, W. (2016) 'Orebody modelling : An integrated

geological- geostatistical approach Orebody Modelling : An Integrated Geological-', (March).

Saeidi, F. (2016) *New Approach for Characterising a Breakage Event as a Multi-stage Process*. The University of Queensland.

Sargent, R. G. (1998) *Verification And Validation Of Simulation Models*.

Schlesinger, S. (1979) 'Terminology for Model Credibility', *Simulation*, 32(3), pp. 103–104.

Schubert, H. (1999) 'On the turbulence-controlled microprocesses in flotation machines', *International Journal of Mineral Processing*, 56, pp. 257–276.

Singh, K. (2017) 'A Geometallurgical Forecast Model For Predicting Concentrate Quality in WLIMS Process for Leveäniemi Ore', *Lulea University of Technology*.

Talikka, M. *et al.* (2018) 'Copper Ore Variability – Benefits of Advanced Simulation', (July), pp. 10–12.

Tutorialspoint (2019) *Modelling and simulation, Verification & validation*, *tutorialspoint.com*. Available at: https://www.tutorialspoint.com/modelling_and_simulation/modelling_and_simulation_verification_validation.htm (Accessed: 21 May 2019).

Wills, B. A. and Napier-Munn, T. (2006) *Will's mineral processing technology: an introduction to the practical aspects of ore treatment and mineral recovery*. 7th edn. Oxford: Elsevier/Butterworth-Heinemann.

7 APPENDICES

Appendix 1. Particle sizes of each unit after different grinding times.

Appendix 2. Fitted kinetic curves drawn using HSC Sim model fit tool.

Appendix 3. Mass balances of each flotation test.

Appendix 4. Element and mineral kinetics of rougher flotations.

Appendix 5. HSC Sim simulated and experimental results of flotation tests.

Appendix 6. Parity charts of rougher flotation results.

Appendix 7. Compared results between experimental and simulated tests.

Appendix 8. Elemental copper and copper mineral grades from mineralogy report and mass balances.

Appendix 1 (1). Particle sizes of each unit after 5, 15, 20 and 30 minutes grinding.

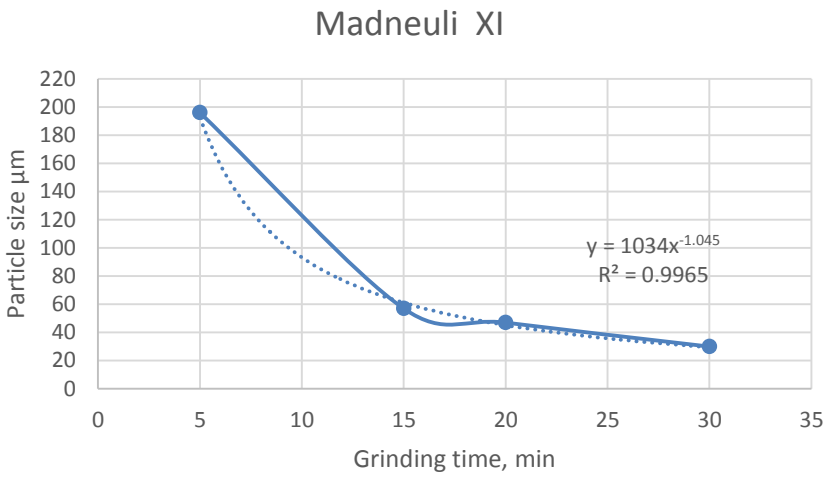

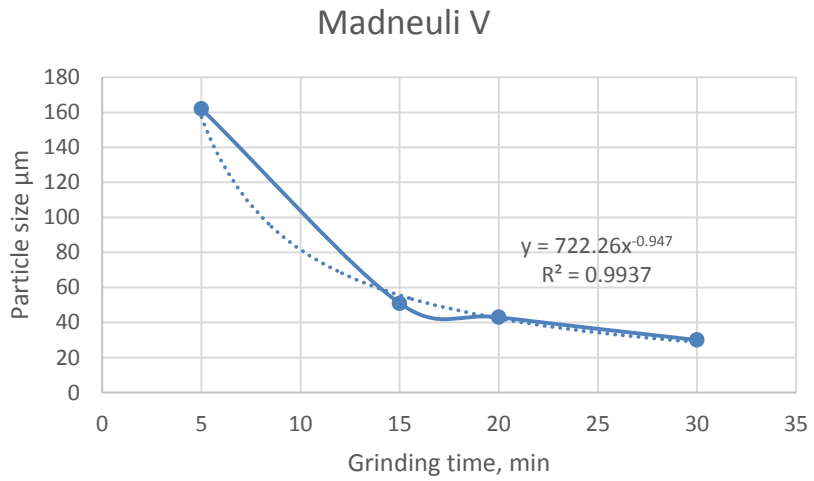

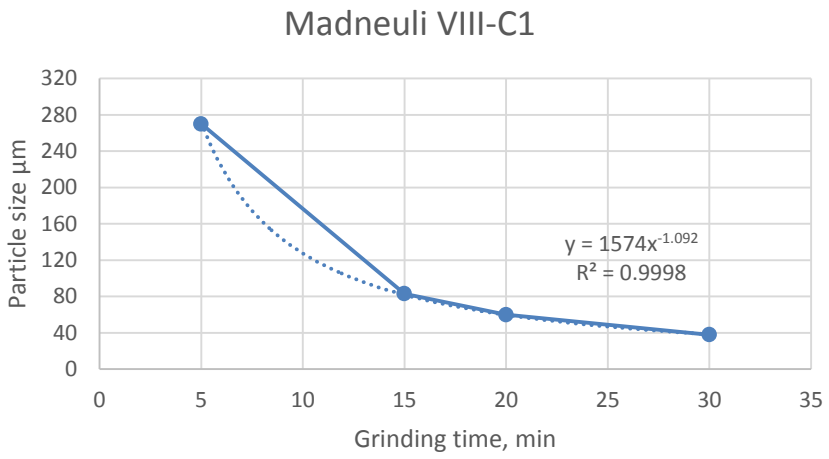

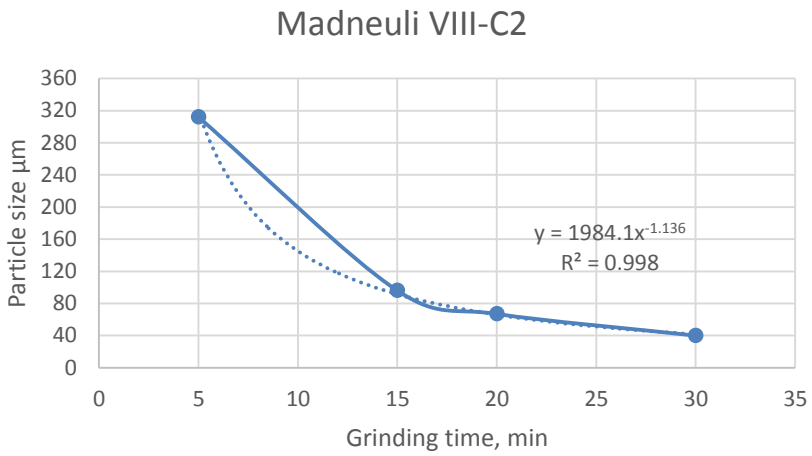

Appendix 1 (2). Particle size distribution charts of each grinding and sieving test.

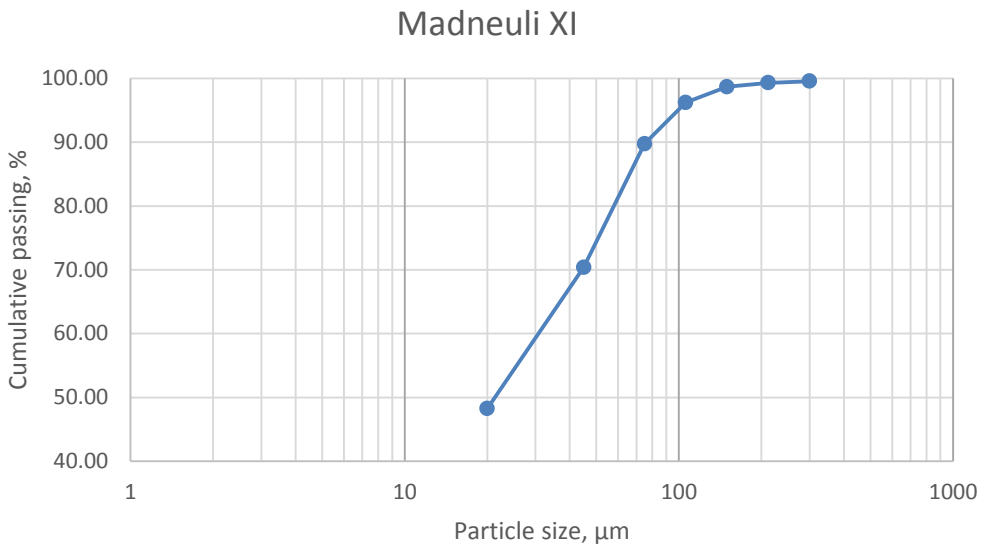

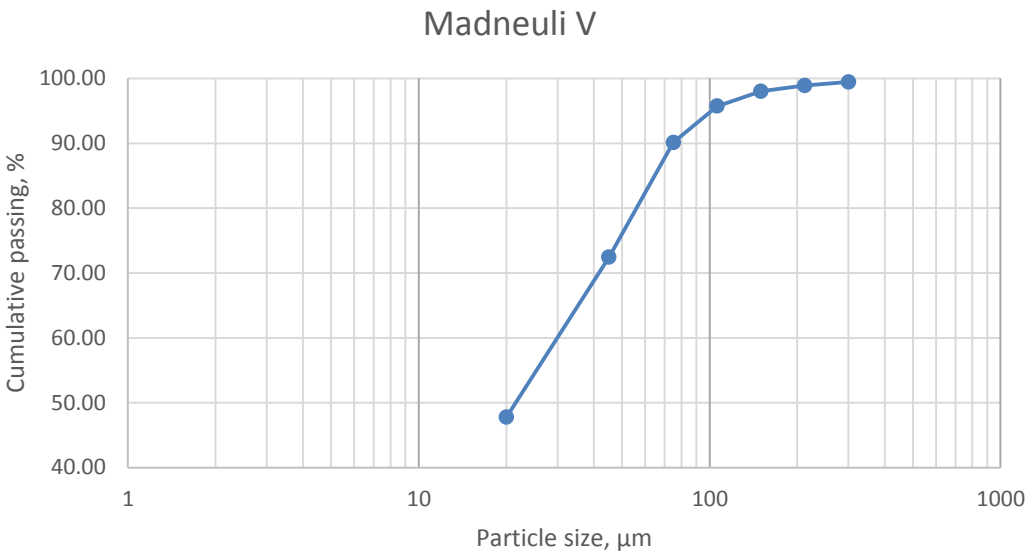
Madneuli V
100.00
90.00
80.00
70.00
60.00
50.00
40.00
Cumulative passing, %
1
10
100
1000
Particle size, µm

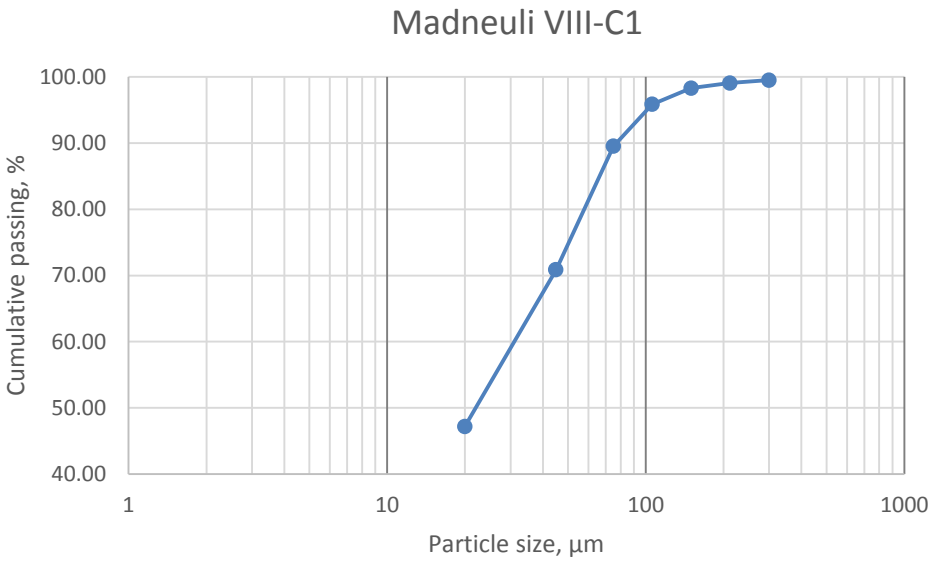
Madneuli VIII-C1
100.00
90.00
80.00
70.00
60.00
50.00
40.00
Cumulative passing, %
1
10
100
1000
Particle size, µm

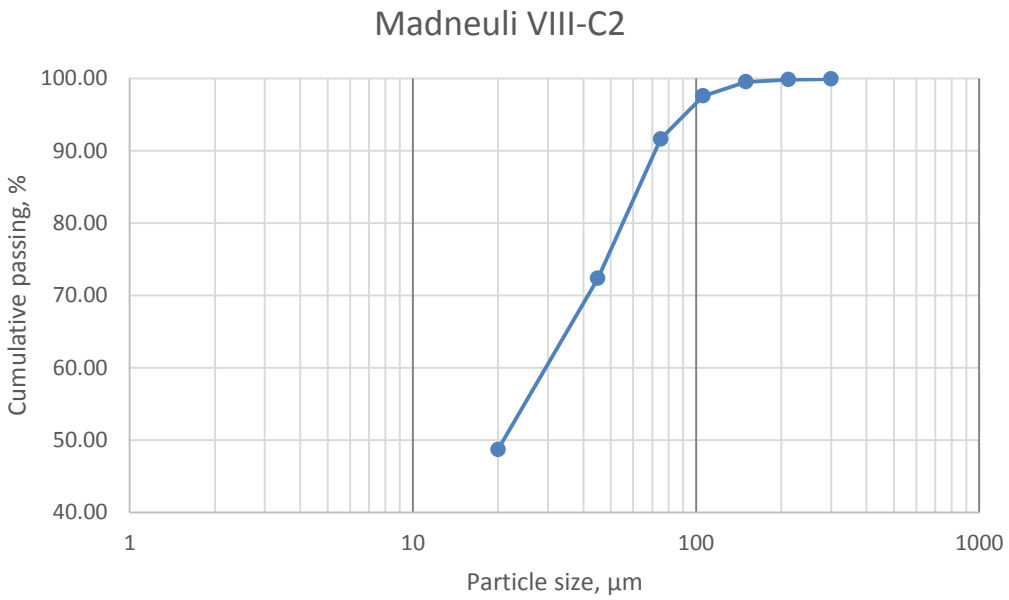
Madneuli VIII-C2
100.00
90.00
80.00
70.00
60.00
50.00
40.00
Cumulative passing, %
1
10
100
1000
Particle size, µm

Appendix 2 (1). Fitted kinetic curves drawn using HSC Sim model fit tool. RMG1 – Madneuli XI

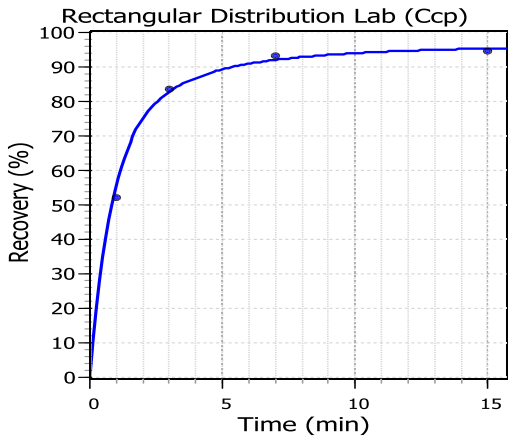

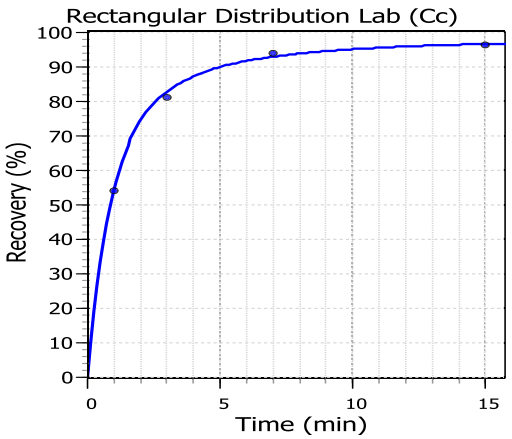

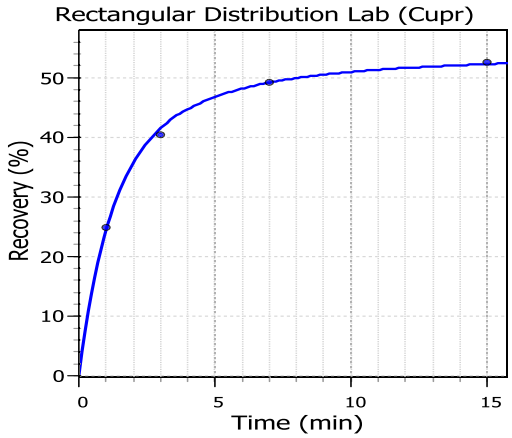

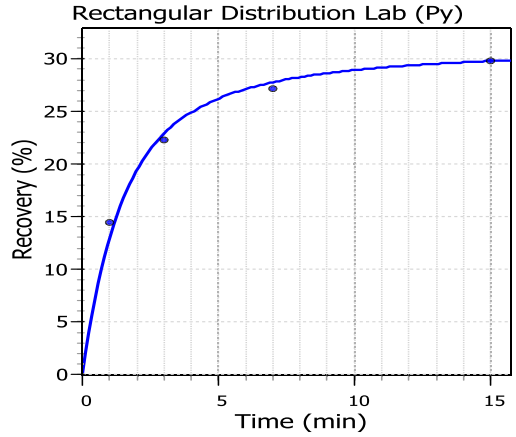

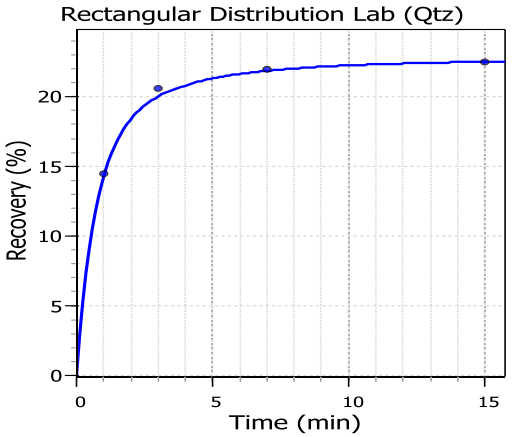

Appendix 2 (2). Fitted kinetic curves drawn using HSC Sim model fit tool. RMG2 – Madneuli V

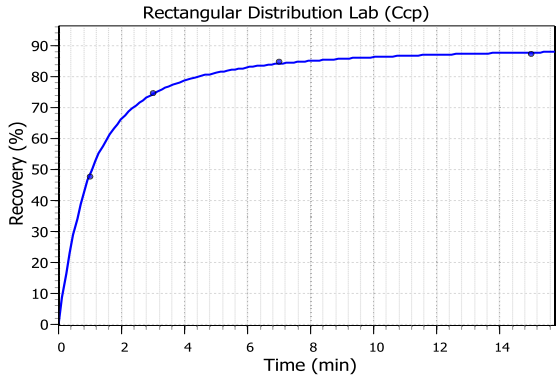

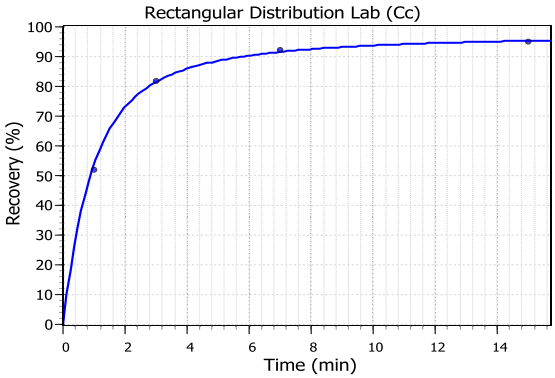

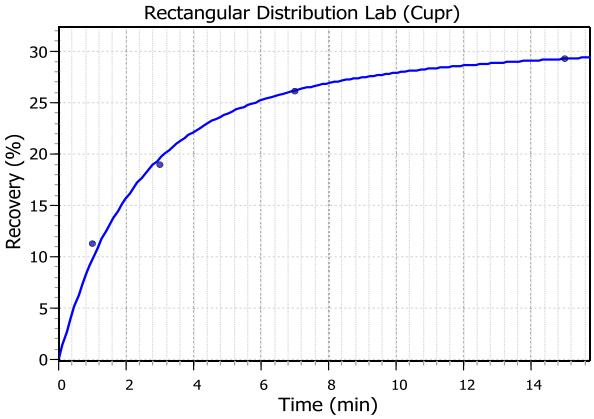

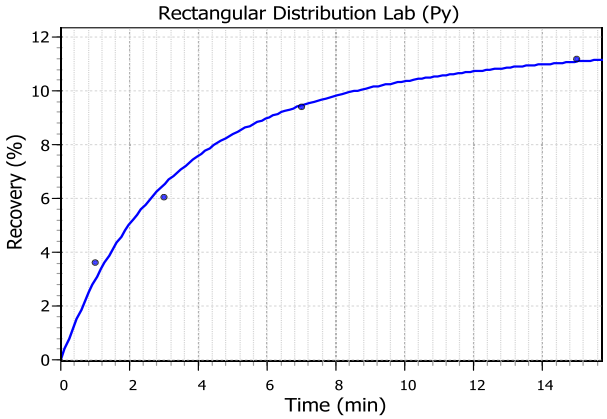

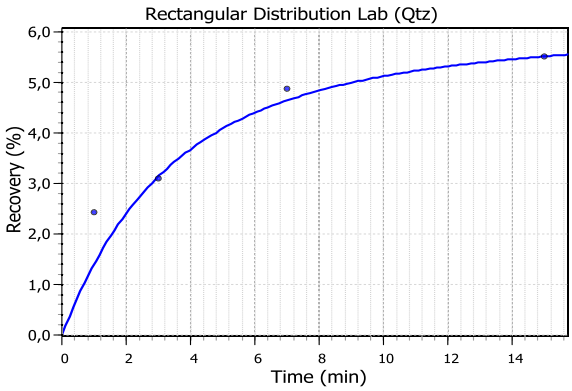

Appendix 2 (3). Fitted kinetic curves drawn using HSC Sim model fit tool. RMG5 – Cleaner flotation Madneuli XI

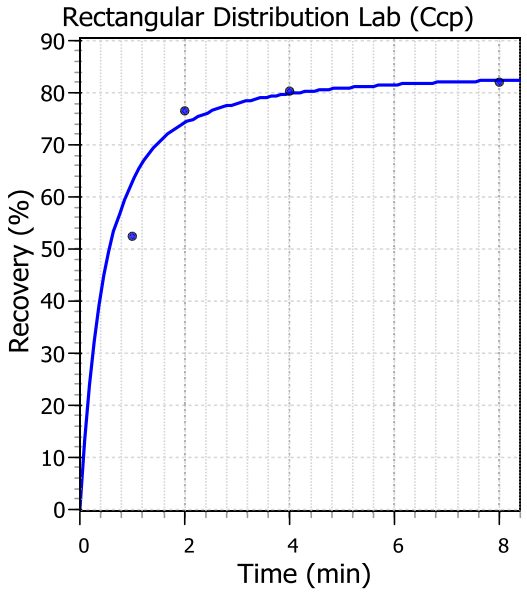

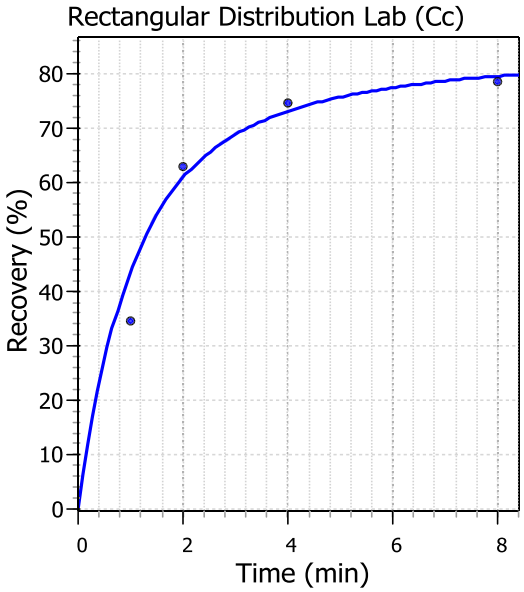

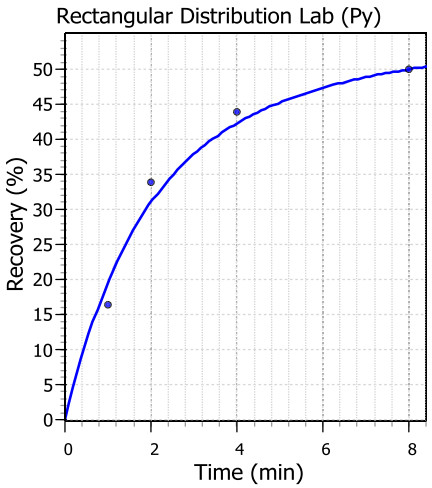

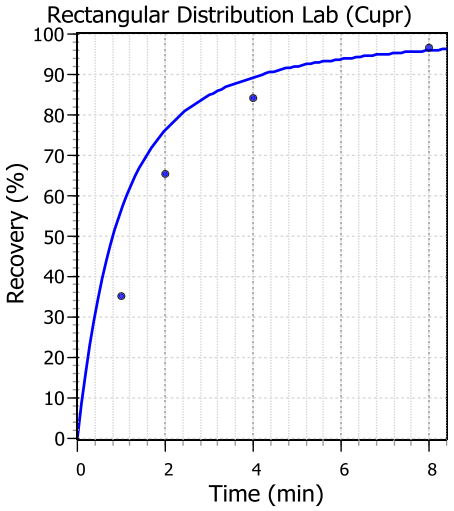

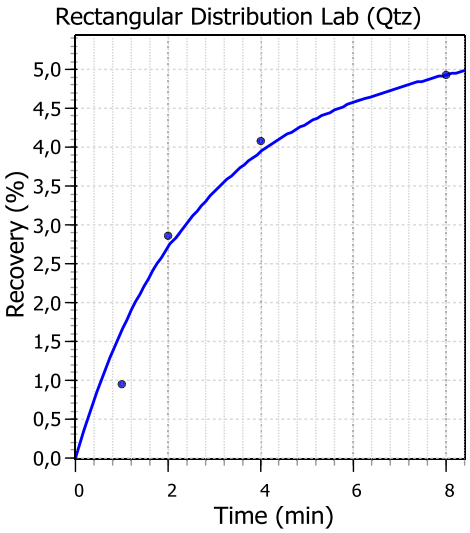

Appendix 2 (5). Fitted kinetic curves drawn using HSC Sim model fit tool. RMG6 – Cleaner flotation Madneuli V

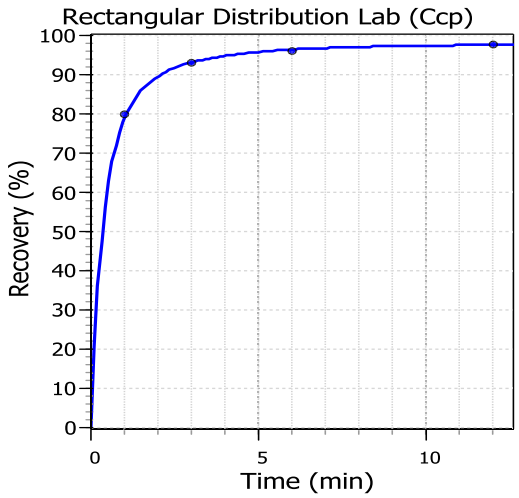

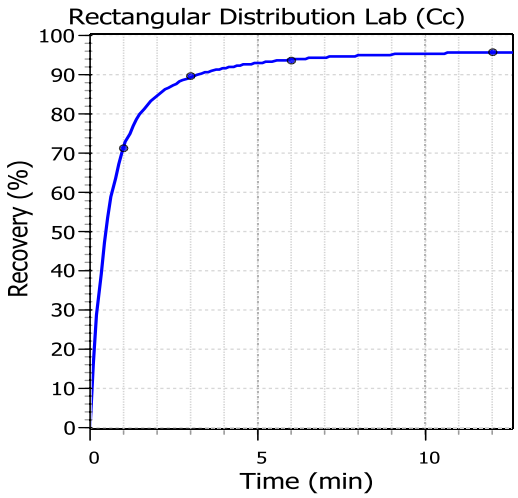

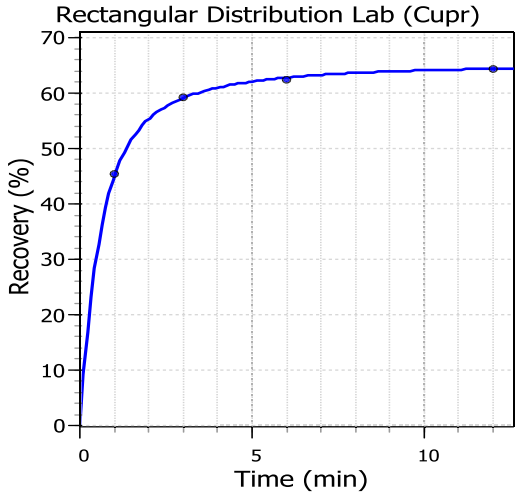

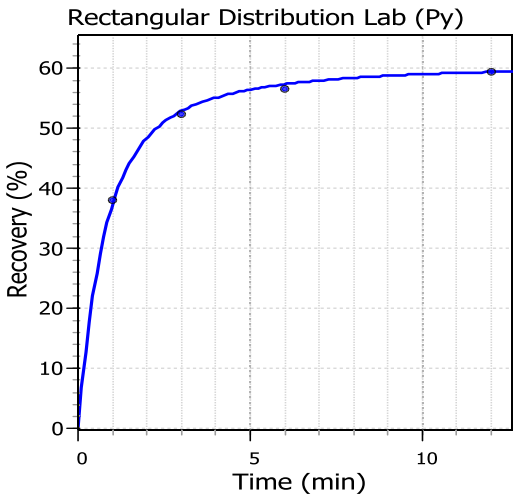

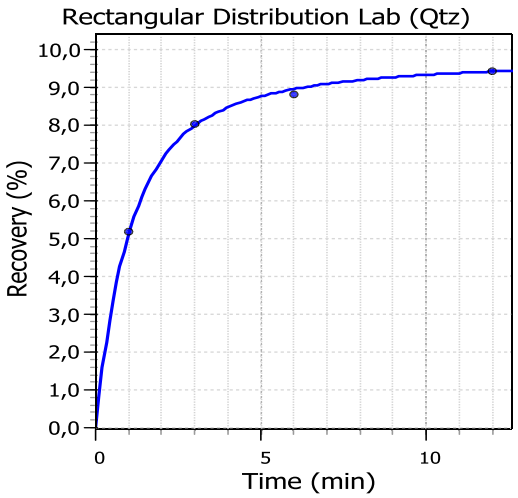

Streams Madneuli XI	Stream type	Weight		CuTOT		Chalcopyrite		Chalcocite		Cuprite		S		Py		Qtz	
		g	%	%	Rec-%	%	Rec-%	%	Rec-%	%	Rec-%	%	Rec-%	%	Rec-%	%	Rec-%
Feed	Analyzed	1499.9	100.00														
Ground feed	Analyzed	1499.9	100.00														
Flotation feed	Calculated	1499.9	100.00	0.48	100.00	0.45	100.00	0.26	100.00	0.12	100.00	2.81	100.00	4.87	100.00	94.29	100.00
RC1	Analyzed	221.4	14.8	1.51	46.89	1.590	52.26	0.980	54.61	0.20	25.40	3.3	17.30	4.770	14.46	92.460	14.47
RT1	Calculated	1278.5	85.2	0.25	53.11							2.33	82.70				
RC2	Analyzed	95.8	6.4	1.93	25.93	2.220	31.57	1.130	27.24	0.29	15.93	4.2	9.53	5.980	7.85	90.380	6.12
RT2	Calculated	1182.7	78.9	0.13	27.17							2.06	73.17				
RC3	Analyzed	24.3	1.6	3.19	10.87	2.690	9.70	2.100	12.84	0.65	9.06	9.2	5.29	14.660	4.88	79.890	1.37
RT3	Calculated	1158.4	77.2	0.08	16.30							1.91	67.87				
RC4	Analyzed	9.5	0.6	1.71	2.28	0.960	1.35	1.010	2.41	0.64	3.49	11.4	2.57	20.320	2.64	77.070	0.52
RT4	Analyzed	1148.9	76.6	0.087	14.02	0.030	5.12	0.010	2.89	0.07	46.12	2.4	65.31	4.460	70.17	95.420	77.51
RC1	Combined	221.4	14.8	1.510	46.89	1.590	52.26	0.980	54.606	0.200	25.396	3.30	17.30	4.77	14.46	92.46	14.47
RC1+RC2	Combined	317.2	21.1	1.637	72.83	1.780	83.83	1.025	81.851	0.227	41.329	3.57	26.83	5.14	22.31	91.83	20.60
RC1+RC2+RC3	Combined	341.5	22.8	1.747	83.70	1.845	93.53	1.102	94.694	0.257	50.388	3.97	32.13	5.81	27.19	90.98	21.97
RC1+RC2+RC3+RC4	Combined	351.0	23.4	1.746	85.98	1.821	94.88	1.099	97.109	0.268	53.875	4.17	34.69	6.21	29.83	90.61	22.49

Streams Madneuli V	Stream type	Weight		CuTOT		Chalcopyrite		Chalcocite		Cuprite		S		Py		Qtz	
		g	%	%	Rec-%	%	Rec-%	%	Rec-%	%	Rec-%	%	Rec-%	%	Rec-%	%	Rec-%
Feed	Analyzed	1488.2	100.00	0.52								3.36					
Ground feed	Analyzed	1488.2	100.00	0.52								3.36					
Flotation feed	Calculated	1488.2	100.00	0.53	100.00	0.23	100.00	0.31	100.00	0.24	100.00	3.08	100.00	5.49	100.00	93.73	100.00
RC1	Analyzed	41.3	2.8	6.84	35.57	4.040	48.05	5.760	51.38	0.95	11.13	6.4	5.76	7.160	3.62	82.090	2.43
RT1	Calculated	1446.9	97.2	0.34	64.43							2.90	94.24				
RC2	Analyzed	13.9	0.9	11.90	20.83	6.790	27.18	9.830	29.51	1.91	7.53	12.0	3.64	14.310	2.43	67.160	0.67
RT2	Calculated	1433.0	96.3	0.23	43.60							2.79	90.60				
RC3	Analyzed	28.6	1.9	2.53	9.11	1.240	10.21	1.670	10.32	0.87	7.06	5.9	3.68	9.600	3.36	86.630	1.78
RT3	Calculated	1404.4	94.4	0.18	34.49							2.68	86.92				
RC4	Analyzed	10.7	0.7	2.15	2.90	0.820	2.53	1.200	2.77	1.02	3.10	7.8	1.82	13.610	1.78	83.350	0.64
RT4	Analyzed	1393.7	93.7	0.180	31.59	0.030	12.04	0.020	6.02	0.18	71.18	2.8	85.10	5.210	88.81	94.560	94.48
RC1	Combined	41.3	2.8	6.840	35.57	4.040	48.05	5.760	51.380	0.950	11.132	6.40	5.76	7.16	3.62	82.09	2.43
RC1+RC2	Combined	55.2	3.7	8.114	56.40	4.732	75.22	6.785	80.891	1.192	18.665	7.81	9.40	8.96	6.05	78.33	3.10
RC1+RC2+RC3	Combined	83.8	5.6	6.208	65.51	3.541	85.43	5.039	91.206	1.082	25.725	7.16	13.08	9.18	9.41	81.16	4.88
RC1+RC2+RC3+RC4	Combined	94.5	6.3	5.749	68.41	3.232	87.96	4.605	93.980	1.075	28.821	7.23	14.90	9.68	11.19	81.41	5.52

Streams Madneuli VIII-C1	Stream type	Weight		CuTOT		Chalcopyrite		Chalcocite		Cuprite		S		Py		Qtz	
		g	%	%	Rec-%	%	Rec-%	%	Rec-%	%	Rec-%	%	Rec-%	%	Rec-%	%	Rec-%
Feed	Analyzed	1406.8	100.00	0.31								5.13					
Ground feed	Analyzed	1406.8	100.00	0.31								5.13					
Flotation feed	Calculated	1406.8	100.00	0.32	100.00	0.33	100.00	0.15	100.00	0.10	100.00	5.10	100.00	9.26	100.00	90.16	100.00
RC1	Analyzed	137.1	9.7	1.42	42.75	2.060	60.71	0.690	43.98	0.170	16.79	6.0	11.47	9.620	10.12	87.457	9.45
RT1	Calculated	1269.7	90.3	0.19	57.25							4.51	88.53				
RC2	Analyzed	27.4	1.9	2.79	16.79	3.080	18.14	1.870	23.82	0.260	5.13	9.3	3.55	14.680	3.09	80.109	1.73
RT2	Calculated	1242.3	88.3	0.13	40.47							4.33	84.97				
RC3	Analyzed	27.7	2.0	1.67	10.16	1.430	8.51	1.180	15.19	0.270	5.39	9.9	3.83	17.150	3.65	79.985	1.75
RT3	Calculated	1214.6	86.3	0.10	30.31							4.14	81.15				
RC4	Analyzed	23.2	1.6	0.81	4.15	0.480	2.39	0.550	5.93	0.240	4.01	9.4	3.04	17.070	3.04	81.670	1.49
RT4	Analyzed	1191.4	84.7	0.100	26.16	0.040	10.24	0.020	11.08	0.080	68.67	4.7	78.10	8.760	80.10	91.100	85.57
RC1	Combined	137.1	9.7	1.420	42.75	2.060	60.71	0.690	43.977	0.170	16.793	6.00	11.47	9.62	10.12	87.46	9.45
RC1+RC2	Combined	164.5	11.7	1.648	59.53	2.230	78.85	0.887	67.796	0.185	21.926	6.55	15.03	10.46	13.21	86.23	11.18
RC1+RC2+RC3	Combined	192.2	13.7	1.651	69.69	2.115	87.36	0.929	82.991	0.197	27.315	7.03	18.85	11.43	16.86	85.33	12.93
RC1+RC2+RC3+RC4	Combined	215.4	15.3	1.561	73.84	1.939	89.76	0.888	88.923	0.202	31.326	7.29	21.90	12.03	19.90	84.94	14.43

Streams Madneuli VIII-C2	Stream type	Weight		CuTOT		Chalcopyrite		Chalcocite		Cuprite		S		Py		Qtz	
		g	%	%	Rec-%	%	Rec-%	%	Rec-%	%	Rec-%	%	Rec-%	%	Rec-%	%	Rec-%
Feed	Analyzed	1446.4	100.00	0.28								5.35					
Ground feed	Analyzed	1446.4	100.00	0.28								5.35					
Flotation feed	Calculated	1446.4	100.00	0.29	100.00	0.14	100.00	0.18	100.00	0.12	100.00	5.07	100.00	9.32	100.00	90.24	100.00
RC1	Analyzed	107.3	7.4	1.25	31.61	1.141	62.49	0.816	33.25	0.229	13.89	8.4	12.30	14.661	11.67	83.153	6.84
RT1	Calculated	1339.1	92.6	0.20	68.39							4.44	87.70				
RC2	Analyzed	28.0	1.9	2.39	15.77	1.672	23.90	1.903	20.24	0.328	5.19	15.1	5.77	26.439	5.49	69.658	1.49
RT2	Calculated	1311.1	90.6	0.15	52.62							4.15	81.93				
RC3	Analyzed	31.5	2.2	1.57	11.65	0.728	11.71	1.302	15.58	0.313	5.57	20.3	8.73	37.011	8.65	60.646	1.46
RT3	Calculated	1279.6	88.5	0.12	40.97							3.71	73.20				
RC4	Analyzed	40.6	2.8	0.62	5.93	0.092	1.91	0.450	6.94	0.261	5.99	13.1	7.26	24.278	7.31	74.919	2.33
RT4	Analyzed	1239.0	85.7	0.120	35.04	0.000	0.00	0.051	24.00	0.099	69.35	3.9	65.94	7.277	66.88	92.573	87.88
RC1	Combined	107.3	7.4	1.250	31.61	1.141	62.49	0.816	33.252	0.229	13.892	8.40	12.30	14.66	11.67	83.15	6.84
RC1+RC2	Combined	135.3	9.4	1.486	47.38	1.251	86.39	1.041	53.488	0.249	19.085	9.79	18.07	17.10	17.16	80.36	8.33
RC1+RC2+RC3	Combined	166.8	11.5	1.502	59.03	1.152	98.09	1.090	69.064	0.261	24.659	11.77	26.80	20.86	25.81	76.64	9.79
RC1+RC2+RC3+RC4	Combined	207.4	14.3	1.329	64.96	0.945	100.00	0.965	76.002	0.261	30.650	12.03	34.06	21.53	33.12	76.30	12.12

Streams RMG5	Stream type	Weight		CuTOT		Chalcopyrite		Chalcocite		Cuprite		S		Py		Qtz	
		g	%	%	Rec-%	%	Rec-%	%	Rec-%	%	Rec-%	%	Rec-%	%	Rec-%	%	Rec-%
Feed	Analyzed	1490.8															
Ground feed	Calculated	1490.8															
Flotation feed	Calculated	1490.8		0.44		0.30		0.33		0.09		2.55		4.44		94.83	
RC	Calculated	412.1	27.6	1.36	86.05												
RT	Analyzed	1078.7	72.4	0.08	13.95	0.00	0.00	0.03	5.43	0.07	55.13	2.20	62.42	4.11	66.86	95.80	73.10
Ground CF feed	Calculated	412.1	27.6	1.36	86.05	1.093	100.00	1.139	94.57	0.153	44.87	3.467	37.58	5.328	33.14	92.287	26.90
CC1	Analyzed	64.8	4.3	5.35	53.37	5.47	78.69	3.76	49.04	0.52	23.69	7.70	13.12	9.42	9.21	80.85	3.71
CT1	Calculated																
CC2	Analyzed	17.8	1.2	6.73	18.44	4.53	17.93	5.57	19.98	0.80	10.10	10.40	4.87	14.39	3.87	74.70	0.94
CT2	Calculated																
CC3	Analyzed	8.8	0.6	4.18	5.66	1.18	2.31	3.81	6.75	0.82	5.13	11.10	2.57	18.56	2.46	75.63	0.47
CT3	Calculated																
CC4	Analyzed	9.8	0.7	1.56	2.35	0.49	1.08	1.18	2.32	0.51	3.52	8.90	2.29	15.32	2.27	82.50	0.57
CT4	Analyzed	310.9	20.9	0.13	6.22	0.00	0.00	0.26	16.47	0.01	2.43	1.80	14.72	3.27	15.34	96.46	21.21
CC1	Combined	64.8	4.3	5.35	53.37	5.47	78.685	3.76	49.042	0.52	23.689	7.70	13.125	9.42	9.209	80.85	3.706
CC1+CC2	Combined	82.6	5.5	5.65	71.81	5.27	96.611	4.15	69.024	0.58	33.785	8.28	17.994	10.49	13.076	79.52	4.646
CC1+CC2+CC3	Combined	91.4	6.1	5.51	77.48	4.87	98.925	4.12	75.773	0.60	38.920	8.55	20.563	11.26	15.541	79.15	5.117
CC1+CC2+CC3+CC4	Combined	101.2	6.8	5.12	79.83	4.45	100.000	3.83	78.096	0.59	42.440	8.59	22.857	11.66	17.807	79.47	5.689

Streams RMG6	Stream type	Weight		CuTOT		Chalcopyrite		Chalcocite		Cuprite		S		Py		Qtz	
		g	%	%	Rec-%	%	Rec-%	%	Rec-%	%	Rec-%	%	Rec-%	%	Rec-%	%	Rec-%
Feed	Analyzed	1466.9															
Ground feed	Calculated	1466.9															
Flotation feed	Calculated	1466.9		0.49		0.14		0.28		0.24		2.90		5.23		94.10	
RC	Calculated	75.0	5.1	6.12	63.43												
RT	Analyzed	1391.9	94.9	0.19	36.57	0.00	0.00	0.02	6.70	0.19	75.16	2.70	88.23	5.04	91.44	94.74	95.54
Ground CF feed	Calculated	75.0	5.1	6.12	63.43	2.758	100.00	5.168	93.30	1.165	24.84	6.683	11.77	8.753	8.56	82.157	4.46
CC1	Analyzed	10.5	0.7	29.80	43.27	15.74	79.91	26.30	66.47	3.77	11.25	23.50	5.79	23.76	3.25	30.43	0.23
CT1	Calculated																
CC2	Analyzed	3.8	0.3	20.30	10.67	7.16	13.16	18.78	17.18	3.18	3.43	19.50	1.74	24.72	1.22	46.16	0.13
CT2	Calculated																
CC3	Analyzed	1.0	0.1	16.80	2.32	6.18	2.99	15.28	3.68	2.77	0.79	20.00	0.47	27.62	0.36	48.15	0.03
CT3	Calculated																
CC4	Analyzed	0.7	0.0	13.30	1.29	4.91	1.66	11.83	1.99	2.42	0.48	18.40	0.30	26.75	0.24	54.08	0.03
CT4	Analyzed	59.0	4.0	0.72	5.87	0.08	2.28	0.28	3.98	0.53	8.89	2.50	3.46	4.52	3.48	94.59	4.04
CC1	Combined	10.5	0.7	29.80	43.27	15.74	79.912	26.30	66.473	3.77	11.250	23.50	5.793	23.76	3.252	30.43	0.231
CC1+CC2	Combined	14.3	1.0	27.28	53.94	13.46	93.068	24.30	83.651	3.61	14.684	22.44	7.533	24.02	4.476	34.61	0.359
CC1+CC2+CC3	Combined	15.3	1.0	26.59	56.26	12.98	96.056	23.71	87.329	3.56	15.472	22.28	8.002	24.25	4.836	35.49	0.393
CC1+CC2+CC3+CC4	Combined	16.0	1.1	26.01	57.55	12.63	97.718	23.19	89.322	3.51	15.953	22.11	8.305	24.36	5.081	36.31	0.421

Streams RMG7	Stream type	Weight		CuTOT		Chalcopyrite		Chalcocite		Cuprite		S		Py		Qtz	
		g	%	%	Rec-%	%	Rec-%	%	Rec-%	%	Rec-%	%	Rec-%	%	Rec-%	%	Rec-%
Feed	Analyzed	1468.0															
Ground feed	Calculated	1468.0															
Flotation feed	Calculated	1468.0		0.30		0.27		0.15		0.11		4.85		8.85		90.63	
RC	Calculated	301.8	20.6	1.101	74.60												
RT	Analyzed	1166.2	79.4	0.097	25.40	0.02	5.85	0.02	10.88	0.09	65.35	4.80	78.57	8.96	80.46	90.92	79.69
Ground CF feed	Calculated	301.8	20.6	1.101	74.60	1.244	94.15	0.633	89.12	0.184	34.65	5.060	21.43	8.409	19.54	89.522	20.31
CC1	Analyzed	21.4	1.5	7.920	38.06	11.41	61.21	4.57	45.62	0.36	4.80	13.20	3.96	15.51	2.56	68.15	1.10
CT1	Calculated																
CC2	Analyzed	10.1	0.7	7.250	16.44	8.20	20.76	5.06	23.84	0.42	2.64	15.40	2.18	21.54	1.68	64.78	0.49
CT2	Calculated																
CC3	Analyzed	9.9	0.7	2.830	6.29	2.19	5.44	2.20	10.16	0.35	2.16	11.60	1.61	19.44	1.48	75.82	0.56
CT3	Calculated																
CC4	Analyzed	8.5	0.6	1.600	3.05	1.09	2.32	1.21	4.80	0.29	1.53	10.90	1.30	19.23	1.26	78.19	0.50
CT4	Analyzed	251.9	17.2	0.190	10.75	0.07	4.42	0.04	4.70	0.15	23.52	3.50	12.37	6.48	12.57	93.25	17.65
CC1	Combined	21.4	1.5	7.92	38.06	11.41	61.212	4.57	45.621	0.36	4.796	13.20	3.965	15.51	2.556	68.15	1.096
CC1+CC2	Combined	31.5	2.1	7.71	54.50	10.38	81.975	4.73	69.462	0.38	7.437	13.91	6.148	17.44	4.231	67.07	1.588
CC1+CC2+CC3	Combined	41.4	2.8	6.54	60.80	8.42	87.410	4.12	79.622	0.37	9.595	13.35	7.760	17.92	5.713	69.16	2.152
CC1+CC2+CC3+CC4	Combined	49.9	3.4	5.70	63.85	7.17	89.732	3.63	84.419	0.36	11.129	12.94	9.060	18.14	6.972	70.70	2.652

Streams RMG8	Stream type	Weight		CuTOT		Chalcopyrite		Chalcocite		Cuprite		S		Py		Qtz	
		g	%	%	Rec-%	%	Rec-%	%	Rec-%	%	Rec-%	%	Rec-%	%	Rec-%	%	Rec-%
Feed	Analyzed	1490.4															
Ground feed	Calculated	1490.4															
Flotation feed	Calculated	1490.4		0.30		0.12		0.18		0.14		4.84		8.91		90.67	
RC	Calculated	228.4	15.3	1.229	63.11												
RT	Analyzed	1262.0	84.7	0.130	36.89	0.00	0.00	0.05	23.98	0.11	67.41	3.90	68.27	7.28	69.22	92.57	86.45
Ground CF feed	Calculated	228.4	15.3	1.229	63.11	0.786	100.00	0.876	76.02	0.294	32.59	10.014	31.73	17.887	30.78	80.155	13.55
CC1	Analyzed	24.2	1.6	5.250	28.57	4.85	65.35	3.94	36.23	0.47	5.52	27.80	9.33	47.35	8.63	43.38	0.78
CT1	Calculated																
CC2	Analyzed	12.8	0.9	4.570	13.15	2.57	18.32	4.03	19.60	0.52	3.23	28.50	5.06	50.12	4.83	42.76	0.41
CT2	Calculated																
CC3	Analyzed	9.6	0.6	2.680	5.78	1.13	6.04	2.38	8.68	0.44	2.05	22.90	3.05	41.21	2.98	54.85	0.39
CT3	Calculated																
CC4	Analyzed	8.8	0.6	1.990	3.94	0.92	4.51	1.67	5.58	0.38	1.62	20.70	2.53	37.49	2.49	59.53	0.39
CT4	Analyzed	173.0	11.6	0.300	11.67	0.06	5.78	0.09	5.92	0.24	20.16	4.90	11.76	9.09	11.85	90.52	11.59
CC1	Combined	24.2	1.6	5.25	28.57	4.85	65.354	3.94	36.234	0.47	5.523	27.80	9.332	47.35	8.633	43.38	0.777
CC1+CC2	Combined	37.0	2.5	5.01	41.72	4.06	83.672	3.97	55.837	0.49	8.755	28.04	14.392	48.31	13.467	43.17	1.182
CC1+CC2+CC3	Combined	46.6	3.1	4.53	47.50	3.46	89.712	3.64	64.519	0.48	10.806	26.98	17.442	46.85	16.447	45.57	1.572
CC1+CC2+CC3+CC4	Combined	55.4	3.7	4.13	51.44	3.05	94.220	3.33	70.104	0.46	12.430	25.98	19.969	45.36	18.933	47.79	1.959

Streams RMG9	Stream type	Weight		CuTOT		Chalcopyrite		Chalcocite		Cuprite		S		Py		Qtz	
		g	%	%	Rec-%	%	Rec-%	%	Rec-%	%	Rec-%	%	Rec-%	%	Rec-%	%	Rec-%
Feed	Analyzed	1495.3	100.00														
Ground feed	Analyzed	1495.3	100.00														
Flotation feed	Calculated	1495.3	100.00	0.48	100.00	0.38	100.00	0.28	100.00	0.15	100.00	2.66	100.00	4.64	100.00	94.56	100.00
RC1	Analyzed	209.0	14.0	1.51	43.58	1.560	57.63	0.940	47.63	0.25	23.91	3.1	16.26	4.430	13.35	92.830	13.72
RT1	Calculated	1286.3	86.0	0.27	56.42							2.23	83.74				
RC2	Analyzed	99.0	6.6	1.99	27.21	1.710	29.93	1.370	32.88	0.35	15.86	3.6	8.95	5.100	7.28	91.480	6.40
RT2	Calculated	1187.3	79.4	0.14	29.21							1.99	74.79				
RC3	Analyzed	22.9	1.5	3.39	10.72	1.770	7.17	2.500	13.88	0.87	9.12	9.4	5.40	15.480	5.11	79.370	1.29
RT3	Calculated	1164.4	77.9	0.09	18.49							1.85	69.39				
RC4	Analyzed	11.7	0.8	1.59	2.57	0.580	1.20	0.990	2.81	0.68	3.64	9.7	2.85	17.390	2.93	80.360	0.66
RT4	Analyzed	1152.7	77.1	0.100	15.92	0.020	4.08	0.010	2.79	0.09	47.47	2.3	66.54	4.290	71.32	95.590	77.92
RC1	Combined	209.0	14.0	1.510	43.58	1.560	57.63	0.940	47.632	0.250	23.911	3.10	16.26	4.43	13.35	92.83	13.72
RC1+RC2	Combined	308.0	20.6	1.664	70.79	1.608	87.56	1.078	80.516	0.282	39.767	3.26	25.21	4.65	20.63	92.40	20.13
RC1+RC2+RC3	Combined	330.9	22.1	1.784	81.51	1.619	94.73	1.177	94.397	0.323	48.884	3.69	30.61	5.40	25.75	91.49	21.41
RC1+RC2+RC3+RC4	Combined	342.6	22.9	1.777	84.08	1.584	95.92	1.170	97.205	0.335	52.525	3.89	33.46	5.80	28.68	91.11	22.08

Streams RMG10	Stream type	Weight		CuTOT		Chalcopyrite		Chalcocite		Cuprite		S		Py		Qtz	
		g	%	%	Rec-%	%	Rec-%	%	Rec-%	%	Rec-%	%	Rec-%	%	Rec-%	%	Rec-%
Feed	Analyzed	1493.3	100.00														
Ground feed	Analyzed	1493.3	100.00														
Flotation feed	Calculated	1493.3	100.00	0.48	100.00	0.26	100.00	0.29	100.00	0.18	100.00	2.75	100.00	4.85	100.00	94.41	100.00
RC1	Analyzed	139.9	9.4	2.10	41.10	1.680	60.62	1.490	48.39	0.37	19.62	3.5	11.93	4.889	9.44	91.572	9.09
RT1	Calculated	1353.4	90.6	0.28	58.90							2.42	88.07				
RC2	Analyzed	47.9	3.2	3.45	23.12	1.830	22.61	2.820	31.36	0.64	11.55	5.4	6.30	7.841	5.18	86.871	2.95
RT2	Calculated	1305.5	87.4	0.17	35.78							2.25	81.77				
RC3	Analyzed	17.8	1.2	4.29	10.68	1.360	6.24	3.420	14.13	1.23	8.28	10.2	4.42	16.906	4.15	77.091	0.97
RT3	Calculated	1287.7	86.2	0.12	25.09							2.13	77.35				
RC4	Analyzed	11.4	0.8	1.74	2.78	0.220	0.65	1.190	3.15	0.81	3.48	9.8	2.72	17.741	2.79	80.044	0.65
RT4	Analyzed	1276.3	85.5	0.125	22.32	0.030	9.88	0.010	2.96	0.12	57.08	2.4	74.62	4.452	78.43	95.372	86.34
RC1	Combined	139.9	9.4	2.100	41.10	1.680	60.62	1.490	48.394	0.370	19.618	3.50	11.93	4.89	9.44	91.57	9.09
RC1+RC2	Combined	187.8	12.6	2.444	64.22	1.718	83.23	1.829	79.754	0.438	31.163	3.98	18.23	5.64	14.63	90.37	12.04
RC1+RC2+RC3	Combined	205.6	13.8	2.604	74.91	1.687	89.48	1.967	93.887	0.506	39.441	4.52	22.65	6.62	18.78	89.22	13.01
RC1+RC2+RC3+RC4	Combined	217.0	14.5	2.559	77.68	1.610	90.12	1.926	97.037	0.522	42.923	4.80	25.38	7.20	21.57	88.74	13.66

Streams RMG11	Stream type	Weight		CuTOT		Chalcopyrite		Chalcocite		Cuprite		S		Py		Qtz	
		g	%	%	Rec-%	%	Rec-%	%	Rec-%	%	Rec-%	%	Rec-%	%	Rec-%	%	Rec-%
Feed	Analyzed	1474.5	100.00														
Ground feed	Analyzed	1474.5	100.00														
Flotation feed	Calculated	1474.5	100.00	0.53	100.00	0.29	100.00	0.33	100.00	0.19	100.00	2.92	100.00	5.16	100.00	94.03	100.00
RC1	Analyzed	96.5	6.5	3.33	40.92	3.150	71.29	2.240	43.82	0.51	17.40	4.4	9.85	5.330	6.76	88.780	6.18
RT1	Calculated	1378.0	93.5	0.31	59.08							2.64	90.15				
RC2	Analyzed	31.7	2.1	5.56	22.45	2.920	21.71	4.600	29.56	0.99	11.10	6.6	4.85	8.710	3.63	82.790	1.89
RT2	Calculated	1346.3	91.3	0.20	36.63							2.49	85.30				
RC3	Analyzed	15.5	1.1	4.36	8.61	1.300	4.73	3.410	10.71	1.34	7.34	9.2	3.31	15.080	3.07	78.880	0.88
RT3	Calculated	1330.8	90.3	0.15	28.02							2.40	81.99				
RC4	Analyzed	12.6	0.9	1.77	2.84	0.770	2.28	1.000	2.55	0.80	3.56	8.6	2.51	15.210	2.52	82.230	0.75
RT4	Analyzed	1318.2	89.4	0.150	25.18	0.000	0.00	0.050	13.36	0.13	60.59	2.6	79.48	4.850	84.02	94.980	90.30
RC1	Combined	96.5	6.5	3.330	40.92	3.150	71.29	2.240	43.815	0.510	17.402	4.40	9.85	5.33	6.76	88.78	6.18
RC1+RC2	Combined	128.2	8.7	3.881	63.37	3.093	93.00	2.824	73.373	0.629	28.499	4.94	14.70	6.17	10.39	87.30	8.07
RC1+RC2+RC3	Combined	143.7	9.7	3.933	71.98	2.900	97.72	2.887	84.086	0.705	35.843	5.40	18.01	7.13	13.46	86.39	8.95
RC1+RC2+RC3+RC4	Combined	156.3	10.6	3.759	74.82	2.728	100.00	2.735	86.640	0.713	39.407	5.66	20.52	7.78	15.98	86.06	9.70

Streams RMG12	Stream type	Weight		CuTOT		Chalcopyrite		Chalcocite		Cuprite		S		Py		Qtz	
		g	%	%	Rec-%	%	Rec-%	%	Rec-%	%	Rec-%	%	Rec-%	%	Rec-%	%	Rec-%
Feed	Analyzed	1495.4	100.00														
Ground feed	Analyzed	1495.4	100.00														
Flotation feed	Calculated	1495.4	100.00	0.39	100.00	0.32	100.00	0.22	100.00	0.12	100.00	4.02	100.00	7.22	100.00	92.12	100.00
RC1	Analyzed	212.7	14.2	1.09	40.26	1.250	55.30	0.610	39.60	0.19	22.87	4.9	17.35	8.120	16.00	89.830	13.87
RT1	Calculated	1282.7	85.8	0.23	59.74							3.32	82.65				
RC2	Analyzed	109.4	7.3	1.48	28.12	1.520	34.59	0.910	30.38	0.26	16.09	5.6	10.20	9.140	9.26	88.170	7.00
RT2	Calculated	1173.3	78.5	0.12	31.62							2.91	72.45				
RC3	Analyzed	23.7	1.6	2.50	10.29	1.740	8.58	1.790	12.95	0.53	7.11	13.5	5.33	23.440	5.15	72.500	1.25
RT3	Calculated	1149.6	76.9	0.08	21.33							2.70	67.13				
RC4	Analyzed	10.5	0.7	1.39	2.53	0.700	1.53	0.990	3.17	0.40	2.38	15.2	2.66	27.610	2.69	70.300	0.54
RT4	Analyzed	1139.1	76.2	0.095	18.79	0.000	0.00	0.040	13.90	0.08	51.56	3.4	64.47	6.340	66.90	93.540	77.35
RC1	Combined	212.7	14.2	1.090	40.26	1.250	55.30	0.610	39.595	0.190	22.865	4.90	17.35	8.12	16.00	89.83	13.87
RC1+RC2	Combined	322.1	21.5	1.222	68.38	1.342	89.89	0.712	69.976	0.214	38.958	5.14	27.55	8.47	25.26	89.27	20.87
RC1+RC2+RC3	Combined	345.8	23.1	1.310	78.67	1.369	98.47	0.786	82.923	0.235	46.065	5.71	32.87	9.49	30.41	88.12	22.12
RC1+RC2+RC3+RC4	Combined	356.3	23.8	1.312	81.21	1.349	100.00	0.792	86.095	0.240	48.441	5.99	35.53	10.03	33.10	87.59	22.65

Streams RMG13	Stream type	Weight		CuTOT		Chalcopyrite		Chalcocite		Cuprite		S		Py		Qtz	
		g	%	%	Rec-%	%	Rec-%	%	Rec-%	%	Rec-%	%	Rec-%	%	Rec-%	%	Rec-%
Feed	Analyzed	1462.6	100.00														
Ground feed	Analyzed	1462.6	100.00														
Flotation feed	Calculated	1462.6	100.00	0.40	100.00	0.21	100.00	0.25	100.00	0.14	100.00	3.93	100.00	7.11	100.00	92.28	100.00
RC1	Analyzed	185.6	12.7	1.24	39.21	1.011	60.11	0.839	42.76	0.25	21.71	4.6	14.87	7.629	13.61	90.274	12.41
RT1	Calculated	1277.0	87.3	0.24	60.79							3.34	85.13				
RC2	Analyzed	61.8	4.2	2.25	23.69	1.473	29.16	1.753	29.75	0.38	11.17	6.7	7.21	10.911	6.48	85.480	3.91
RT2	Calculated	1215.2	83.1	0.15	37.09							3.06	77.92				
RC3	Analyzed	18.0	1.2	3.76	11.53	1.386	7.99	3.281	16.22	0.74	6.31	15.3	4.80	26.480	4.58	68.109	0.91
RT3	Calculated	1197.2	81.9	0.10	25.56							2.87	73.12				
RC4	Analyzed	12.3	0.8	1.60	3.35	0.404	1.59	1.315	4.44	0.46	2.68	13.8	2.96	25.057	2.96	72.762	0.66
RT4	Analyzed	1184.9	81.0	0.110	22.21	0.003	1.14	0.021	6.83	0.10	58.13	3.4	70.17	6.351	72.36	93.521	82.10
RC1	Combined	185.6	12.7	1.240	39.21	1.011	60.11	0.839	42.760	0.248	21.713	4.60	14.87	7.63	13.61	90.27	12.41
RC1+RC2	Combined	247.4	16.9	1.492	62.91	1.126	89.28	1.067	72.509	0.282	32.879	5.12	22.08	8.45	20.10	89.08	16.33
RC1+RC2+RC3	Combined	265.4	18.1	1.646	74.44	1.144	97.27	1.217	88.726	0.313	39.188	5.81	26.88	9.67	24.68	87.65	17.24
RC1+RC2+RC3+RC4	Combined	277.7	19.0	1.644	77.79	1.111	98.86	1.222	93.167	0.320	41.869	6.17	29.83	10.35	27.64	86.99	17.90

Streams RMG14	Stream type	Weight		CuTOT		Chalcopyrite		Chalcocite		Cuprite		S		Py		Qtz	
		g	%	%	Rec-%	%	Rec-%	%	Rec-%	%	Rec-%	%	Rec-%	%	Rec-%	%	Rec-%
Feed	Analyzed	1490.6															
Ground feed	Calculated	1490.6															
Flotation feed	Calculated	1490.6		0.46		0.29		0.29		0.15		2.71		4.77		94.51	
RC	Calculated	249.5	16.7	2.172	78.44												
RT	Analyzed	1241.1	83.3	0.12	21.56	0.01	4.05	0.03	7.98	0.11	59.38	2.40	73.80	4.47	78.07	95.38	84.03
Ground CF feed	Calculated	249.5	16.7	2.172	78.44	1.649	95.95	1.607	92.02	0.357	40.62	4.239	26.20	6.247	21.93	90.140	15.97
CC1	Analyzed	15.8	1.1	19.30	44.15	18.71	68.94	14.53	52.69	1.37	9.89	19.40	7.59	18.58	4.13	46.80	0.52
CT1	Calculated																
CC2	Analyzed	9.9	0.7	13.30	19.06	8.32	19.20	11.26	25.59	1.61	7.26	16.00	3.92	20.25	2.82	58.56	0.41
CT2	Calculated																
CC3	Analyzed	4.5	0.3	6.81	4.44	2.86	3.00	5.86	6.05	1.28	2.63	14.00	1.56	22.11	1.40	67.88	0.22
CT3	Calculated																
CC4	Analyzed	5.2	0.3	3.63	2.73	1.58	1.92	2.78	3.32	0.97	2.30	11.30	1.46	19.06	1.39	75.61	0.28
CT4	Analyzed	214.1	14.4	0.26	8.06	0.06	2.90	0.09	4.37	0.19	18.53	2.20	11.67	4.04	12.18	95.62	14.53
CC1	Combined	15.8	1.1	19.30	44.15	18.71	68.939	14.53	52.690	1.37	9.891	19.40	7.594	18.58	4.132	46.80	0.525
CC1+CC2	Combined	25.7	1.7	16.99	63.21	14.71	88.138	13.27	78.275	1.46	17.154	18.09	11.518	19.23	6.953	51.33	0.937
CC1+CC2+CC3	Combined	30.2	2.0	15.47	67.65	12.94	91.138	12.16	84.330	1.44	19.786	17.48	13.079	19.66	8.353	53.80	1.153
CC1+CC2+CC3+CC4	Combined	35.4	2.4	13.73	70.38	11.27	93.054	10.79	87.648	1.37	22.089	16.57	14.535	19.57	9.748	57.00	1.432

Streams RMG15	Stream type	Weight		CuTOT		Chalcopyrite		Chalcocite		Cuprite		S		Py		Qtz	
		g	%	%	Rec-%	%	Rec-%	%	Rec-%	%	Rec-%	%	Rec-%	%	Rec-%	%	Rec-%
Feed	Analyzed	1483.5															
Ground feed	Calculated	1483.5															
Flotation feed	Calculated	1483.5		0.48		0.24		0.31		0.17		2.93		5.21		94.07	
RC	Calculated	241.1	16.3	2.25	75.74												
RT	Analyzed	1242.4	83.7	0.14	24.26	0.02	7.11	0.03	8.07	0.12	58.89	2.70	77.17	5.03	80.80	94.80	84.40
Ground CF feed	Calculated	241.1	16.3	2.25	75.74	1.347	92.89	1.761	91.93	0.432	41.11	4.117	22.83	6.158	19.20	90.310	15.60
CC1	Analyzed	15.3	1.0	19.50	41.62	15.62	68.37	15.65	51.84	1.79	10.82	19.30	6.79	19.99	3.95	46.94	0.51
CT1	Calculated																
CC2	Analyzed	10.1	0.7	13.80	19.44	6.01	17.37	12.52	27.37	1.94	7.74	16.40	3.81	22.03	2.88	57.50	0.42
CT2	Calculated																
CC3	Analyzed	4.5	0.3	7.70	4.83	2.83	3.64	6.70	6.53	1.54	2.74	15.00	1.55	23.69	1.38	65.24	0.21
CT3	Calculated																
CC4	Analyzed	3.6	0.2	4.61	2.32	1.10	1.13	3.91	3.05	1.25	1.78	13.60	1.13	23.25	1.08	70.49	0.18
CT4	Analyzed	207.6	14.0	0.26	7.53	0.04	2.38	0.07	3.15	0.22	18.04	2.00	9.55	3.69	9.90	95.99	14.28
CC1	Combined	15.3	1.0	19.50	41.62	15.62	68.373	15.65	51.836	1.79	10.818	19.30	6.793	19.99	3.955	46.94	0.515
CC1+CC2	Combined	25.4	1.7	17.23	61.06	11.80	85.739	14.41	79.211	1.85	18.557	18.15	10.603	20.80	6.832	51.14	0.931
CC1+CC2+CC3	Combined	29.9	2.0	15.80	65.89	10.45	89.382	13.25	85.738	1.80	21.294	17.67	12.156	21.24	8.210	53.26	1.141
CC1+CC2+CC3+CC4	Combined	33.5	2.3	14.60	68.21	9.44	90.515	12.24	88.785	1.74	23.072	17.24	13.282	21.45	9.292	55.11	1.323

Streams RMG16	Stream type	Weight		CuTOT		Chalcopyrite		Chalcocite		Cuprite		S		Py		Qtz	
		g	%	%	Rec-%	%	Rec-%	%	Rec-%	%	Rec-%	%	Rec-%	%	Rec-%	%	Rec-%
Feed	Analyzed	1480.8															
Ground feed	Calculated	1480.8															
Flotation feed	Calculated	1480.8		0.49		0.20		0.31		0.20		2.90		5.19		94.10	
RC	Calculated	189.3	12.8	2.71	70.04												
RT	Analyzed	1291.5	87.2	0.17	29.96	0.06	24.10	0.03	7.25	0.15	64.31	2.70	81.07	5.01	84.18	94.77	87.83
Ground CF feed	Calculated	189.3	12.8	2.71	70.04	1.182	75.90	2.268	92.75	0.553	35.69	4.301	18.93	6.418	15.82	89.580	12.17
CC1	Analyzed	12.6	0.9	25.70	44.19	13.72	58.64	23.29	63.40	2.65	11.37	21.70	6.36	22.85	3.75	37.49	0.34
CT1	Calculated																
CC2	Analyzed	5.7	0.4	15.70	12.21	6.07	11.73	14.40	17.73	2.36	4.60	18.60	2.46	25.40	1.89	51.77	0.21
CT2	Calculated																
CC3	Analyzed	3.1	0.2	8.73	3.69	2.40	2.52	7.93	5.31	1.77	1.87	15.90	1.15	25.19	1.02	62.72	0.14
CT3	Calculated																
CC4	Analyzed	2.9	0.2	5.19	2.05	1.07	1.05	4.50	2.82	1.39	1.37	13.40	0.90	22.68	0.86	70.38	0.15
CT4	Analyzed	165.0	11.1	0.35	7.88	0.04	1.96	0.10	3.49	0.29	16.49	2.10	8.06	3.87	8.31	95.71	11.33
CC1	Combined	12.6	0.9	25.70	44.19	13.72	58.641	23.29	63.398	2.65	11.370	21.70	6.357	22.85	3.749	37.49	0.339
CC1+CC2	Combined	18.3	1.2	22.59	56.41	11.33	70.369	20.52	81.129	2.56	15.966	20.73	8.822	23.64	5.635	41.94	0.551
CC1+CC2+CC3	Combined	21.4	1.4	20.58	60.10	10.04	72.890	18.70	86.437	2.44	17.835	20.03	9.968	23.87	6.652	44.95	0.690
CC1+CC2+CC3+CC4	Combined	24.3	1.6	18.74	62.15	8.97	73.942	17.00	89.254	2.32	19.205	19.24	10.871	23.73	7.508	47.98	0.837

Appendix 4 (1) Elemental copper and copper mineral kinetics of rougher flotation tests.

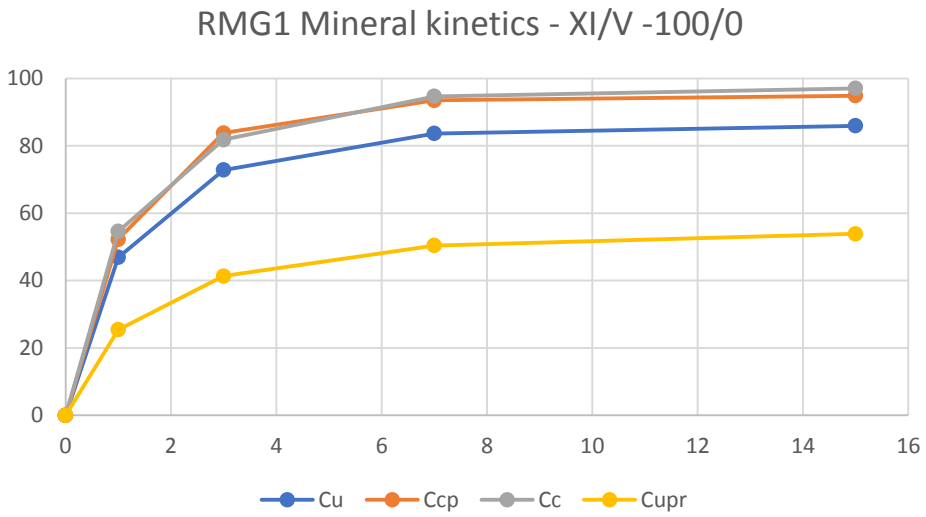

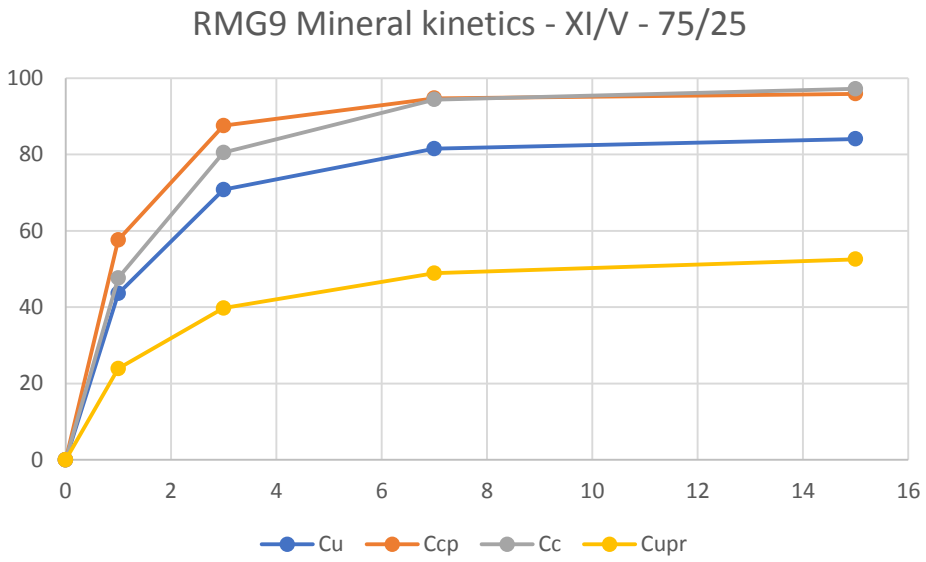

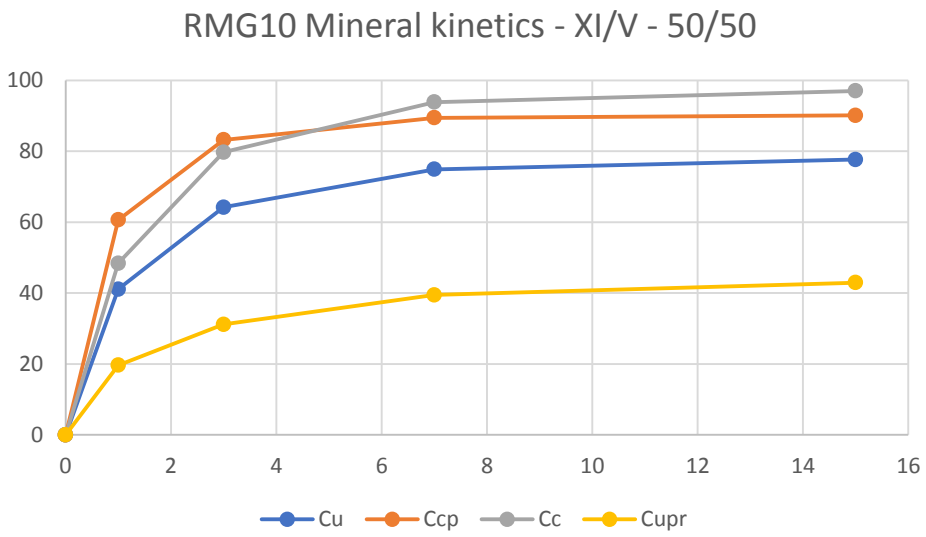
RMG10 Mineral kinetics - XI/V - 50/50
100
80
60
40
20
0
0
2
4
6
8
10
12
14
16
Cu
Ccp
Cc
Cupr

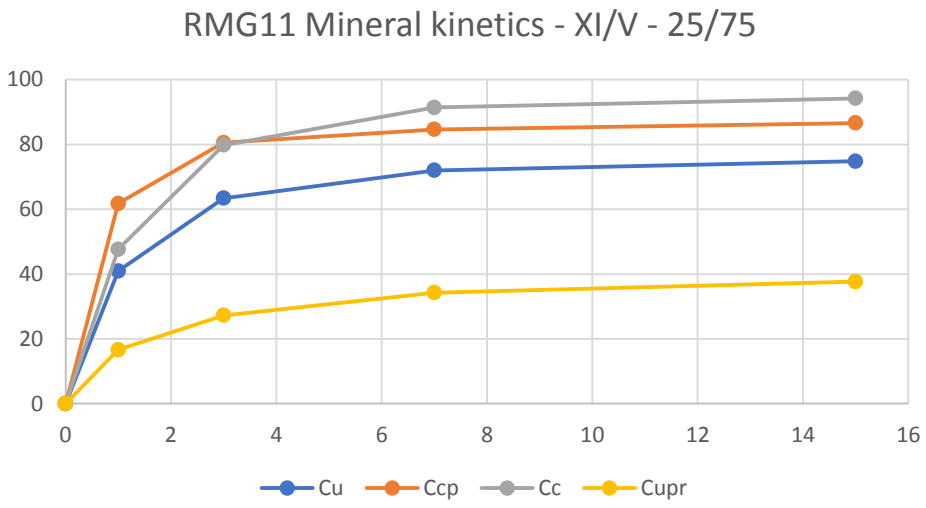
RMG11 Mineral kinetics - XI/V - 25/75
100
80
60
40
20
0
0
2
4
6
8
10
12
14
16
Cu
Ccp
Cc
Cupr

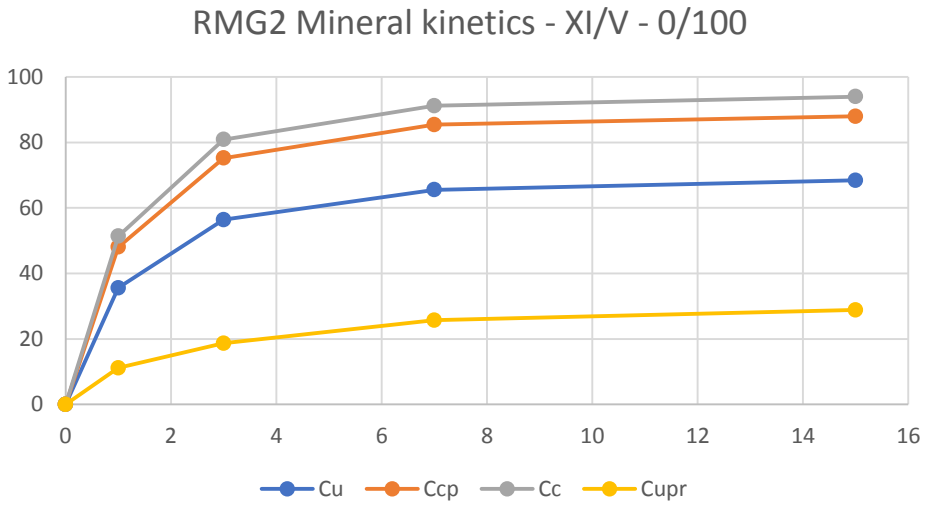
RMG2 Mineral kinetics - XI/V - 0/100
100
80
60
40
20
0
0
2
4
6
8
10
12
14
16
Cu
Ccp
Cc
Cupr

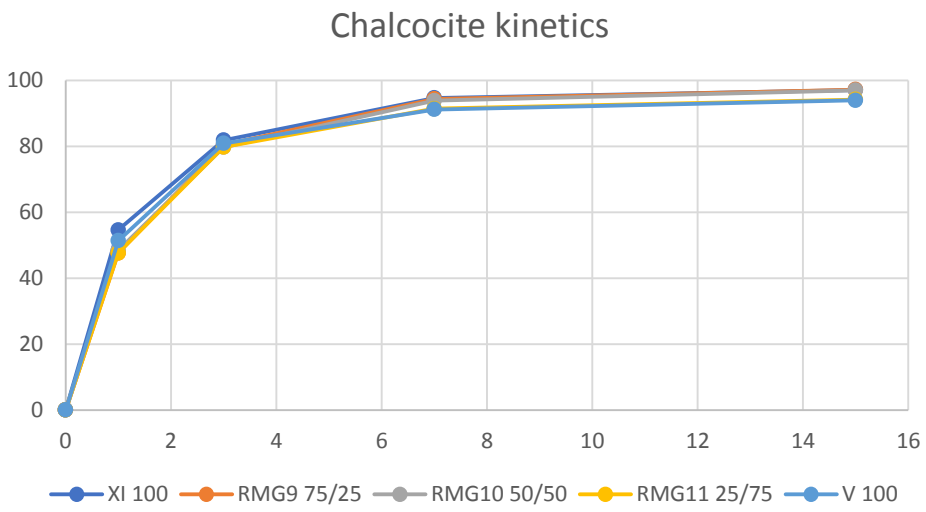
Chalcocite kinetics
100
80
60
40
20
0
0
2
4
6
8
10
12
14
16
XI 100
RMG9 75/25
RMG10 50/50
RMG11 25/75
V 100

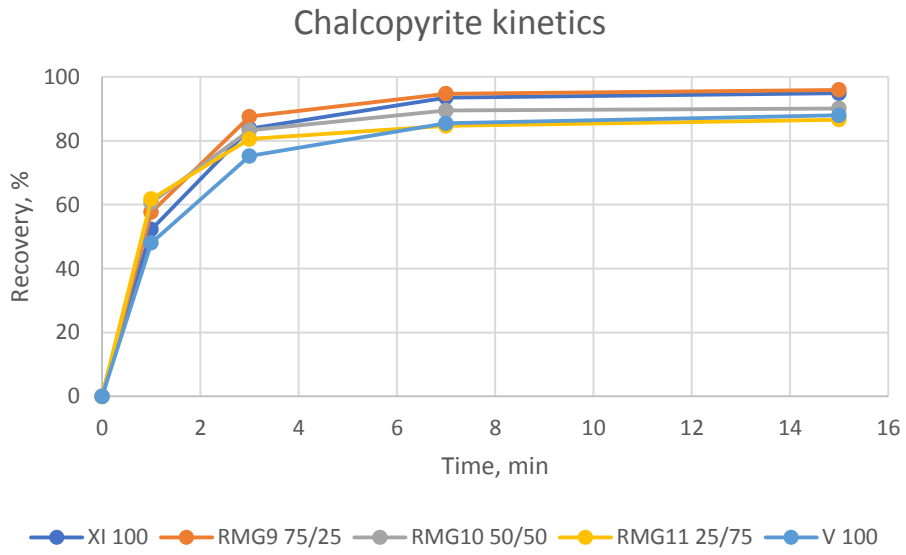
Chalcopyrite kinetics
Recovery, %
100
80
60
40
20
0
0
2
4
6
8
10
12
14
16
Time, min
XI 100
RMG9 75/25
RMG10 50/50
RMG11 25/75
V 100

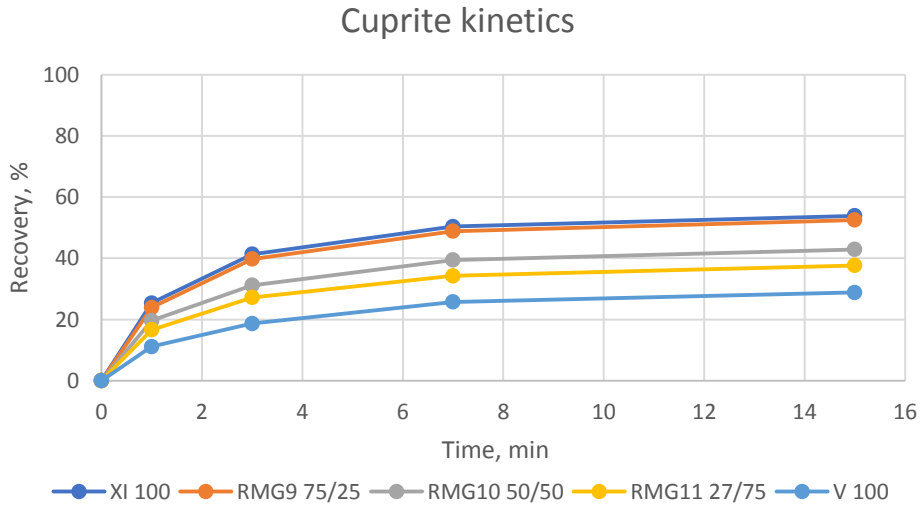
Cuprite kinetics
Recovery, %
100
80
60
40
20
0
0
2
4
6
8
10
12
14
16
Time, min
XI 100
RMG9 75/25
RMG10 50/50
RMG11 27/75
V 100

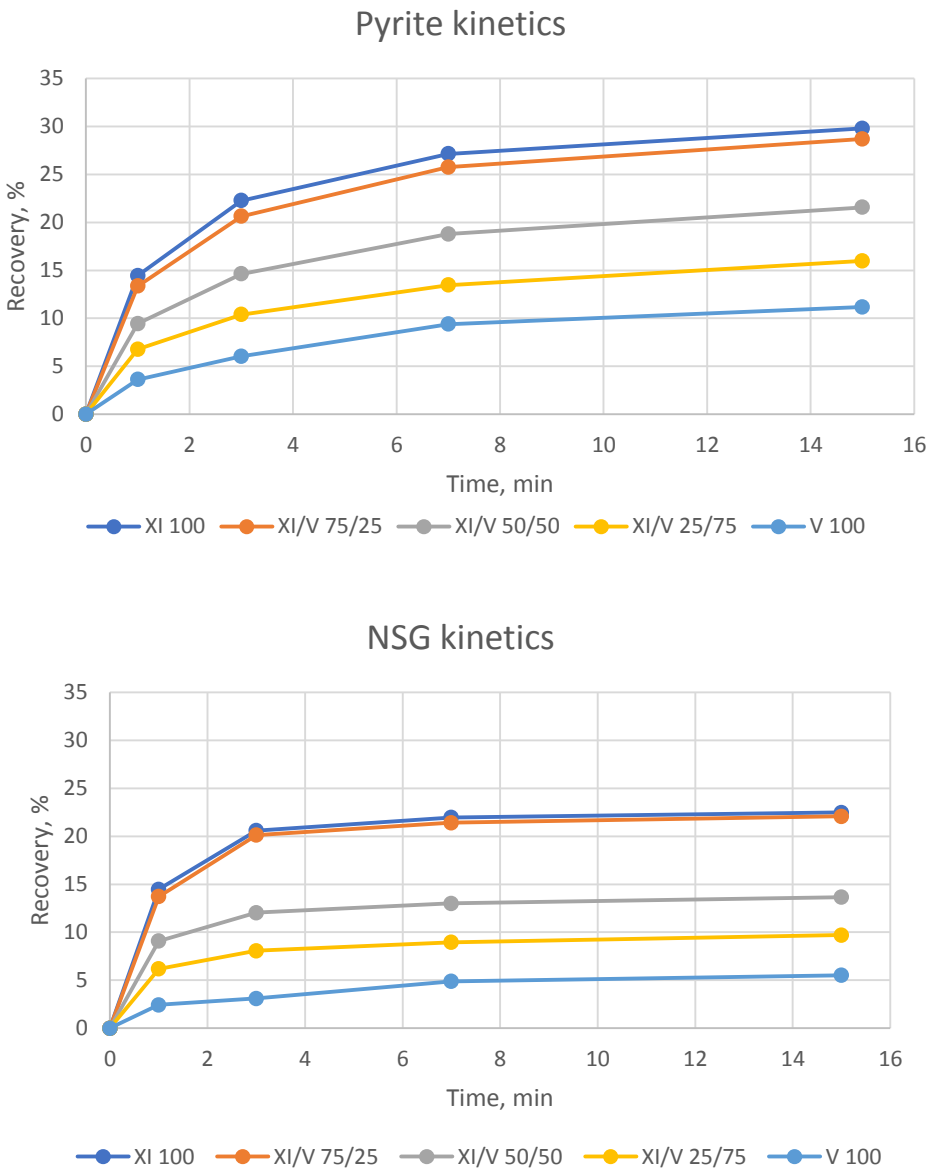

Appendix 4 (2) Elemental copper and copper mineral kinetics of cleaner flotation tests.

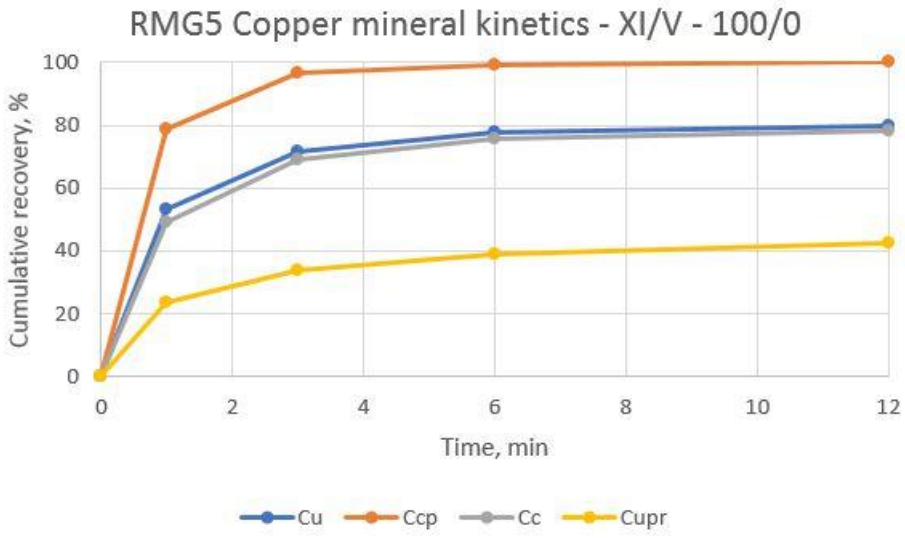
RMG5 Copper mineral kinetics - XI/V - 100/0
Cumulative recovery, %
100
80
60
40
20
0
0
2
4
6
8
10
12
Time, min
Cu
Ccp
Cc
Cupr

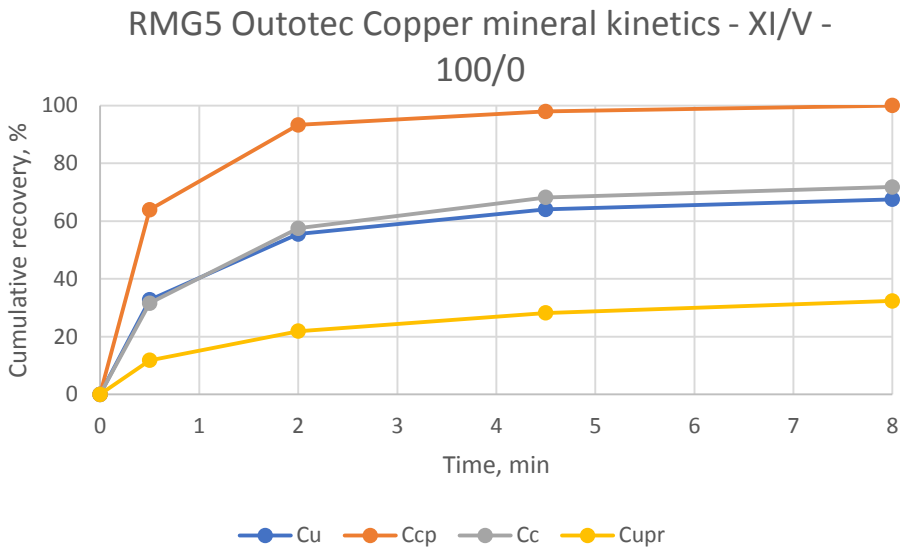
RMG5 Outotec Copper mineral kinetics - XI/V - 100/0
Cumulative recovery, %
100
80
60
40
20
0
0
1
2
3
4
5
6
7
8
Time, min
Cu
Ccp
Cc
Cupr

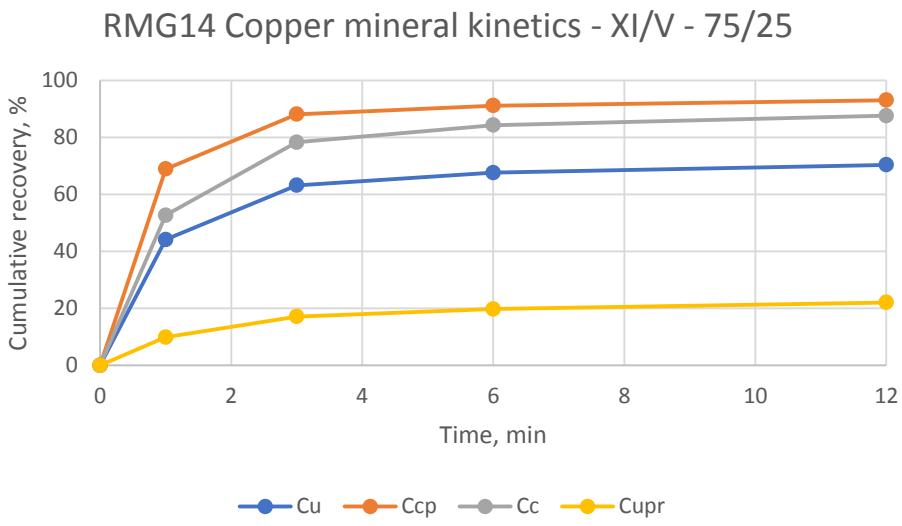
RMG14 Copper mineral kinetics - XI/V - 75/25
Cumulative recovery, %
100
80
60
40
20
0
0
2
4
6
8
10
12
Time, min
Cu
Ccp
Cc
Cupr

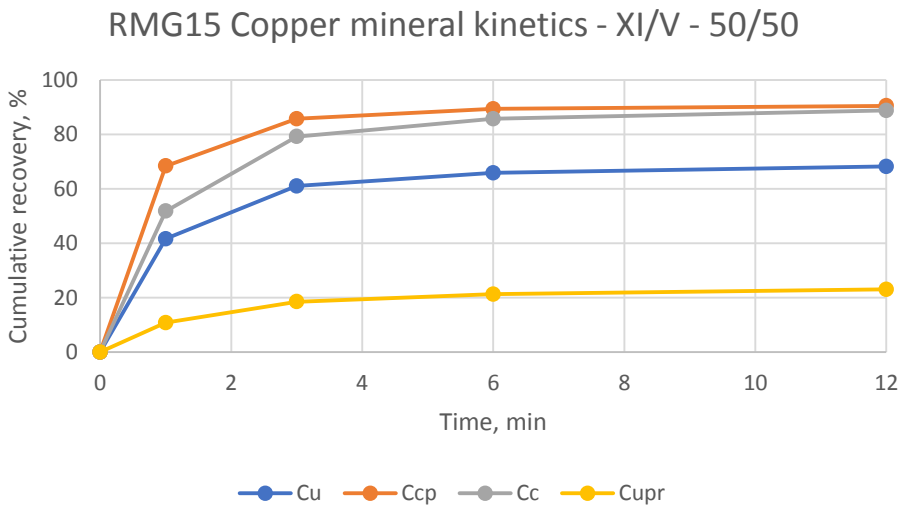
RMG15 Copper mineral kinetics - XI/V - 50/50
Cumulative recovery, %
100
80
60
40
20
0
0
2
4
6
8
10
12
Time, min
Cu
Ccp
Cc
Cupr

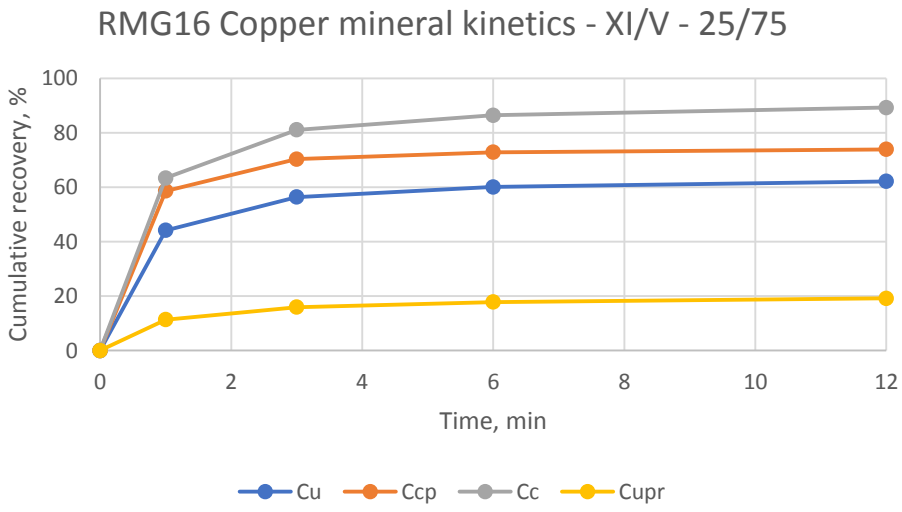
RMG16 Copper mineral kinetics - XI/V - 25/75
Cumulative recovery, %
100
80
60
40
20
0
0
2
4
6
8
10
12
Time, min
Cu
Ccp
Cc
Cupr

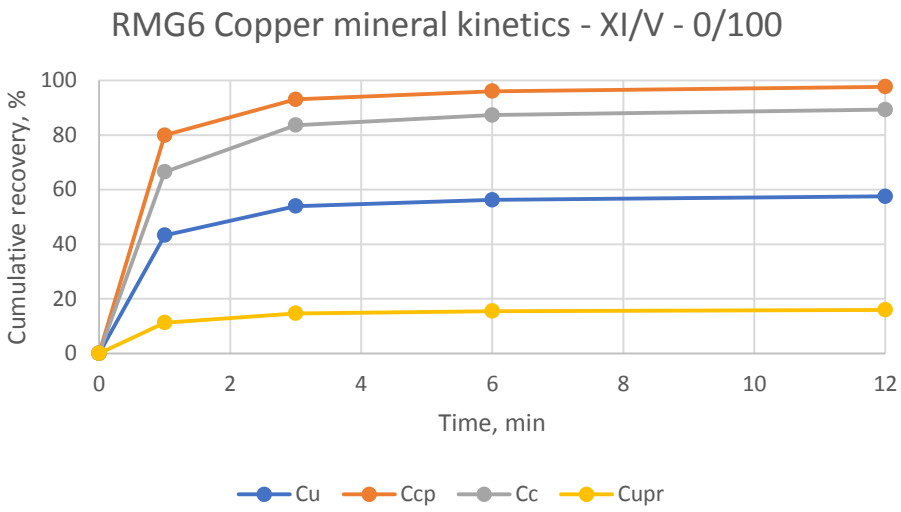
RMG6 Copper mineral kinetics - XI/V - 0/100
Cumulative recovery, %
100
80
60
40
20
0
0
2
4
6
8
10
12
Time, min
Cu
Ccp
Cc
Cupr

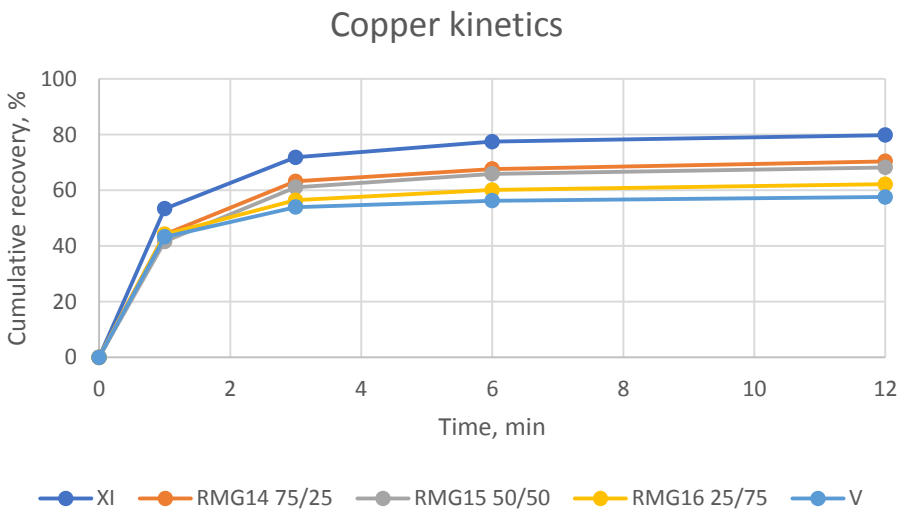
Copper kinetics
Cumulative recovery, %
100
80
60
40
20
0
0
2
4
6
8
10
12
Time, min
XI
RMG14 75/25
RMG15 50/50
RMG16 25/75
V

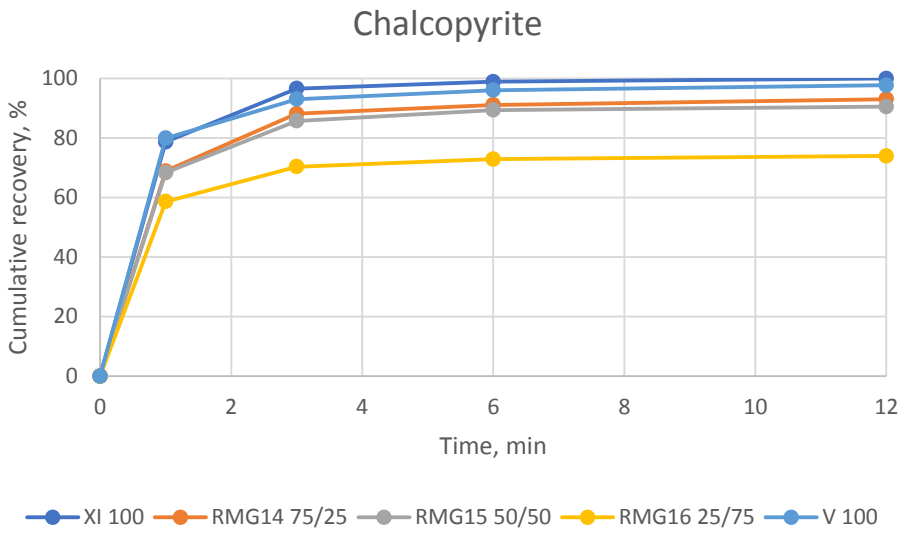
Chalcopyrite
Cumulative recovery, %
100
80
60
40
20
0
0
2
4
6
8
10
12
Time, min
XI 100
RMG14 75/25
RMG15 50/50
RMG16 25/75
V 100

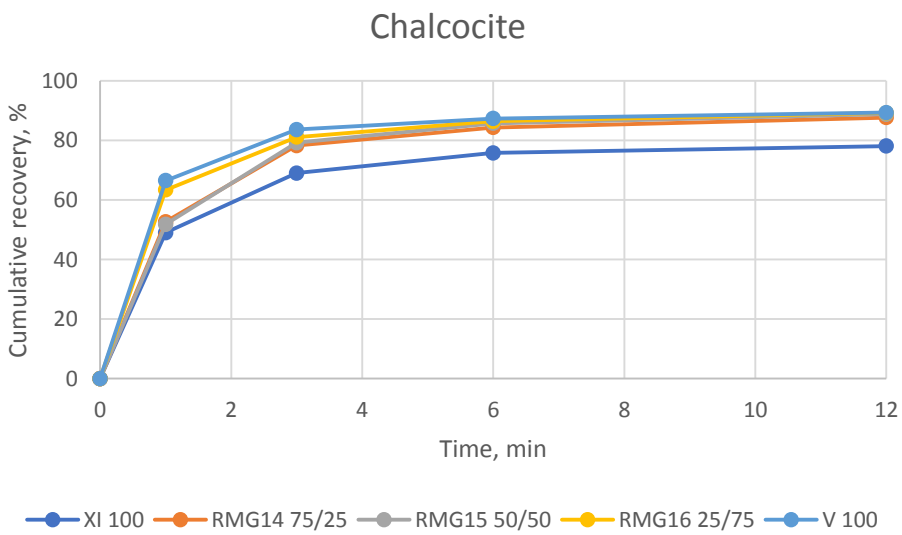
Chalcocite
Cumulative recovery, %
100
80
60
40
20
0
0
2
4
6
8
10
12
Time, min
XI 100
RMG14 75/25
RMG15 50/50
RMG16 25/75
V 100

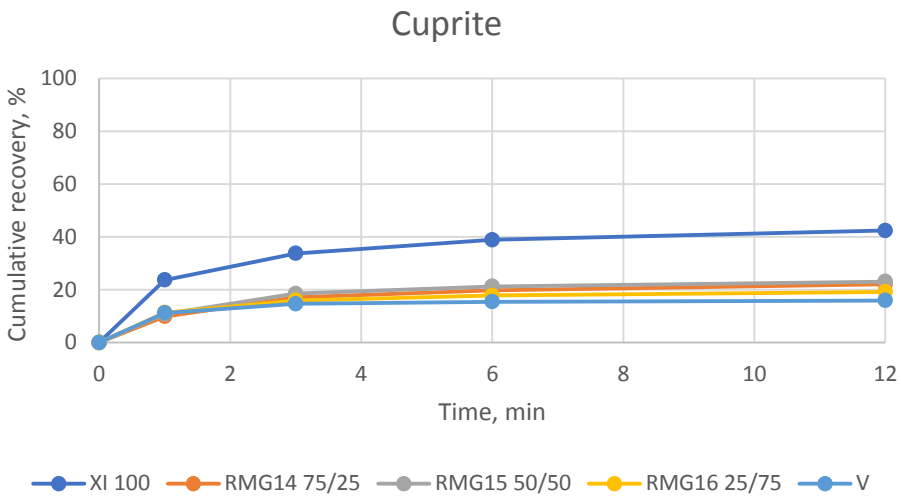
Cuprite
Cumulative recovery, %
100
80
60
40
20
0
0
2
4
6
8
10
12
Time, min
XI 100
RMG14 75/25
RMG15 50/50
RMG16 25/75
V

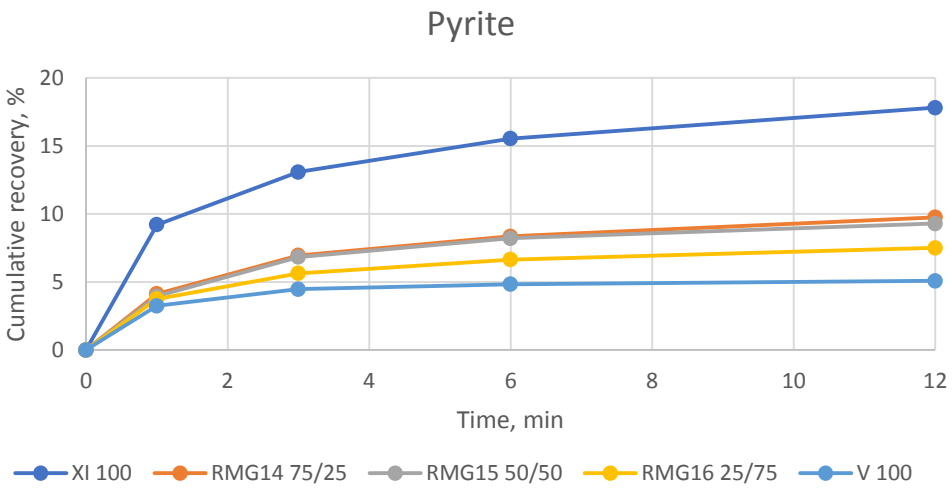
Pyrite
Cumulative recovery, %
20
15
10
5
0
0
2
4
6
8
10
12
Time, min
XI 100
RMG14 75/25
RMG15 50/50
RMG16 25/75
V 100

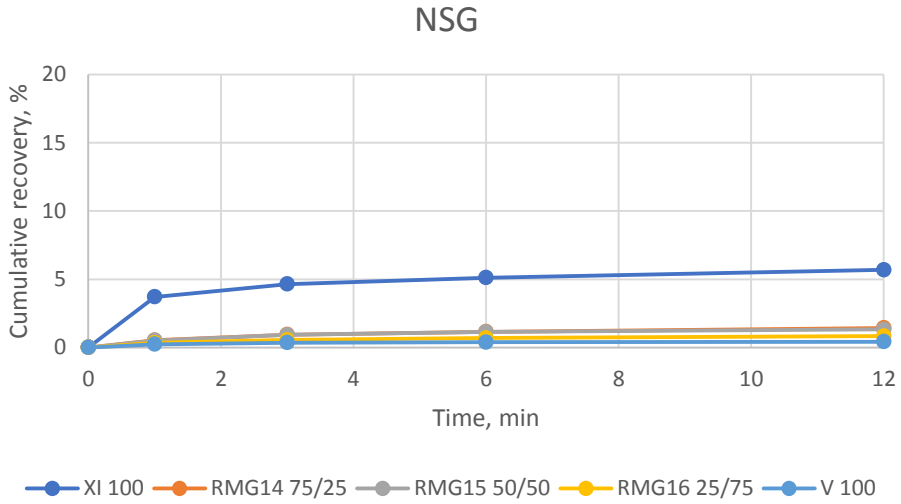
NSG
Cumulative recovery, %
20
15
10
5
0
0
2
4
6
8
10
12
Time, min
XI 100
RMG14 75/25
RMG15 50/50
RMG16 25/75
V 100

Appendix 5 (1). HSC Sim simulated results of rougher flotation tests.

Scenario 1	Rounds					
Unit Name	-	XI feed	V feed	RF	RF	RF
Variable Name	-	XI share	V share	Cu grade	Cu Rec	RC mass flow
Measurement Unit	-	t/h	t/h	%	%	t/h
SET / GET	-	SET	SET	GET	GET	GET
Cell Reference	-	0.0	100.0	5.76	67.66	6.35
Run 1	4	100.0	0.0	1.76	86.18	23.42
Run 2	4	90.0	10.0	1.88	84.14	21.71
Run 3	4	75.0	25.0	2.10	81.19	19.15
Run 4	4	60.0	40.0	2.38	78.36	16.59
Run 5	4	50.0	50.0	2.63	76.54	14.89
Run 6	4	40.0	60.0	2.94	74.77	13.18
Run 7	4	25.0	75.0	3.60	72.21	10.62
Run 8	4	10.0	90.0	4.70	69.75	8.06
Run 9	4	0.0	100.0	5.95	68.16	6.35

Scenario 1	Rounds					
Unit Name	-	XI feed	V feed	RF	RF	RF
Variable Name	-	XI share	V share	Cupr grade	Cc grade	Ccp grade
Measurement Unit	-	t/h	t/h	%	%	%
SET / GET	-	SET	SET	GET	GET	GET
Cell Reference	-	0.0	100.0	1.10	4.60	3.31
Run 1	4	100.0	0.0	0.28	1.10	1.84
Run 2	4	90.0	10.0	0.31	1.20	1.88
Run 3	4	75.0	25.0	0.35	1.39	1.96
Run 4	4	60.0	40.0	0.41	1.63	2.06
Run 5	4	50.0	50.0	0.45	1.84	2.15
Run 6	4	40.0	60.0	0.52	2.11	2.26
Run 7	4	25.0	75.0	0.65	2.66	2.49
Run 8	4	10.0	90.0	0.86	3.58	2.88
Run 9	4	0.0	100.0	1.10	4.60	3.31

Scenario 1	Rounds						
Unit Name	-	XI feed	V feed	RF	RF	RF	RF
Variable Name	-	XI share	V share	Py Rec	NSG Rec	Py grade	NSG grade
Measurement Unit	-	t/h	t/h	%	%	%	%
SET / GET	-	SET	SET	GET	GET	GET	GET
Cell Reference	-	0.0	100.0	11.02	5.47	9.62	81.38
Run 1	4	100.0	0.0	29.68	22.50	6.18	90.60
Run 2	4	90.0	10.0	27.60	20.81	6.28	90.33
Run 3	4	75.0	25.0	24.58	18.26	6.47	89.84
Run 4	4	60.0	40.0	21.67	15.71	6.71	89.19
Run 5	4	50.0	50.0	19.79	14.01	6.91	88.64
Run 6	4	40.0	60.0	17.96	12.31	7.17	87.95
Run 7	4	25.0	75.0	15.28	9.75	7.72	86.48
Run 8	4	10.0	90.0	12.70	7.18	8.62	84.07
Run 9	4	0.0	100.0	11.02	5.47	9.62	81.38

Appendix 5 (2). Experimental flotation results of rougher flotation.

Rougher flotation

Test	XI/V	RC mass pull	RC Cu grade-%	RC Cu Rec-% 10 min
RMG1	100/0	23.4	1.75	84.55
RMG9	75/25	22.9	1.78	82.5
RMG10	50/50	14.5	2.6	76
RMG11	25/75	10.6	3.76	73
RMG2	0/100	6.3	5.75	66.5

Test	XI/V	Ccp Rec	Cc Rec	Cupr Rec	Cupr grade	Cc grade	Ccp grade
RMG1	100/0	94.88	97.11	53.9	0.27	1.1	1.8
RMG9	75/25	95.9	97.2	52.5	0.34	1.2	1.6
RMG10	50/50	90.1	97	42.9	0.52	1.9	1.6
RMG11	25/75	100	86.6	39.4	0.71	2.7	2.7
RMG2	0/100	88.0	94.0	28.8	1.1	4.6	3.2

Test	XI/V	Py Rec	NSG Rec	Py grade	NSG grade
RMG1	100/0	29.78	22.49	6.21	90.61

RMG9	75/25	28.68	22.08	5.8	91.11
RMG10	50/50	21.57	13.66	7.2	88.74
RMG11	25/75	15.98	9.7	7.78	86.06
RMG2	0/100	11.17	5.52	9.68	81.41

Appendix 5 (3). Experimental results of cleaner blend flotation.

Test	XI/V	CC mass pull	CC Cu grade-%	CC Cu Rec-%
RMG5	100/0	6.8	5.12	79.83
RMG14	75/25	2.4	13.73	70.4
RMG15	50/50	2.3	14.6	68.2
RMG16	25/75	1.6	18.74	62.15
RMG6	0/100	1.1	26	57.55

Test	XI/V	Ccp grade	Ccp Rec	Cc grade	Cc Rec	Cupr grade	Cupr Rec
RMG5	100/0	4.45	100	3.83	78.1	0.59	42.4
RMG14	75/25	11.3	93.1	10.8	87.6	1.37	22.1
RMG15	50/50	9.44	90.5	12.2	88.8	1.74	23.1
RMG16	25/75	9	73.9	17	89.3	2.3	19.2
RMG6	0/100	12.6	97.7	23.2	89.3	3.51	16

Test	XI/V	Py grade	Py Rec	NSG grade	NSG Rec
RMG5	100/0	11.7	17.8	79.5	5.7
RMG14	75/25	19.6	9.7	57	1.4
RMG15	50/50	21.5	9.3	55.1	1.3
RMG16	25/75	23.7	7.5	48	0.84
RMG6	0/100	24.4	5.1	36.3	0.42

Appendix 6. Parity charts of rougher flotation results.

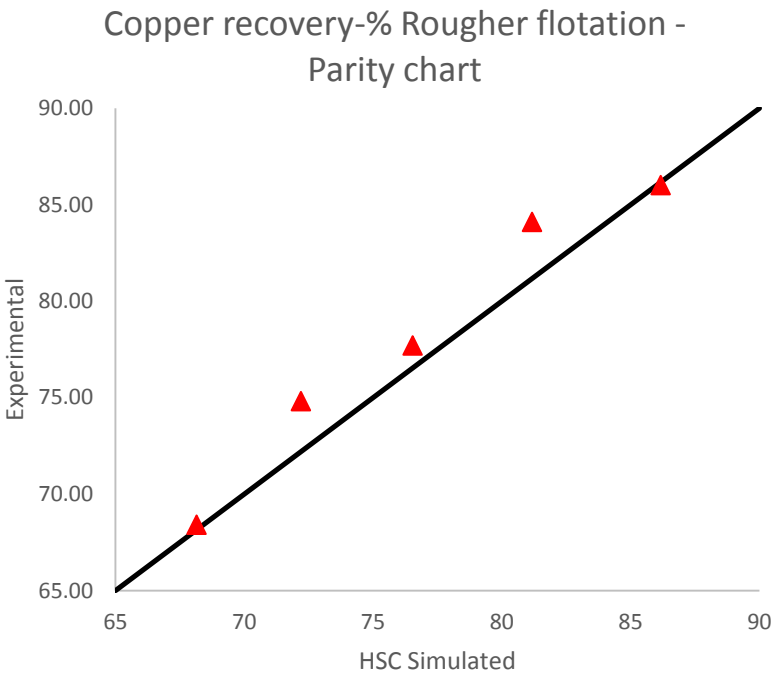

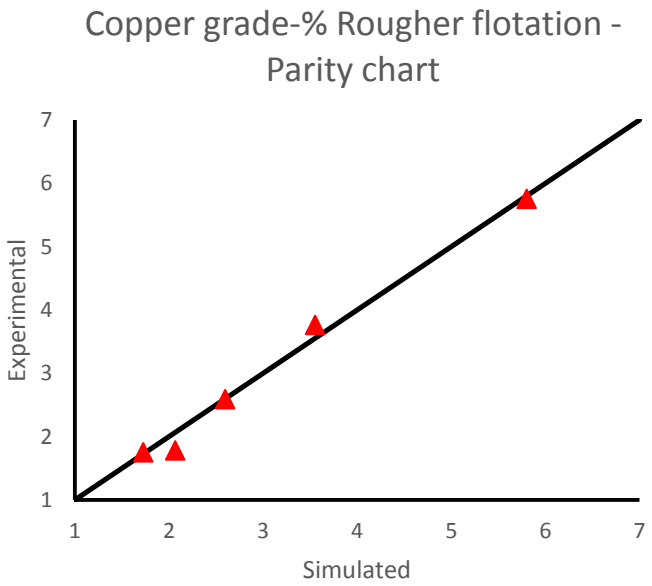

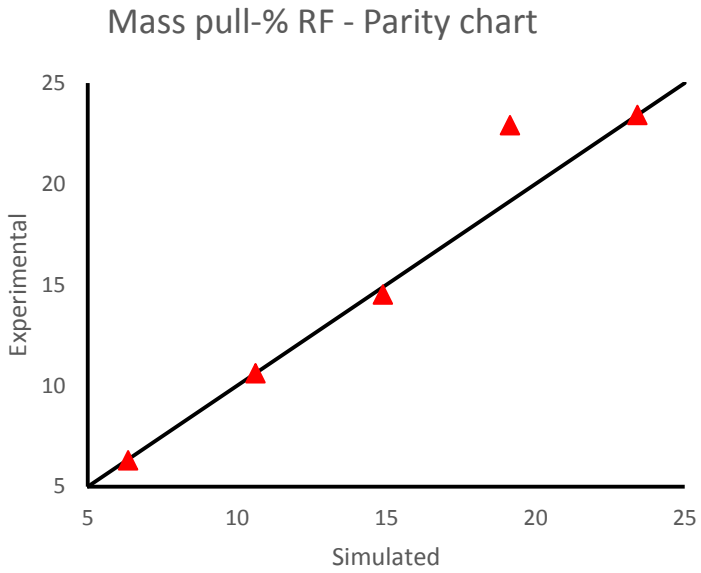

Appendix 7 (1). Compared results between experimental and simulated tests.

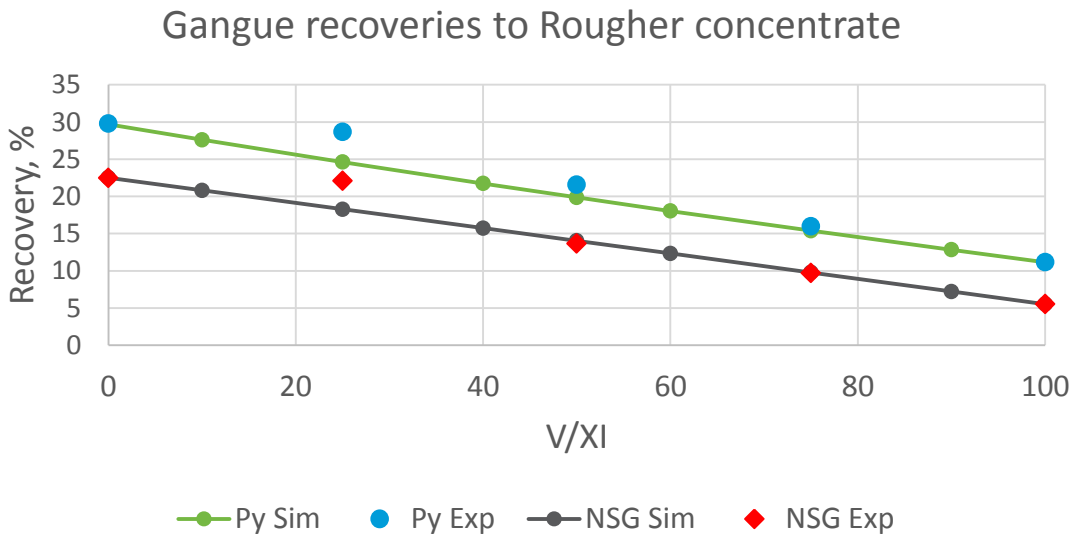

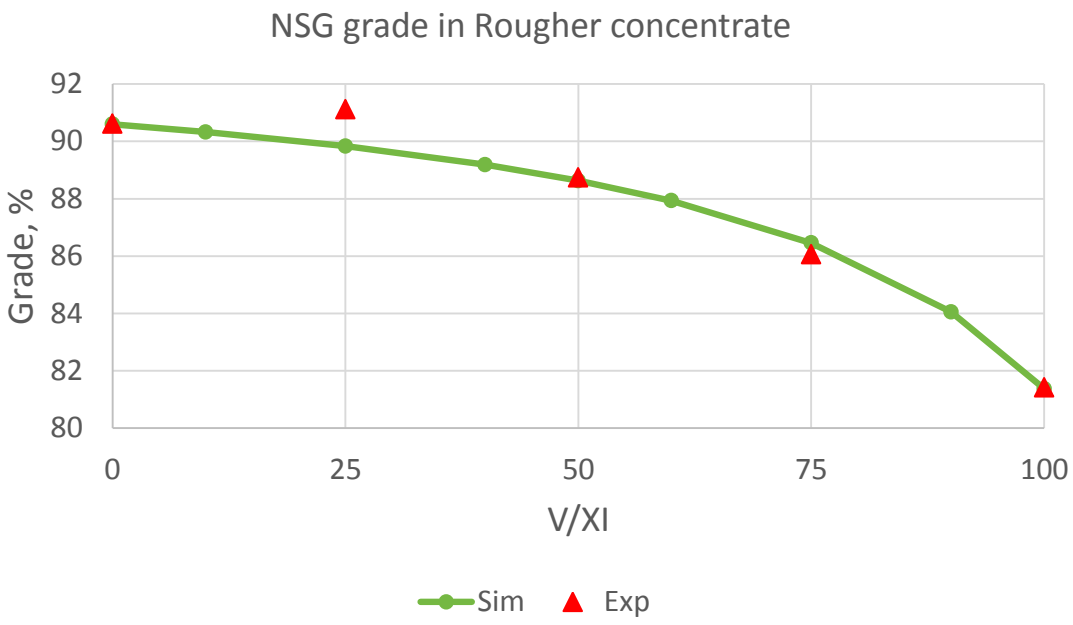
NSG grade in Rougher concentrate
Grade, %
92
90
88
86
84
82
80
0
25
50
75
100
V/XI
Sim
Exp

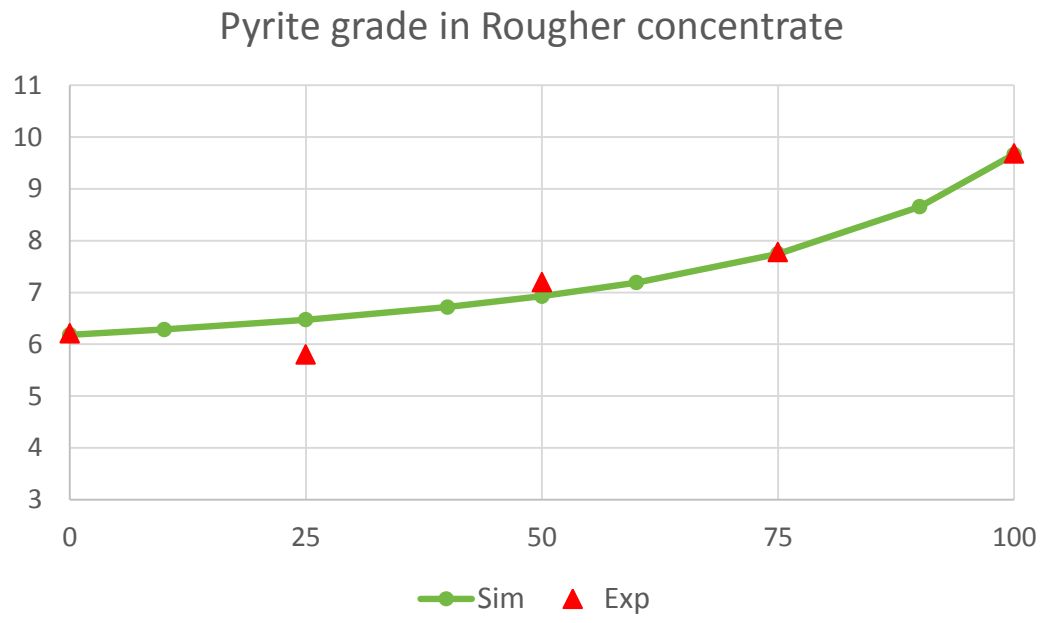
Pyrite grade in Rougher concentrate
11
10
9
8
7
6
5
4
3
0
25
50
75
100
Sim
Exp

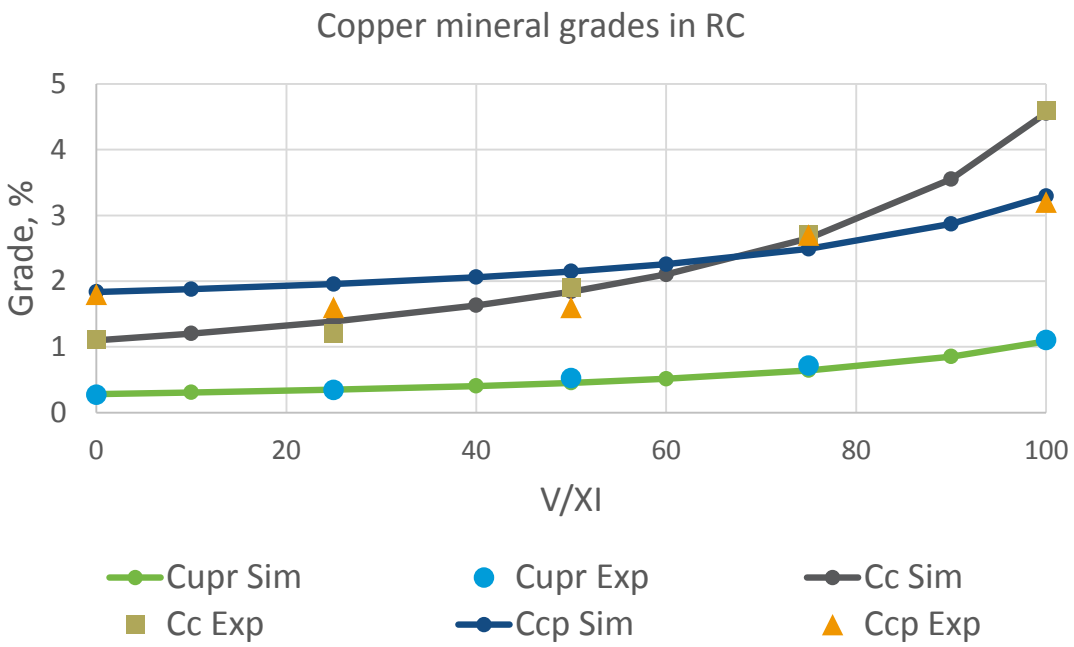

Appendix 7 (2). Simulated and experimental results in cleaner flotation tests.

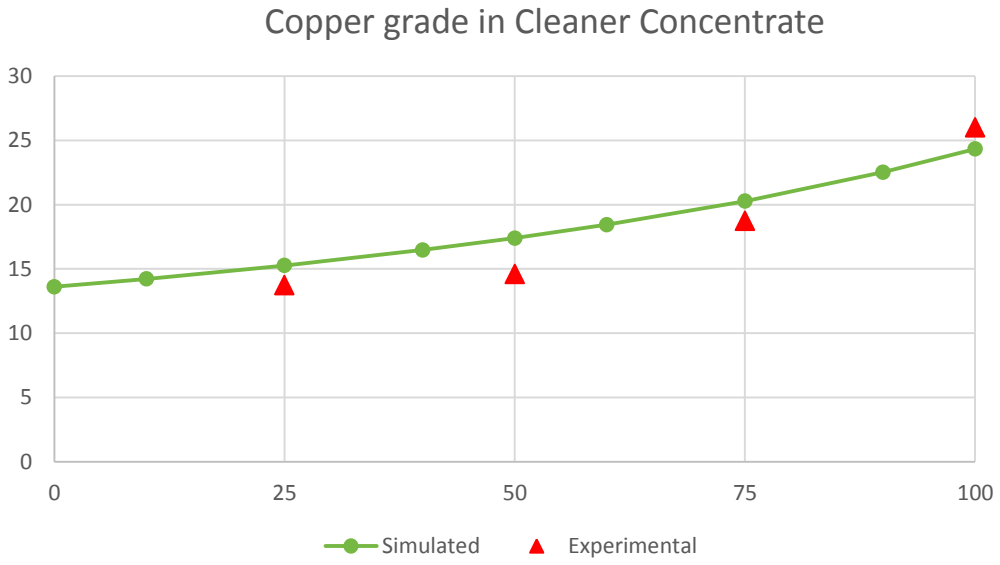

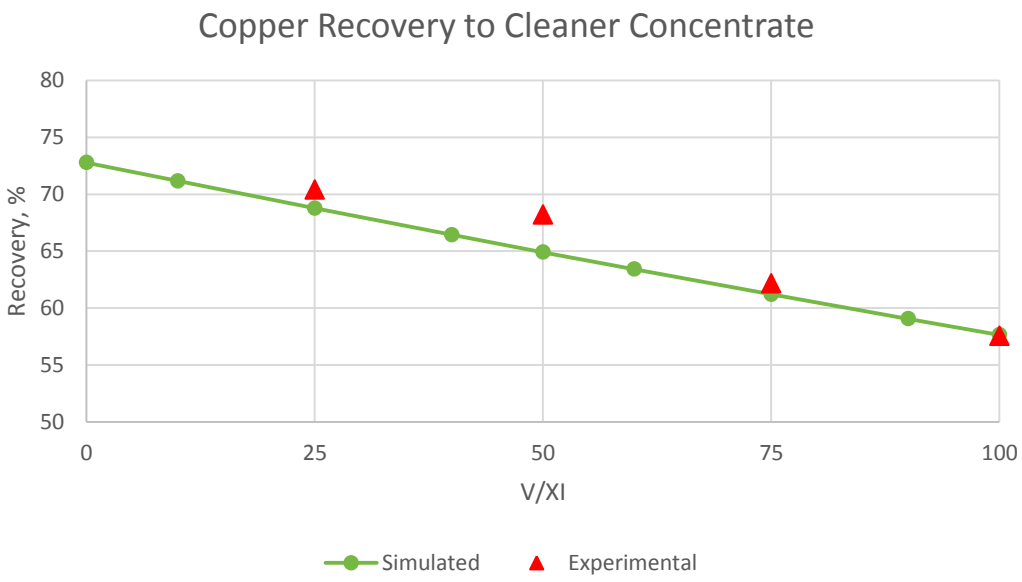
Copper Recovery to Cleaner Concentrate
Recovery, %
80
75
70
65
60
55
50
0
25
50
75
100
V/XI
Simulated
Experimental

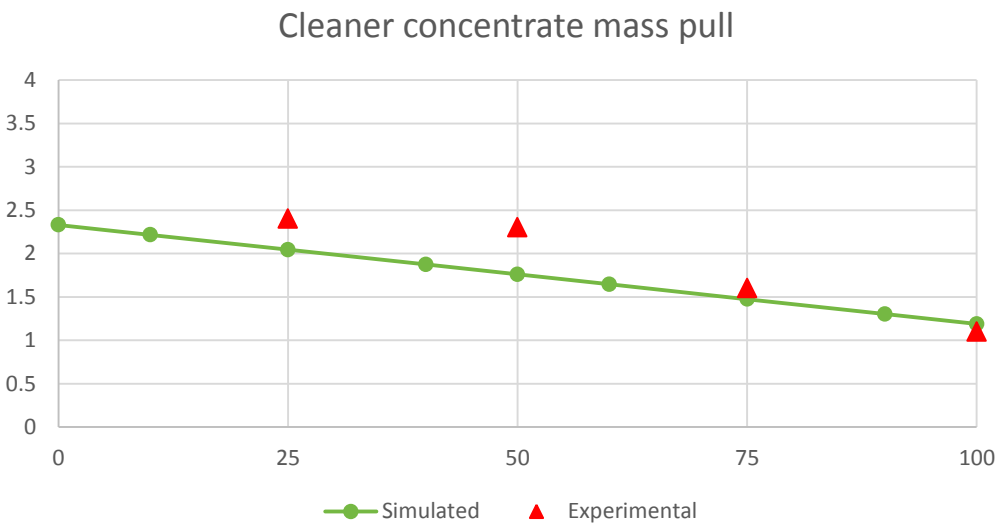
Cleaner concentrate mass pull
4
3.5
3
2.5
2
1.5
1
0.5
0
0
25
50
75
100
Simulated
Experimental

Appendix 8. Elemental copper and copper mineral grades from mineralogy report and mass balances.

	RF/CF	Sample	Cu	S	Ccp	Cc	Cupr	Py	NSG
Analyzed	Analyzed	XI	0.45	3.04	0.35	0.29	0.21	5.4	93.8
Back calculated	RF	XI	0.48	2.81	0.45	0.26	0.12	4.9	94.3
Back calculated	CF	XI	0.44	2.55	0.3	0.33	0.09	4.4	94.8
Analyzed	Analyzed	V	0.52	3.15	0.12	0.49	0.2	5.6	93.6
Back calculated	RF	V	0.53	3.08	0.23	0.31	0.24	5.5	93.7
Back calculated	CF	V	0.49	2.9	0.14	0.28	0.24	5.2	93.5
Analyzed	Analyzed	VIII-C1	0.31	5.13	0.25	0.17	0.11	9.4	90.1
Back calculated	RF	VIII-C1	0.32	5.1	0.33	0.15	0.1	9.3	90.2
Back calculated	CF	VIII-C1	0.3	4.85	0.27	0.15	0.11	8.9	90.6
Analyzed	Analyzed	VIII-C2	0.28	5.35	0.11	0.19	0.14	9.9	89.7
Back calculated	RF	VIII-C2	0.29	5.1	0.14	0.18	0.12	9.3	90.2
Back calculated	CF	VIII-C2	0.3	4.84	0.12	0.18	0.14	8.9	90.7

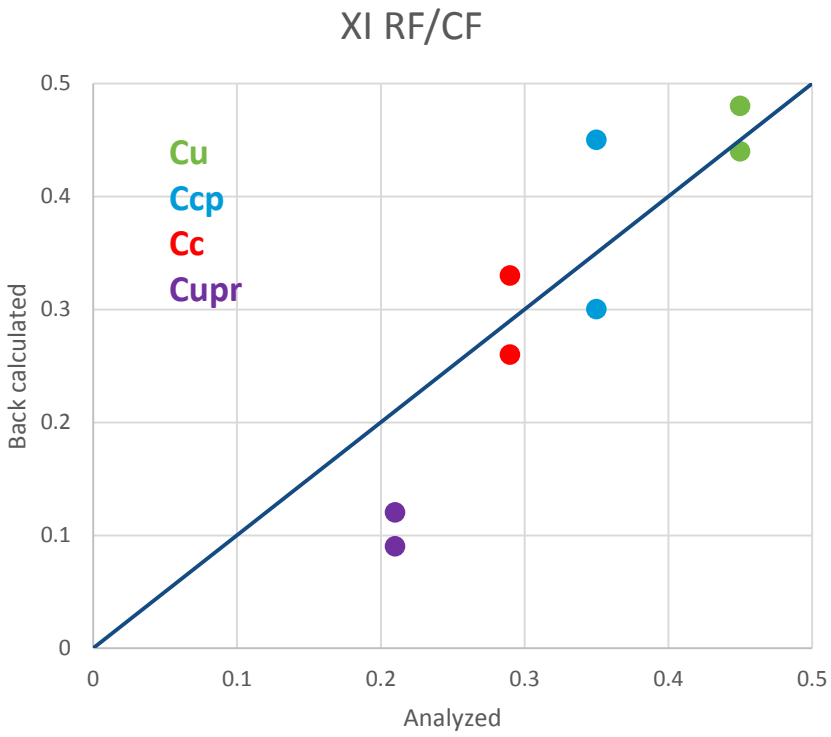

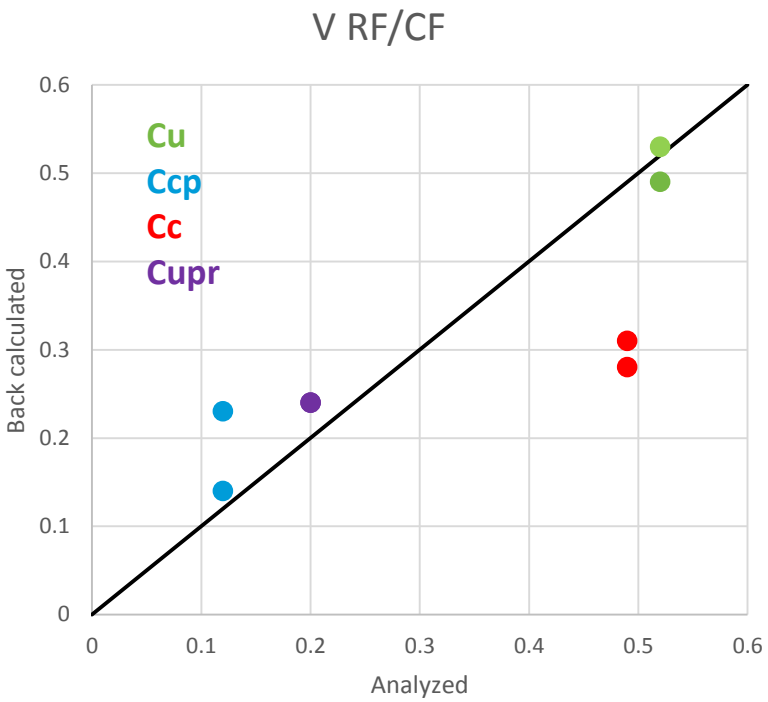
V RF/CF
Cu
Ccp
Cc
Cupr
Back calculated
Analyzed
0
0.1
0.2
0.3
0.4
0.5
0.6

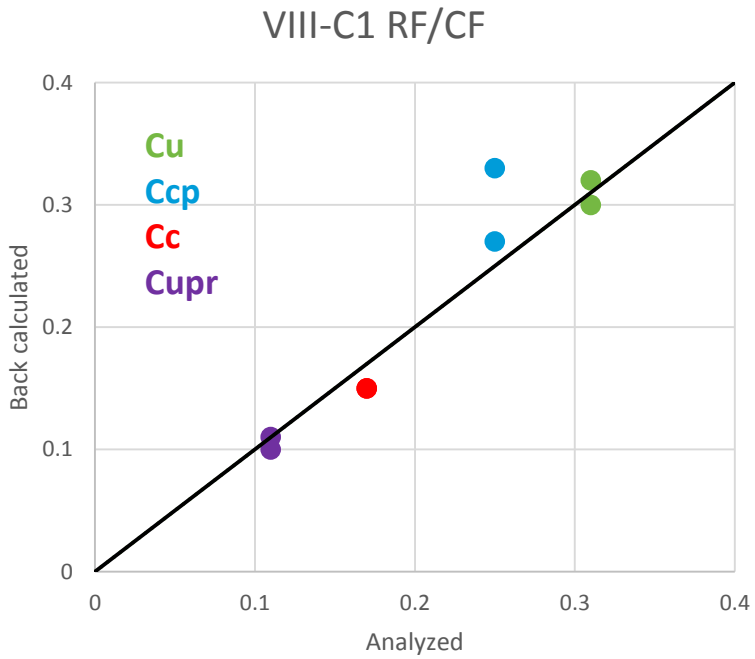
VIII-C1 RF/CF
Cu
Ccp
Cc
Cupr
Back calculated
Analyzed
0
0.1
0.2
0.3
0.4

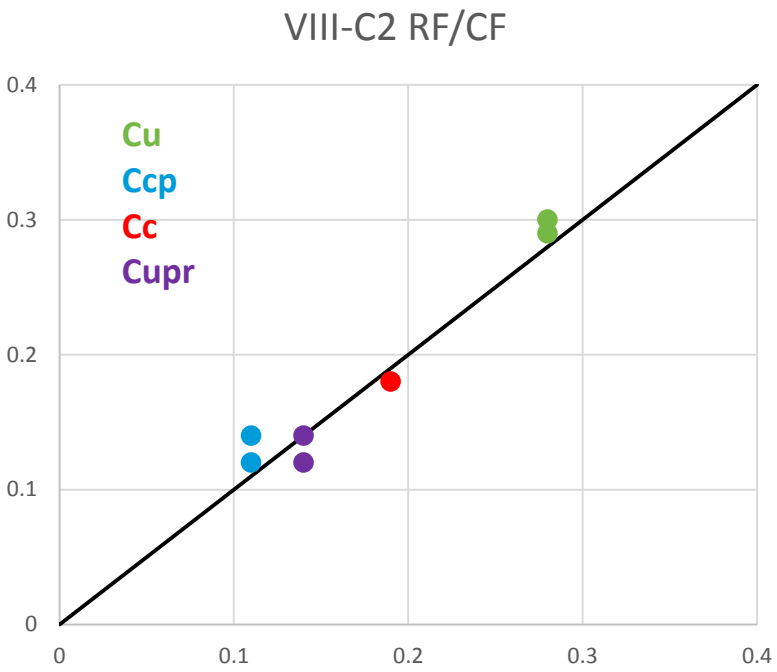
VIII-C2 RF/CF
0.4
0.3
0.2
0.1
0
0
0.1
0.2
0.3
0.4
Cu
Ccp
Cc
Cupr